



Umwelt-Campus
Birkenfeld

H O C H
S C H U L E
T R I E R



Høgskulen
på Vestlandet

The environmental signal of diatoms in recent (0-90 years) sediments from the Lærdalsfjord, Western Norway

A Bachelor's thesis submitted to Trier Hochschule (Umwelt Campus) and Høgskulen på Vestlandet (Western Norway University of Applied Sciences) in fulfilment of the requirements for the degree of B.Eng. Sustainable Business and Technology

Supervisor from Western Norway University of Applied Sciences (Sogndal):

Prof. Dr. Matthias Paetzel

Supervisor from Trier Hochschule (Umwelt Campus):

Prof. Dr. Stefan Stoll

Submitted by:

YANG YANG

Matrikelnummer: 974981

Mühlenstraße 35

67271 Kleinkarlbach

+491633837347

Email: ynyn3088@umwelt-campus.de

Date of submission: 05/2023

Table of Contents

ABSTRACT	8
ACKNOWLEDGEMENTS.....	9
1. INTRODUCTION	10
2. OBJECTIVE	13
Objective 1.....	13
Objective 2.....	13
Objective 3.....	14
3. SETTINGS	15
3.1. Environmental Settings.....	15
3.1.1 Bathymetry	15
3.1.2 Hydrography	16
3.1.3. Climate change.....	19
3.1.4 Recent human activities.....	20
3.2 Diatoms.....	22
3.2.1 Morphology.....	22
3.2.2 Classification.....	24
3.2.3 Ecological preferences	25
3.2.4 Application of diatoms in scientific research	26
3.3 Scientific settings.....	26
4. MATERIALS AND METHODS	29
4.1. Data collection.....	29
4.1.1. Sampling of sediment cores (material).....	29
4.1.2 Preparation of smear slides.....	30
4.1.3. Diatom counting.....	31
4.2. Data analysis.....	33
4.2.1 Data processing	33
4.2.2 Diatom-based dating	35
4.2.3 Analysis of major changes.....	36
5. RESULTS	37
5.1. General description of both sediment cores.....	37
5.2. Dating based on the relationship between precipitation and the relative abundance of freshwater diatoms	38
5.3. Dating based on the relationship between temperature and the relative abundance of <i>Paralia sulcata</i>	40
5.4. Major changes of the freshwater diatom compositions in both sediment cores.....	42
5.5. Major changes in the marine diatom compositions in both sediment cores.....	45
5.6. Major results of the correlation test	48
5.7. Major changes of common and abundant diatoms in both cores	51
5.8. Table of the morphology, classification, and ecological preferences of common and abundant diatoms	57

6. DISCUSSION	62
6.1. Reliability of diatom-based dating methods	62
6.2. Causes of changes in the freshwater planktonic diatom compositions	63
6.3. Causes of changes in the freshwater benthic diatom compositions	64
6.4. Causes of changes in the marine planktonic diatom compositions	65
6.5. Causes of changes in the marine benthic diatom compositions	67
6.6. Differences in the environmental setting between the Inner and Outer Lærdalsfjord	68
7. CONCLUSION.....	70
8. REFERENCE.....	71
9. APPENDIX.....	79
Appendix 1. Diatom counting result of the smear slides from the core MF2022-2 (raw data).....	79
Appendix 2. Diatom counting result of the smear slides from the core MF2022-3 (raw data).....	80
Appendix 3. The relative abundances (in % of total diatoms) of each diatom genus and each category in the core MF2022-2 and their mean occurrence	81
Appendix 4. The relative abundances (in % of total diatoms) of each diatom genus and each category in the core MF2022-3 and their mean occurrence	82
Appendix 5. X-Y scatter graphs of the relative abundance of each category and each diatom genus (in % of total diatoms) in the core MF2022-2	83
Appendix 6. X-Y scatter graphs of the relative abundance of each category and each diatom genus (in % of total diatoms) in the core MF2022-3	84
Appendix 7. Historical annual precipitation records between 1896 and 2022 from the Maristova meteorological station	85
Appendix 8. Historical annual average temperature records, the data from the meteorological stations in Lærdal, Lærdal/Tønjum, Lærdal/Moldo, and Lærdal IV	86
Appendix 9. Results of the correlation test in the core MF2022-2, red numbers indicate the absolute values of correlation coefficients (r) being ≥ 0.44 (Howarth & Sinding-Larsen, 1983), grey highlighted lines indicate the correlation between different genus and subcategories (e.g. total marine planktonic diatoms).....	87
Appendix 10. Results of the correlation test in the core MF2022-3, red numbers indicate the absolute values of correlation coefficients (r) being ≥ 0.44 (Howarth & Sinding-Larsen, 1983), grey highlighted lines indicate the correlation between different genus and subcategories (e.g. total marine planktonic diatoms).....	87

List of Figures

Figure 1. a). Location of Sognefjord b). Location of Lærdalsfjord c). Locations of Inner and Outer Lærdalsfjord, Lærdal Tunnel, River Lærdalselv and Erdalselv, Mountain Grånosi, Såta, and Vetanosi, the delta, two hydropower plants and two measuring stations (White dot lines indicate the main road E16).	11
Figure 2. Bathymetry profile of the Lærdalsfjord, and its depth profile with depth curves of 50m, 100m, 200m, 400m, 600m and 800m below sea level (Norgeskart, n.d.). Red letters (A, B, C, D) indicate the transect used for reconstruction of bathymetry profile.	15
Figure 3. Three vertical layers (brackish water, intermediate layer, basin water) of a Norwegian fjord, and basin circulation principle (Aksnes et al., 2019). Dissolved oxygen concentrations in basin water and in ocean water are shown as O_B and O_S respectively.	16
Figure 4. Salinity, temperature, density, and oxygen values of the Inner and Outer Lærdalsfjord in September 2022, vertical layers (brackish water, intermediate layer, basin water) in Inner and Outer Lærdalsfjord (No basin water layer in the Outer Lærdalsfjord). The red solid line is used for comparison at 50m water depth between the Inner and Outer Lærdalsfjord.	17
Figure 5. Oxygen levels in different water depths in Inner and Outer Lærdalsfjord measured in September 2022 with classification standards set by the European Environmental Agency (2022)	18
Figure 6. Historical records of oxygen concentration with water in Inner and Outer Lærdalsfjord in 1987, 2006 and 2022 (Johannessen & Lønning, 1988; Heggøy et al., 2007).	18
Figure 7. Historical temperature records in the Outer Lærdalsfjord at 10m water depth (blue line) and at 50m water depth (yellow line) and that in the Inner Lærdalsfjord at 10m water depth (blue line) and 20m water depth (green line) during the period between 1968 and 2022 (Torbjørn Dale 2023, personal communication).	19
Figure 8. (a). Annual average temperature records from 1870 to 2022 in Lærdal (Meteorologisk institutt, 2022b). (b). Annual average precipitation records from 1896 to 2022 in Maristova meteorological station (Meteorologisk institutt, 2022b).	20
Figure 9. River regulation of Borgund and Stuvane hydropower plants (hydropower plants are marked with two triangles, the regulated river flow is marked by solid red lines, Sælthun and Stuvane measuring stations are marked with two dots).	21
Figure 10. Differences between natural delta in Lærdal in 1961 and human-built delta in 2017 (Klamer, 2017) (delta is marked with red dot lines).	21
Figure 11. Girdle view (a) and valve view (b) of a marine benthic diatom, <i>Achnanthes brevipes</i> Agardh, its frustule consists of an epitheca, a hypotheca and girdle bands (Matthias Paetzel 2023, personal communication).	23
Figure 12. A Scanning Electron Microscope (SEM) Image of <i>Cavinula cocconeiformis</i> with sternum, raphe, central nodule, and striae (Otu & Spaulding,2011).....	24
Figure 13. Example of diatom classification based on the CMB (Coscinodiscophyceae (marked in yellow), Mediophyceae (marked in green) and Bacillariophyceae (marked in blue)) hypothesis (Theriot et al., 2009). ...	25

Figure 14. Bathymetry profile of the Inner Lærdalsfjord (Station 1) and the Outer Lærdalsfjord (Station 2). Sampling stations 1 and 2 marked with red numbers. Red letters (A, B, C, D) indicate the transect used for the reconstruction of the bathymetry.	29
Figure 15. (a) A collection of smear slides for a whole sediment core. (b) A single smear slide with a label showing the sediment core number and the core depth.	31
Figure 16. Different diatom valves:(1) <i>Achnanthes</i> (2) <i>Fragilaria pulchella</i> (3) <i>Caloneis</i> (4) <i>Thalassiosira nordenskiöldii</i> (5) <i>Skeletonema costatum</i> (6) <i>Cymbella</i> (7) <i>Eunotia</i> (8) <i>Tabellaria flocculosa</i> (9) <i>Rhoicosphenia</i> (10) <i>Nitzschia</i> (Smith, 1853).....	32
Figure 17. Sediment core MF2022-2 from the Inner Lærdalsfjord and its layers with different colours and structures.....	37
Figure 18. Sediment core MF2022-3 from the Outer Lærdalsfjord and its layers with different colours and structures.....	38
Figure 19. Dating result of core MF2022-2 from the Inner and core MF2022-3 from the Outer Lærdalsfjord based on the relationship between total freshwater diatoms and precipitation levels until 1969(except for 1936 in the Outer Lærdalsfjord).	39
Figure 20. Dating result of core MF2022-2 from the Inner Lærdalsfjord based on the relationship between the relative abundance of <i>Paralia sulcata</i> and temperature level until 1973 (the part before 1973 is highlighted in grey in both graphs).....	41
Figure 21. Dating result of core MF2022-2 from the Outer Lærdalsfjord based on the relationship between the relative abundance of <i>Paralia sulcata</i> and temperature level until 1973 (the part before 1973 is highlighted in grey in both graphs).....	42
Figure 22. The relative abundances of total freshwater diatoms, freshwater planktonic diatoms, and freshwater benthic diatoms in core MF2022-2 from the Inner Lærdalsfjord presented versus depths.....	43
Figure 23. The relative abundances of total freshwater diatoms, freshwater planktonic diatoms, and freshwater benthic diatoms in core MF2022-2 from the Inner Lærdalsfjord presented versus time (part before 1969 without certain dating results is highlighted in grey).....	43
Figure 24. The relative abundances of total freshwater diatoms, freshwater planktonic diatoms, freshwater benthic diatoms in the core MF2022-3 from the Outer Lærdalsfjord presented versus sediment depth.	44
Figure 25. The relative abundances of total freshwater diatoms, freshwater planktonic diatoms, freshwater benthic diatoms in the core MF2022-3 from the Outer Lærdalsfjord presented versus time (parts before 1969 without certain dating results are highlighted in grey).	44
Figure 26. The relative abundances of total marine diatoms, marine planktonic diatoms, and marine benthic diatoms in core MF2022-2 from the Inner Lærdalsfjord presented versus sediment depth.....	45
Figure 27. The relative abundances of total marine diatoms, marine planktonic diatoms, and marine benthic diatoms in core MF2022-2 from the Inner Lærdalsfjord presented versus time (parts before 1969 without certain dating results are highlighted in grey).	46
Figure 28. The relative abundances of total marine diatoms, marine planktonic diatoms, and marine benthic diatoms in core MF2022-3 from the Outer Lærdalsfjord presented versus sediment depth.	47

Figure 29. The relative abundances of total marine diatoms, marine planktonic diatoms, and marine benthic diatoms in core MF2022-3 from the Outer Lærdalsfjord presented versus time (parts before 1969 without certain dating results are highlighted in grey).	47
Figure 30. X-Y scatter graphs of the relative abundances of major freshwater planktonic diatom genus, <i>Eunotia</i> sp. and <i>Tabellaria flocculosa</i> , presented versus sediment depths, in core MF2022-2 from the Inner Lærdalsfjord	51
Figure 31. X-Y scatter graphs of the relative abundances of major freshwater planktonic diatoms, <i>Eunotia</i> sp. and <i>Tabellaria flocculosa</i> , presented versus time, in core MF2022-2 (part before 1969 without certain dating results is highlighted in grey).	52
Figure 32. X-Y scatter graphs of the relative abundances of major freshwater planktonic diatom genus, <i>Eunotia</i> sp., <i>Tabellaria flocculosa</i> , presented versus, in core MF2022-3 from the Outer Lærdalsfjord.....	52
Figure 33. X-Y scatter graphs of the relative abundances of major freshwater planktonic diatoms, <i>Eunotia</i> sp. and <i>Tabellaria flocculosa</i> , presented versus time, in core MF2022-3 (part before 1969 without certain dating results is highlighted in grey).	53
Figure 34. X-Y scatter graphs of the relative abundance of major freshwater benthic diatom, <i>Mastogloia elliptica</i> , presented versus sediment depth, in core MF2022-2 and core MF2022-3.	53
Figure 35. X-Y scatter graphs of the relative abundance of major freshwater benthic diatom, <i>Mastogloia elliptica</i> , presented versus time, in core MF2022-2 and core MF2022-3 (part before 1969 without certain dating results is highlighted in grey).	54
Figure 36. X-Y scatter graphs of the relative abundances of major marine planktonic diatom genus, <i>Chaetoceros</i> sp. and <i>Thalassiosira nordenskiöldii</i> , presented versus sediment depths, in core MF2022-2 from the Inner Lærdalsfjord.	54
Figure 37. X-Y scatter graphs of the relative abundances of major marine planktonic diatom genus, <i>Chaetoceros</i> sp. and <i>Thalassiosira nordenskiöldii</i> , presented versus time, in core MF2022-2 (parts before 1969 without certain dating results are highlighted in grey).....	55
Figure 38. X-Y scatter graphs of the relative abundances of major marine planktonic diatom genus, <i>Chaetoceros</i> sp. and <i>Thalassiosira nordenskiöldii</i> , presented versus sediment depths, in core MF2022-3 from the Outer Lærdalsfjord.	56
Figure 39. X-Y scatter graphs of the relative abundances of major marine planktonic diatom genus, <i>Chaetoceros</i> sp. and <i>Thalassiosira nordenskiöldii</i> , presented versus time, in core MF2022-3 (parts before 1969 without certain dating results are highlighted in grey).....	56
Figure 40. X-Y scatter graphs of the relative abundance of major marine benthic diatom genus, <i>Paralia sulcata</i> , presented versus sediment depths, in core MF2022-2 and core MF2022-3 with trendlines and trendline equations.....	57
Figure 41. X-Y scatter graphs of the relative abundance of major marine benthic diatom genus, <i>Paralia sulcata</i> , presented versus time, in core MF2022-2 and core MF2022-3 (part before 1969 without certain dating results is highlighted in grey).	57
Figure 42. X-Y scatter graphs of total freshwater diatoms and <i>Paralia sulcata</i> presented versus time based on two dating results of the core MF2022-2 (Figure 24; Figure 25) (part before 1969 without certain dating results is highlighted in grey).....	63

Figure 43. X-Y scatter graphs of total freshwater diatoms and *Paralia sulcata* presented versus time based on two dating results of the core MF2022-3 (Figure 24; Figure 26) (part before 1969 without certain dating results is highlighted in grey)..... 63

Figure 44. The box model of the Lærdalsfjord, which shows similarities and differences in how the main external influential factors (the precipitation, the inflow of North Atlantic Oceanic Water, river runoff of the river Lærdalselv and the river Erdalselv) exert impacts on the diatom composition in the Inner and Outer Lærdalsfjord. The runoff of the river Lærdalselv is influenced by hydropower plants and loss of natural delta. 69

List of Tables

Table 1. Coordinates, water depth and sediment penetration (core length) of two sediment cores MF2022-2 (Station 1, Inner Lærdalsfjord) and MF2022-3 (Station 2, Outer Lærdalsfjord). 30

Table 2. Significant correlations in Core MF2022-2 with absolute value of correlation coefficient (r) of $r \geq 0,44$ (Howarth & Sinding-Larsen, 1983). Variable A and B refer to the two variables whose correlation coefficient is calculated. 49

Table 3. Significant correlations in Core MF2022-3 with absolute value of correlation coefficient (r) of $r \geq 0,44$ (Howarth & Sinding-Larsen, 1983). Variable A and B refer to the two variables whose correlation coefficient is calculated. 50

Table 4. Morphology, classification, and ecological preferences of the six common and abundant diatoms; read from left to right. Pictures without references are taken from the Lærdalsfjord smear slides.58-62

Abstract

Two sediment cores were retrieved from the oxic Inner and Outer Lærdalsfjord, Western Norway. The fossil diatom record of these cores was used to reconstruct environmental and climate change over the past 90 years, providing a basis for future ecosystem management of the Lærdalsfjord.

Two relationships have been observed between climate factors and the fossil diatom composition. These are (a) a positive relationship between precipitation levels and the relative abundance of total freshwater diatoms, and (b) a negative relationship between decreased nutrient upwelling driven by increasing temperatures and the relative abundance of the marine benthic diatom species *Paralia sulcata*. These two relationships have also been used to date the sediment cores.

The gradually decreasing sedimentation rates in the Inner Lærdalsfjord after the construction of a first hydropower plant at Borgund in 1974 and a second hydropower plant at Stuvane in 1988 indicate an impact of the two hydropower plants on the river flow pattern. This impact has also been observed in decreasing relative abundance of freshwater planktonic diatoms in the Inner Lærdalsfjord. The relatively stable sedimentation rates and stable relative abundance of freshwater planktonic diatoms in the Outer Lærdalsfjord suggest that the Outer Lærdalsfjord is impacted less by the changes in flow pattern of the partially regulated river Lærdalselv compared to the Inner Lærdalsfjord.

After the construction of the second hydropower plant in 1988 and the loss of the natural delta between 1995 and 2000, the already existing impact of hydropower plants on the resulting reduction in flow velocity of the river Lærdalselv has been enhanced. As a result, the low river flow velocity caused the reduction in nutrients transported out to the Inner and Outer Lærdalsfjord, which furthermore led to the decreasing relative abundance of marine planktonic diatoms in the Inner and Outer Lærdalsfjord after 1988. This enhanced effect has also been shown in an increase in the freshwater benthic diatoms in the Inner Lærdalsfjord and their decrease in the Outer Lærdalsfjord after 2000.

This thesis shows that fossil diatom records in recent (0-90 years) Lærdalsfjord sediments contain environmental signals and can help reconstruct environmental and climate change.

Acknowledgements

A huge heartfelt “thank you” to my supervisor in Norway, Matthias Paetzel, for his effort, and patience in supporting me during the fieldwork, the laboratory work and the writing of the thesis. He has invested a lot of time to help me with the diatom counting, the interpretation of diatom analysis results, the development of dating results, as well as the scientific writing. With his help, I have learned a lot of new knowledge and overcome many obstacles during these two semesters. I am really grateful for his help and for having such an inspiring supervisor when writing my thesis.

In addition, I would like to thank Sarah and Alicia, my laboratory partners, who spent a lot of time together with me in the laboratory during the diatom counting. Without their help, it would have been impossible for me to collect the diatom counting results within a reasonable time frame. I also want to thank all the students in the “From Mountain to Fjord” exchange program in 2022 for collecting and analysing data that was helpful for my thesis and for all the help during the fieldwork.

Last but not least, I would like to thank my supervisor in Germany, Stephan Stoll for his help in dealing with the formalities, his amazing ecology lectures, and the recommendation of this amazing exchange programme.

1. Introduction

Fjords are transition areas between land and ocean environments. They store around 18 Mt of organic carbon every year with an organic carbon burial rate per unit area being twice that of the global ocean average (Smith et al., 2015). As such, they are one of the most important ecosystems on earth (Bianchi et al., 2020). Considering their important role in the global ecosystem, there is no doubt that the health of fjord ecosystems should be ensured by taking necessary protection measures. One of the protection measures, the EU Water Framework Directive, has hence been implemented in Norwegian fjords. Its goal is to achieve good ecological and chemical conditions in all European aquatic ecosystems, including Norwegian fjords, by 2021, with a recently extended deadline of 2025 (European Commission, 2014). Good ecological and chemical conditions are defined in the EU Water Framework Directive as showing no or only slight deviations from the natural conditions under no anthropogenic pressures (European Commission, 2014). To achieve this goal in Norway, the ecological and chemical conditions of Norwegian fjords and aquatic ecosystems are monitored, and the relevant information is made available to the public in the database “Vann-nett.no” (Vann-nett.no, 2022).

The Lærdalsfjord is a southern side inlet of the Sognefjord in Western Norway (Figure 1a;1b). It is one of the Western Norwegian fjords whose chemical and ecological conditions are under monitoring of the EU Water Framework Directive. However, the data about chemical conditions and risk evaluation in the Lærdalsfjord is sparse. The most recent reports about the ecological conditions were published in 1988 and 2007 (Johannessen & Lønning, 1988; Heggøy et al., 2007).

Since the Lærdalsfjord is exposed to climate change of increasing temperature and precipitation level (Meteorologisk Institutt, 2022b) and potential environmental changes due to human activities (e.g., Johnsen & Golmen, 1992; Borgund kraftverk, 2021; Engineering.com, 2006), it is crucial to investigate and monitor its environmental conditions closely. In this thesis, special emphasis is put on potential environmental impacts of major human induced events, including the regulation of the river Lærdalselv by the Borgund hydropower plant built in 1974 and the Stuvane hydropower plant built in 1988 (Borgund kraftverk, 2021), and the Lærdal Tunnel building and following reconstruction of a human-built delta between 1995 and 2000 (Engineering.com, 2006) (Figure 1c).

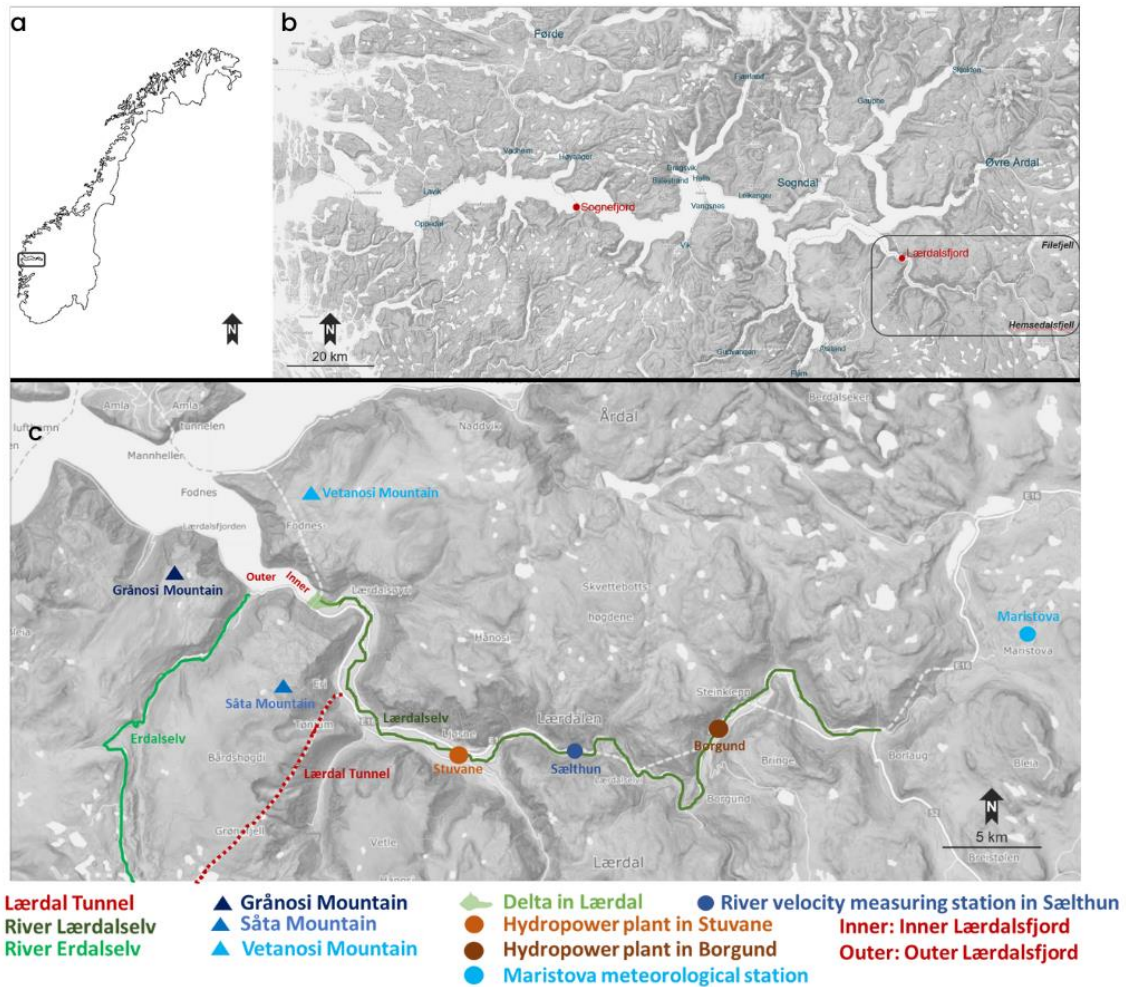


Figure 1. a). Location of Sognefjord b). Location of Lærdalsfjord c). Locations of Inner and Outer Lærdalsfjord, Lærdal Tunnel, River Lærdalselv and Erdalselv, Mountain Grånosi, Sâta, and Vetanosi, the delta, two hydropower plants and two measuring stations (White dot lines indicate the main road E16).

To provide the water management agencies with detailed up-to-date information about the hydrographical, ecological, and chemical conditions of the Lærdalsfjord, the Western Norway University of Applied Science (HVL) has conducted a marine environmental project in the Lærdalsfjord in 2022. As part of the project, this thesis aims to identify environmental signals from the fossil diatom records in sediment cores and to reconstruct past environmental and climate changes in the Lærdalsfjord based on the major changes in the diatom composition over the past 90 years.

Diatoms, which are used as biological indicators in this thesis, are single-celled microalgae with wide ecological niche breadth (Dixit et al., 1992). They are widely employed for environmental research due to their quick response to environmental and climate changes and their wide distribution (Dixit et al., 1992).

Most diatom-based environmental research focuses mainly on fossil marine diatom records, such as past environmental changes in the Koljö Fjord, Sweden (McQuoid & Nordberg, 2003a), paleoclimate reconstructions in the Skalafjord, Faroe Islands (Witon et al., 2006), and past hydrographic changes in the Igaliku Fjord, South Greenland (Jensen et al., 2004). However, Paetzel & Dale (2010) has pointed out the significance of freshwater diatoms as indicators of changes in river runoff and precipitation levels on land, when using fossil diatom records in fjord sediment of the Inner Sognefjord region in Western Norway to reconstruct past climate changes. Thus, this paper will focus on both marine and freshwater diatoms in sediment cores in the Lærdalsfjord and interpret their environmental signals.

In addition, Paetzel & Dale (2010) suggested a new relative dating method based on fossil freshwater diatoms to date their sediment cores retrieved from the glacially influenced Sogndalsfjord. Compared to absolute radioactive sediment dating methods, this relative diatom-based dating method is rather time- and cost-efficient. To explore the potential of fossil diatom records in sediment dating, this thesis will adopt the basic principle of this new dating method and examine the method in a different, non-glacially influenced fjord system, i.e., the Lærdalsfjord in Western Norway.

2. Objective

This thesis will present possibilities of utilizing fossil freshwater and marine diatom records to date sediment cores and using the dated record to investigate potential impacts of past climate changes and human activities on the ecosystem of the Lærdalsfjord. The major aim of this thesis is thus to shed light on the following main question: Do the diatoms in recent (0-90 years) sediments from the Lærdalsfjord hold signals of past natural and/or human-caused environmental and/or climate change?

To answer this main question, the three following objectives are formulated:

Objective 1

Can changes in the diatom composition be used to date two sediment cores from the Inner and Outer Lærdalsfjord?

A timescale needs to be obtained by dating the sediment cores for the detailed analysis of diatom composition changes. The timescale will help link a changing diatom composition to a certain time and help determine the possible causes of these changes. Instead of traditional dating methods like the recognition of ^{137}Cs from the Chernobyl accident (Paetzel & Schrader, 1991), or the ^{210}Pb dating method (Koide et al., 1972), a new relative dating method has been used by Paetzel & Dale (2010) to date young (0-20 years) fjord sediment cores. This new method is based on the positive relationship between precipitation level and the mineral matter and freshwater diatom content in fjord sediment cores. This thesis will utilize this dating method to provide a main timescale for the two sediment cores. An additional relationship between diatom composition changes and local air (and thus surface water) temperature will also be examined to suggest another diatom-based relative dating possibility.

Objective 2

Can changes in the freshwater diatom composition in the Inner and Outer Lærdalsfjord sediment cores be linked to past natural and/or human-caused environmental and/or climate change?

Certain environmental and climate changes may cause changes in the freshwater diatom composition. Thus, this thesis aims to explore the potential of freshwater diatoms as indicators for past natural and/or human-caused environmental and/or climate changes. Linkages between changes in the freshwater diatom compositions and past environmental and/or climate changes

will be constructed by analysing the causes of freshwater diatom composition changes. Additionally, despite the distance between the core locations in the Inner and Outer Lærdalsfjord being only around 1km (Figure 1), the Inner and Outer Lærdalsfjord may be impacted by environmental and/or climate changes in different ways due to their different surrounding environments. Thus, a comparison will be made between the freshwater diatom composition changes in the Inner and Outer Lærdalsfjord in this thesis.

Objective 3

Can changes in the marine diatom composition in the Inner and Outer Lærdalsfjord sediment cores be linked to past natural and/or human-caused environmental and/or climate change?

Since marine diatoms are one of the main primary producers in fjords (Dixit et al., 1992), changes in marine diatom concentration (in percentage of the total diatom concentration) can imply changes in primary productivity in a fjord. In addition, changes in certain environmental or climate factors, such as stratification, nutrient availability, and temperature (e.g., Paetzel & Dale 2010), may lead to changes in the relative abundance of certain marine diatom species with specific ecological tolerances. Hence, this thesis aims to examine the potential of marine diatoms as indicators for past natural and/or human-caused environmental and/or climate changes. Linkages between changes in the marine diatom compositions and past environmental and/or climate changes will be constructed by analysing the causes of marine diatom composition changes. In addition, since the Inner and Outer Lærdalsfjord may be impacted differently by environmental and climate changes due to their different surrounding environments (Figure 1), this thesis will compare the marine diatom composition changes in the Inner Lærdalsfjord with that in the Outer Lærdalsfjord.

3. Settings

To facilitate further diatom-based analysis, this chapter provides background information about the environmental settings of the Lærdalsfjord. These settings include the bathymetry profile, recent hydrographical and climate changes, and recent human activities in the area close to the Lærdalsfjord. In addition, detailed information about diatoms will be given, including their morphology, classification, ecological preferences, and their significance in environmental research. Furthermore, published literature about the Lærdalsfjord will be summarised in the scientific setting as a theoretical foundation for this thesis.

3.1. Environmental Settings

3.1.1 Bathymetry

The Lærdalsfjord, consisting of the Inner and the Outer Lærdalsfjord basin, is a NW-SE-oriented tributary of the Sognefjord in Western Norway (Figure 1). It is around 9 km long and around 700 to 2300 m wide and is located around 130 km inland east of the Norwegian coast (Norgeskart, n.d.). The Lærdalsfjord is surrounded by the 1408m high Såta mountain to the south, the 1209 m high Grånosi mountain to the southwest, and the 1134 m high Vetanosi mountain to the northeast (Figure 1).

The Inner Lærdalsfjord basin is connected to the Outer Lærdalsfjord basin by a 46 m deep sill (Figure 2). The Inner Lærdalsfjord basin has a maximum water depth of 55 m (Figure 2) and the Outer Lærdalsfjord basin has a water depth gradually increasing from the sill to 845 m over a distance of 7 km (Figure 2).

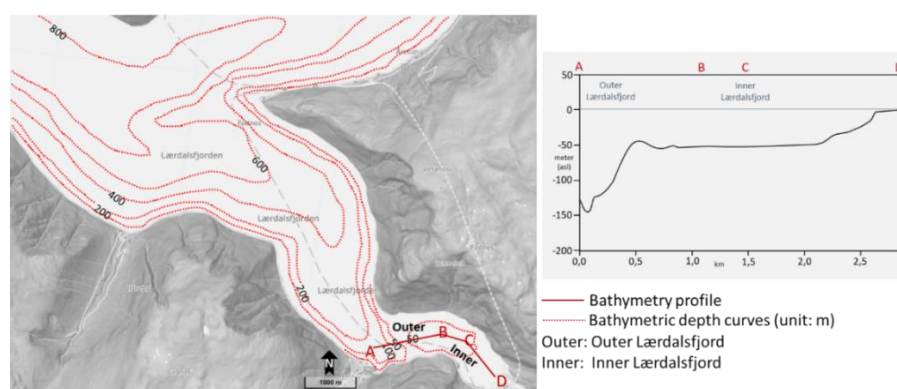


Figure 2. Bathymetry profile of the Lærdalsfjord, and its depth profile with depth curves of 50m, 100m, 200m, 400m, 600m and 800m below sea level (Norgeskart, n.d.). Red letters (A, B, C, D) indicate the transect used for reconstruction of bathymetry profile.

The river Lærdalselv is the major freshwater inlet into the eastern end of the Inner Lærdalsfjord (Figure 1). It runs into the Inner Lærdalsfjord by a reconstructed human-built delta (Figure 1; Figure 10). It gains its freshwater mainly by precipitation and melted snow since the river is not fed by glacial meltwater. In contrast, the Outer Lærdalsfjord receives freshwater supply from both the river Lærdalselv and the river Erdalselv (Figure 1).

3.1.2 Hydrography

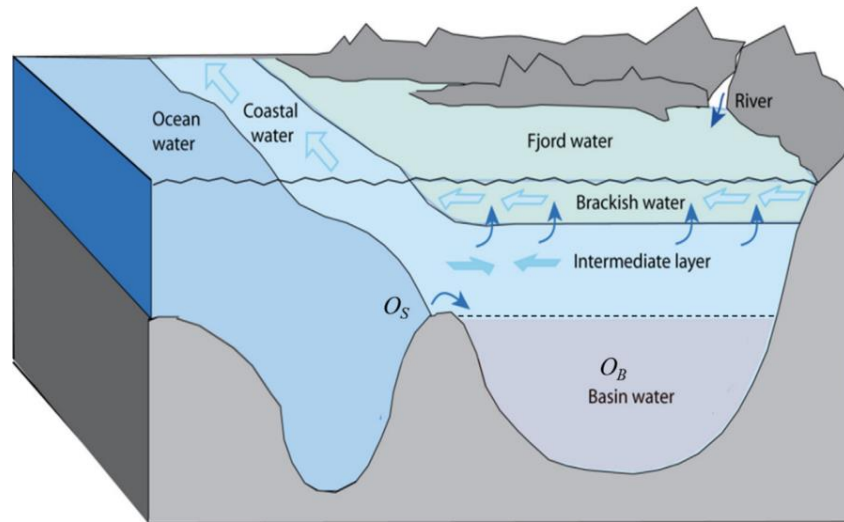


Figure 3. Three vertical layers (brackish water; intermediate layer; basin water) of a Norwegian fjord, and basin circulation principle (Aksnes et al., 2019). Dissolved oxygen concentrations in basin water and in ocean water are shown as O_B and O_S respectively.

The Lærdalsfjord contains three vertical water layers due to temperature differences and salinity caused density differences (Figure 3). The thin surface layer consists of brackish water with the lowest density. The intermediate layer is composed of Norwegian Coastal Water (Aksnes et al., 2019). Depending on the sill depth, the basin water contains either Norwegian Coastal Water or North Atlantic Water or a mixture of both (Aksnes et al., 2019).

Based on the data of CTD (Conductivity, Temperature, and Depth) measurements (Figure 4), the Inner Lærdalsfjord has a surface brackish layer from 0m to 9m with a salinity level lower than 28PSU and a density level lower than 20g/cm^3 . In contrast, the salinity and density of the intermediate layer from 9m to 46m increases continuously to a maximum level of 33PSU and 26g/cm^3 , respectively, at the water depth of 46m (Figure 4). The oxygen level of the basin water layer below 48m decreases to a minimum level of $3.9\text{mgO}_2/\text{l}$ (Figure 4).

Compared to the Inner Lærdalsfjord, the surface brackish layer in the Outer Lærdalsfjord is thinner and there is no basin water layer (Figure 4). The surface brackish layer ranges from 0m

to 8m with a salinity level lower than 28PSU and a density level lower than 23g/cm³ (Figure 4). The intermediate layer consists of a shallow intermediate layer from 8m to 46m and a deep intermediate layer below 46m water depth (Figure 4). The salinity and density of the water shows a first gradual increase in the shallow intermediate layer to 33PSU and 26g/cm³, followed by a second increase in the deep intermediate layer to 34PSU and 27g/cm³ (Figure 4). The oxygen level decreases gradually in the intermediate layer from 9mgO₂/l to 6.3mgO₂/l (Figure 4).

The basin water in the Inner Lærdalsfjord at the depth of 50m shows a slightly higher density of 27g/cm³ and a slightly lower temperature of 8°C compared to the Outer Lærdalsfjord in the same depth (Figure 4). This can be explained by a basin water exchange in the Inner Lærdalsfjord in the winter in 2021.

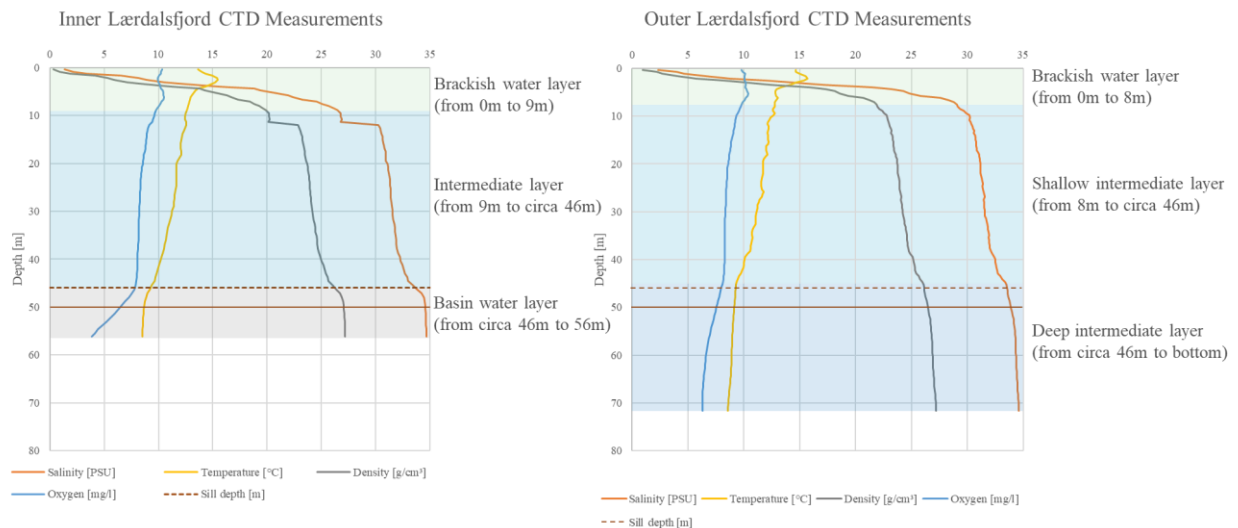


Figure 4. Salinity, temperature, density, and oxygen values of the Inner and Outer Lærdalsfjord in September 2022, vertical layers (brackish water; intermediate layer; basin water) in Inner and Outer Lærdalsfjord (No basin water layer in the Outer Lærdalsfjord). The red solid line is used for comparison at 50m water depth between the Inner and Outer Lærdalsfjord.

Regarding the oxygen level in the Lærdalsfjord, the dissolved oxygen concentration in the Inner Lærdalsfjord drops in the basin water layer from 8mgO₂/l to 3.9mgO₂/l, while the Outer Lærdalsfjord shows a good dissolved oxygen concentration with the lowest value of 6.3mgO₂/l based on the dissolved oxygen concentration standards (European Environmental Agency, 2022) (Figure 5).

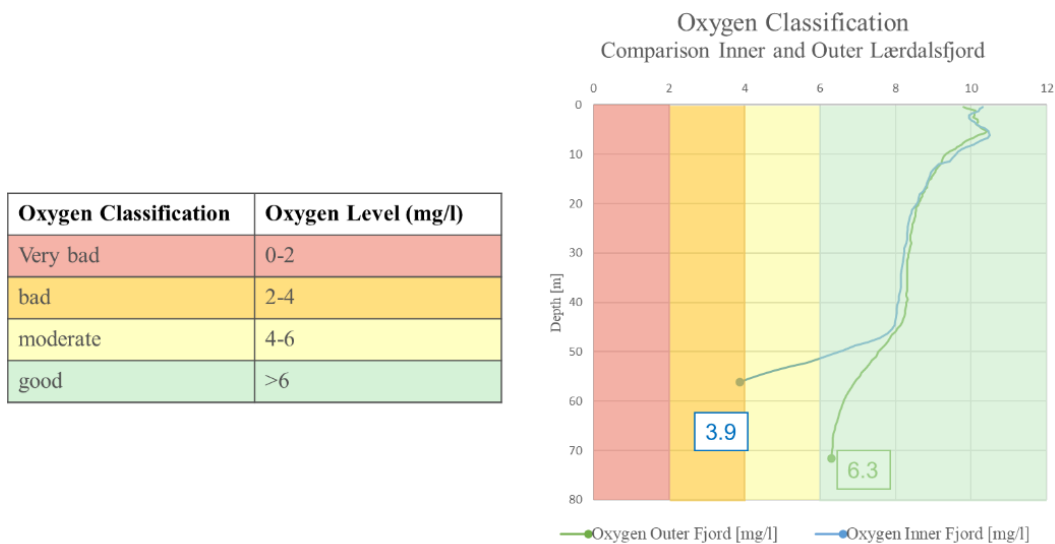


Figure 5. Oxygen levels in different water depths in Inner and Outer Lærdalsfjord measured in September 2022 with classification standards set by the European Environmental Agency (2022)

Compared to 1987 and 2006, the dissolved oxygen concentration in the Inner and Outer Lærdalsfjord in 2022 is lower (Figure 6). For example, the dissolved oxygen concentrations in the Inner and Outer Lærdalsfjord at the depth of 5m in 2022 are around 10.5mgO₂/l while the values in 1987 and 2006 are around 12mgO₂/l (Figure 6).

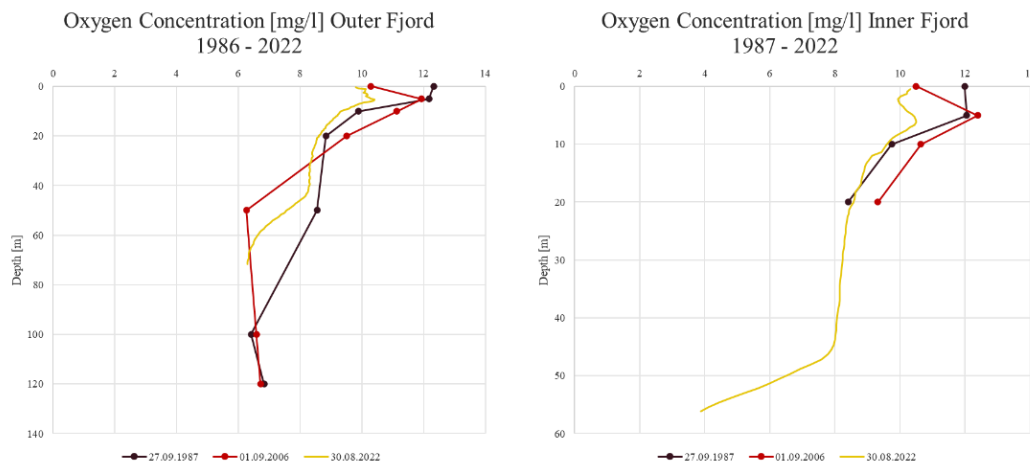


Figure 6. Historical records of oxygen concentration with water in Inner and Outer Lærdalsfjord in 1987, 2006 and 2022 (Johannessen & Lønning, 1988; Heggøy et al., 2007).

Considering that increasing temperature can lead to decrease in dissolved oxygen concentration (Blumberg & Di Toro, 1990), the low dissolved oxygen concentration in the Lærdalsfjord in 2022 can be caused by a gradual increase in water temperature in both Inner and Outer Lærdalsfjord since the 1970s (Figure 7). The water temperatures at water depth of 10m in the Inner and Outer Lærdalsfjord show an increase from 7°C in 1968 to 12.5°C in 2022 (Figure 7).

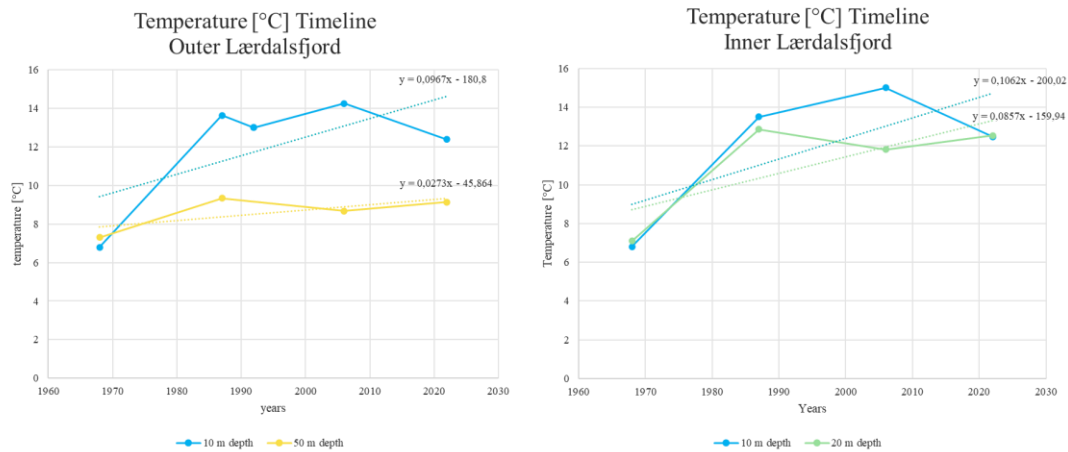


Figure 7. Historical temperature records in the Outer Lærdalsfjord at 10m water depth (blue line) and at 50m water depth (yellow line) and that in the Inner Lærdalsfjord at 10m water depth (blue line) and 20m water depth (green line) during the period between 1968 and 2022 (Torbjørn Dale 2023, personal communication).

Another possible reason for the low dissolved oxygen concentration in the Lærdalsfjord in 2022 can be the less frequent basin water circulation. Basin water circulation plays a key role in supplying new oxygen to the stagnant basin water with a low oxygen level (Aksnes et al., 2019). When the density of the Norwegian Coastal Water or North Atlantic Water at sill level outside the basin exceeds the density of the basin water, the coastal or oceanic oxygen rich water will flow into the basin and replace the stagnant basin water (Darelius, 2020). With the rising temperature and decreasing oceanic water density observed along the Norwegian coast, basin water circulation in the Norwegian fjords has become less frequent, which can furthermore lead to longer stratification periods in the Norwegian fjords and lower oxygen levels in the fjord basins (Darelius, 2020).

3.1.3. Climate change

The Lærdalsfjord is located within a generally mild and rainy marine climate zone (Meteorologisk institutt, 2022a). However, since the Lærdalsfjord is relatively far away from the coast, the temperature in winter can drop below 0°C and the average precipitation level of 750mm/year is rather moderate compared to the coastal areas with an average precipitation level of over 3,500mm/year (Meteorologisk institutt, 2022a).

The historical annual average temperature data from the meteorological stations Lærdal, Lærdal/Tønjum, Lærdal/Moldo, and Lærdal IV (Appendix 8) between the years 1870 and 2022 is used in this thesis to show the past air temperature changes in Lærdal (and hence surface water temperature changes in the Lærdalsfjord). The annual air temperature remains at a stable

level of 6.5°C on average between 1870 and 1920, followed by an increase to 7.5°C between 1920 and 1940 (Figure 8a). Between 1940 and 1980 the annual air temperature decreases to 5.5°C on average (Figure 8a). After 1980 the annual air temperature shows a continuous increase and reaches a current average level of around 7.5°C (Figure 8a).

To show the past changes in runoff of the river Lærdalselv into the Lærdalsfjord, the historical annual precipitation records between 1896 and 2022 from the Maristova meteorological station are used in this thesis (Appendix 7). The data from the Maristova meteorological station is chosen since this station is close to the main water source area of the river Lærdalselv. The annual precipitation level shows a gradual increase from 700mm on average in 1970 to 800mm on average in 2022 (Figure 8b). The continuous increase in both precipitation and temperature level after 1980 indicates a climate warming trend after 1980.

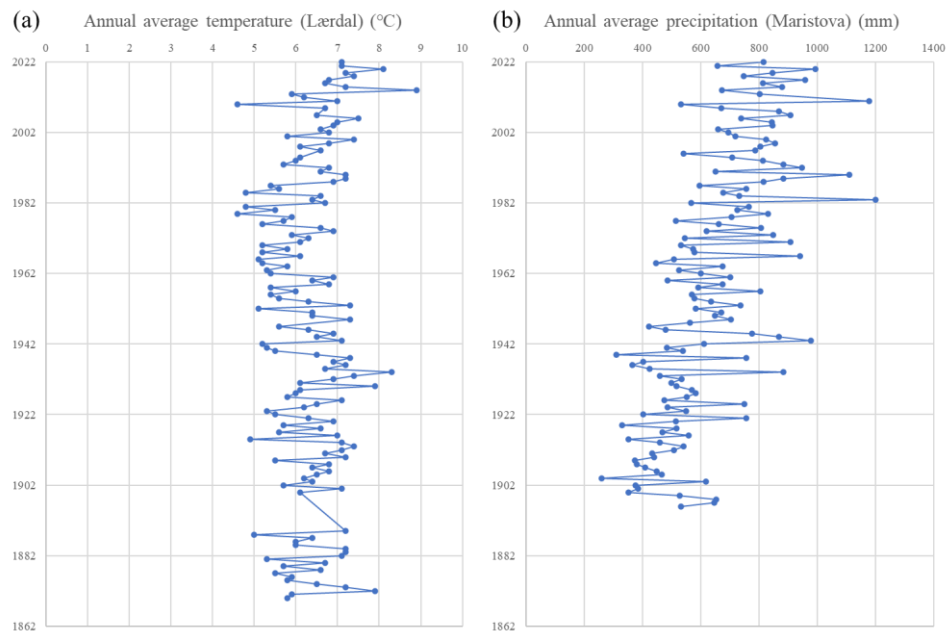


Figure 8. (a). Annual average temperature records from 1870 to 2022 in Lærdal (Meteorologisk institutt, 2022b). (b). Annual average precipitation records from 1896 to 2022 in Maristova meteorological station (Meteorologisk institutt, 2022b).

3.1.4 Recent human activities

The Lærdalsfjord is located close to the township of Lærdal with a population of 2117 people in January 2022 (SSBS API, 2022). Human activities in this region may exert an influence on the ecological and chemical conditions of the Lærdalsfjord. In the following section, the details of several major human activities and their potential environmental impacts will be illustrated.

The first hydropower plant with a capacity of 212MW was constructed in Borgund in 1974, while the second hydropower plant with a relatively low capacity of 19MW was built in Stuvane in 1988 (Borgund kraftverk, 2021). To facilitate hydropower-based energy production, the river flow in the river Lærdalselv is partially regulated although the river still maintains a natural seasonal flow pattern (Figure 9). Based on the data from the Sælthun measuring station (Figure 9) between 1961 and 2008 and the data from the Stuvane measuring station (Figure 9) between 1987 and 2008, the mean flow velocity in Sælthun has decreased by 20% from 24m³/s by 1974 to 19m³/s by 2008, while the mean flow velocity in Stuvane has increased by 30% from 22.4m³/s by 1988 to 30.7m³/s by 2008 (Torbjørn Dale 2023, personal communication).

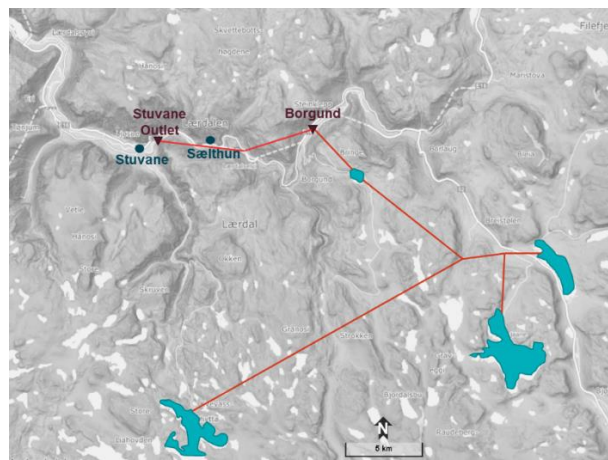


Figure 9. River regulation of Borgund and Stuvane hydropower plants (hydropower plants are marked with two triangles, the regulated river flow is marked by solid red lines, Sælthun and Stuvane measuring stations are marked with two dots).

In addition, to boost the local economy and attract more tourists, the original natural delta has been reconstructed with the rock masses from building of the Lærdal Tunnel between 1995 and 2000 (Engineering.com, 2006). As a result, 70% the natural delta has been lost and the equilibrium between the river and the natural ecosystem in the delta cease to exist after the loss of natural delta (Figure 10).

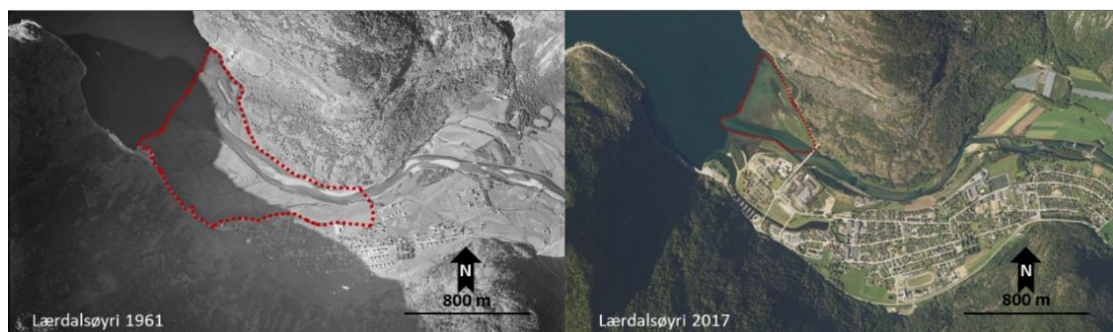


Figure 10. Differences between natural delta in Lærdal in 1961 and human-built delta in 2017 (Klamer, 2017) (delta is marked with red dot lines).

3.2 Diatoms

Diatoms are single-celled microalgae from the algal class Bacillariophyceae with sizes ranging from 1µm to over 1mm (Kociolek et al., 2023). As primary producers in aquatic ecosystems, they can be found in almost all marine, brackish, and freshwater ecosystems with sufficient light and nutrient conditions (Dixit et al., 1992). The Chlorophylls a and c and the golden-brown pigments contained in their cells allow them to perform photosynthesis efficiently (Kociolek et al., 2023). Apart from their role in the global cycling of oxygen and carbon, they are also crucial to the global cycling of silica since they need opaline silica ($\text{SiO}_2 \cdot 2\text{H}_2\text{O}$) for the cell walls of their frustules (Kociolek et al., 2023). Due to their resistant opaline cell walls, they are well-preserved even in sediments with a period of millions of years and thus are widely utilized for sediment analysis (Dixit et al., 1992). In the following section, the morphology, classification, ecological preferences, and application of diatoms in scientific research will be explained in detail to facilitate further diatom analysis.

3.2.1 Morphology

The opaline cell wall of diatoms, also known as frustule, fully encloses the protoplast and is located outside of the plasma membrane (Kotzsch et al., 2017). The frustule consists of two nanopatterned porous bio-silica building blocks, namely two valves resembling a pillbox bottom and lid, and one girdle band that connects the two valves (Kotzsch et al., 2017; Lewis, 1984; Mitra et al., 2018) (Figure 11). The lid or the older and bigger valve is called epitheca, while the bottom or the younger and smaller valve is called hypotheca (Mitra et al., 2018) (Figure 11). In most diatom cells, the valves are radially or bilaterally symmetrical and connected by a cylindrical girdle (Figure 11), while there are some exceptions with asymmetrical valves or bent girdle bands (Round et al., 1990). Since the frustule is divided into two building blocks, valves, and girdle bands, the morphology of each diatom cell can be determined from two principal orientations, namely the valve view and the girdle view, depending on if the girdle bands or the valves appear in the face view or are parallel to the line of sight (Round et al., 1990) (Figure 11). In the process of asexual reproduction via mitosis, the old epitheca develops a new hypotheca while remaining an epitheca (Lewis, 1984). In contrast, the old hypotheca develops a new hypotheca and becomes an epitheca itself (Lewis, 1984). The cell division in the process of asexual reproduction leads to a decrease in the average size of diatom cells since new valves must fit inside the old valves (Lewis, 1984). To compensate for the decrease in the size of cells due to asexual reproduction, diatoms can also

produce auxospores through sexual reproduction (Pérez-Martínez et al., 1992). Auxospore formation can be triggered by favourable environmental conditions like an increase in nutrient availability and by the high percentage of small-sized cells (Pérez-Martínez et al., 1992).

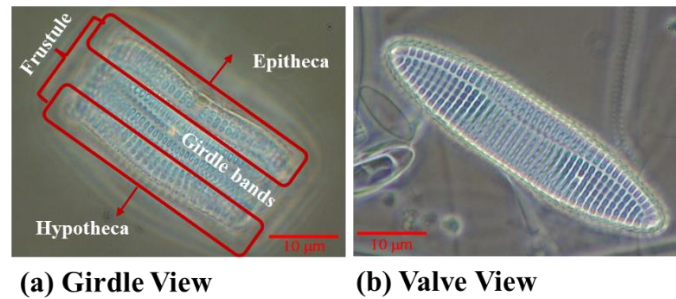


Figure 11. Girdle view (a) and valve view (b) of a marine benthic diatom, *Achnanthes brevipes* Agardh, its frustule consists of an epitheca, a hypotheca and girdle bands (Matthias Paetzl 2023, personal communication).

Despite of critics about this morphogenetic classification method, diatoms can be divided into centric and pennate diatoms in a descriptive sense based on the shape of valves and the pattern of the valve surface (Mitra et al., 2018; Medlin, 2009; Alverson et al., 2006). The centric diatoms with a discoid, solenoid, or cylindrical cell shape show radiating patterns from the centre (Mitra et al., 2018). The pennate diatoms with an elongated and fusiform, oval, sigmoid, or roughly circular shape, on the other hand, contain elongated valves, which are bilaterally symmetric along an apical axis, and a sternum, which is a longitudinal silica element of the valve of pennate diatoms (Mitra et al., 2018; Round et al., 1990). The sternum, known as the first silica deposited in the valve formation process, is positioned either along the apical axis (Figure 12), or along the valve margin as in the *Eunotia* species (Round et al., 1990).

In many raphid diatoms (i.e., diatoms with a raphe system), the sternum contains a raphe system (Round et al., 1990). A raphe system consists of one or two slits (i.e., an opening within diatom cell walls) and is positioned like the sternum either along the apical axis or along the valve margin (Cox, 2012). As shown in Figure 12, if there are two slits, the two branches of raphe can be separated by a central nodule, which is a silica thickening area in raphid diatoms (Cox, 2012; Round et al, 1990).

Another element of a diatom cell is a stria, or striae in the plural (Figure 12). A stria refers to a row of alveoli or a single alveolus when the alveolus spans from the apical axis to the valve margin (Ross et al., 1979). In centric diatoms, striae are positioned along the radius of a valve, while striae are positioned transapically in pennate diatoms (Figure 12) (Ross et al., 1979). Three features of striae are often used for diatom identification, including density, orientation,

and seriation (Ross et al., 1979). Density refers to the number of striae in 10 μm of circumference (Ross et al., 1979). There are three common types of orientation, namely radiate, parallel, or convergent (Ross et al., 1979). The seriation of striae can be uni-, bi-, or multiseriate (Ross et al., 1979).

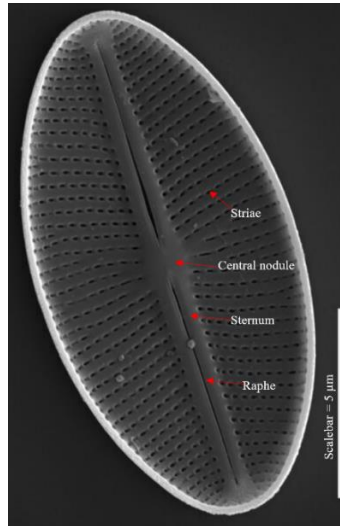


Figure 12. A Scanning Electron Microscope (SEM) Image of *Cavinula cocconeiformis* with sternum, raphe, central nodule, and striae (Otu & Spaulding, 2011).

3.2.2 Classification

Due to its wide distribution around the globe, diatoms have a high phylogenetic diversity and are the most species among autotrophic algae (Kociolek et al., 2023; Archibald, 2017). There are over 75,000 named taxa while more than 200,000 species may exist (Kociolek et al., 2023).

Since centric and araphid diatoms are not monophyletic, the morphological classification of diatoms (i.e., diatoms are divided into centric, araphid pennate and raphid pennate groups) shall not be employed for the taxa classification (Medlin, 2009). A new classification method is introduced by Medlin & Kaczmarek (2004), which takes both morphology and molecular phylogenetic relationships into consideration and reflects more accurately the evolution process of diatoms than the morphological classification method (Medlin & Desdevises, 2020). This diatom classification, also known as CMB (Coscinodiscophyceae, Mediophyceae and Bacillariophyceae) hypothesis, divides diatoms into three categories: Coscinodiscophyceae for radial centric diatoms, Mediophyceae for polar centric diatoms and radial *Thalassiosirales*, and Bacillariophyceae for pennate diatoms (Medlin & Desdevises, 2020) (Figure 13).

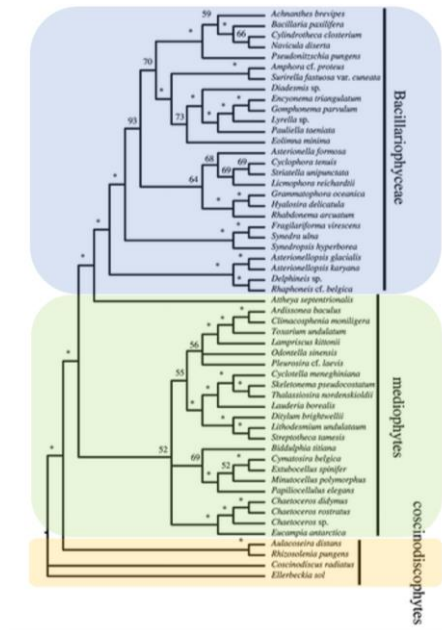


Figure 13. Example of diatom classification based on the CMB (*Coscinodiscophyceae* (marked in yellow), *Mediophyceae* (marked in green) and *Bacillariophyceae* (marked in blue)) hypothesis (Theriot et al., 2009).

3.2.3 Ecological preferences

Diatoms have a wide ecological niche breadth, especially in terms of temperature, salinity, trophic level, and pH level. Their distribution ranges from hot springs in the tropic regions to the ice in the arctic regions, from the most dilute freshwater to salty inland lakes with a salinity level higher than the open ocean, from the most oligotrophic environments to the outlets of sewage treatment plants with a high trophic level, and from acid mine drainage water with a very low pH level of 2.5 to an alkaline water column with a high pH level of above 10 (Kociolek et al., 2023).

Different diatom species possess different levels of ecological tolerance and show the maximum growth rates under different ecological conditions. As primary producers, light is one of the key ecological factors for their bloom. Additionally, given their opaline ($\text{SiO}_2 \cdot 2\text{H}_2\text{O}$) cell walls, the availability of certain nutrients, especially nitrogen (N), phosphorus (P), and silicium (Si), can also impact the growth rate of diatoms. Furthermore, marine diatoms can be more affected by the change in salinity level while freshwater diatoms are more sensitive to a change in pH level (Dixit et al., 1992).

Depending on the habitat preferences, diatoms can be divided into planktonic diatoms that spend most of their life cycle in the water column and benthic diatoms that live at the bottom of the water column. Planktonic diatoms live either as single cells or join each other in chains

to form colonies given their relatively small sizes (Kasim & Mukai, 2006). Benthic diatoms can be either free-living or attached to plants or rocks. Based on their living environments, benthic diatoms can be subdivided into epiphytic (attached to other plants), epipsammic (on sand), epipelagic (on the sediment), and epilithic (attached to rock surfaces) (Dixit et al., 1992).

3.2.4 Application of diatoms in scientific research

Diatoms have been widely employed as biological indicators for both short-term and long-term climate and environmental changes, such as global warming and cooling, eutrophication, acidification, or metal contamination (Dixit et al., 1992). There are various methods to utilize diatoms in environmental research.

Analysis of fossil diatom records in the sediment cores is one of the common methods for the analysis of long-term climate and/or environmental changes. For example, climate and environmental changes in the Skalafjord (Faroe Island) during the past 5400 calibrated ^{14}C years BP (Before Present) have been reconstructed based on the freshwater and marine diatom composition changes in sediment cores (Witton et al., 2006). In another example, Taylor et al. (2001) employed the temperature preferences of different diatom species to reconstruct the Holocene paleoclimate change in the Antarctic Peninsula.

The changes in the abundance, morphology and genetic features of certain diatom species can also be utilized to detect short-term environmental changes since the morphological and genetic features of diatom species may change under certain stress factors. For example, early aging in *Thalassiosira* sp. and *Skeletonema marinoi* is used to indicate a shortage of silicic acid and iron in the paper published by Lauritano et al. (2015). Another example is the monitoring of metal contamination situation in Lac Dufault (Québec, Canada) based on the diatom composition changes and morphological characteristics changes of certain species (Cattaneo et al., n.d.).

3.3 Scientific settings

Considering the significance of the ecosystem in the Lærdalsfjord, several environmental analyses have been carried out in this region during the past 40 years.

The first environmental research in the Lærdalsfjord was conducted in 1987 due to the rising public concerns about potential polluting influences of sewage discharge on the fjord ecosystem (Johannessen & Lønning, 1988). The hydrography, sediment, and benthic fauna in the Lærdalsfjord were examined to evaluate the impacts of sewage discharge (Johannessen &

Lønning, 1988). To alleviate potentially polluting environmental impacts, this research suggested to release sewage water into a deeper level of the fjord (Johannessen & Lønning, 1988).

The second environmental research was carried out in 1992 by the Norwegian Institute for Water Research (Norsk institutt for vannforskning) to examine the potential environmental impacts of the dumping of surplus masses from planned tunnel building on the fjord ecosystem (Johnsen & Golmen, 1992). The hydrographical changes, including temperature, salinity, density, and flow velocity, were monitored between 1980 and 1990 (Johnsen & Golmen, 1992). This environmental investigation has concluded that the overall negative environmental impact is rather insignificant (Johnsen & Golmen, 1992). However, since the released tunnel masses may affect benthic flora and fauna and may change the turbidity and eutrophic level of the Lærdalsfjord, dumping in the summer (from May to August) was not recommended (Johnsen & Golmen, 1992).

A more recent marine biological investigation was conducted between August and September 2006 to examine the biological and chemical conditions of the Lærdalsfjord and to classify the environmental quality of the Lærdalsfjord based on the guidelines from the Norwegian Climate and Pollution Agency (Statens Forurensningstilsyn) (Heggøy et al., 2007). Various ecological factors, including temperature, salinity, density, oxygen content, turbidity, grain size of the sediment, macrofauna, macroalgae, and chemical pollutants, were investigated using the samples collected from chosen locations (Heggøy et al., 2007). This investigation concluded that no pollution is found in these locations, and the environmental quality of the Lærdalsfjord is good based on the definition of good ecological and chemical conditions set by the EU Water Framework Directive in 2014 (European Commission, 2014) (Heggøy et al., 2007).

Two most recent research in 2018 and 2020 aimed to reconstruct the flooding history in the area near the Lærdalsfjord by examining marine sediments cores collected from the Inner Lærdalsfjord (Gjerdingen, 2018; Haflidason, 2020). In these two papers, the sedimentation rates in the Lærdalsfjord were calculated, ranging from 0.25 cm/year to 0.33 cm/year over the last 1000 years (Gjerdingen, 2018; Haflidason, 2020). These ¹⁴C-based sedimentation rates provide benchmarks for the dating of sediment cores from the Lærdalsfjord.

Furthermore, the Western Norway University of Applied Science (HVL) has conducted a marine environmental project in the Lærdalsfjord in 2022. This marine environmental project investigated the ecological and chemical conditions of the Lærdalsfjord from the following

aspects: hydrography of the Lærdalsfjord and the Lærdalselv (the hydrographic data is shown in Figure 4, 5, 6 and 7), chemical pollution in the Lærdalsfjord and the river Lærdalselv, foraminifera, macroalgae, and sediment analysis (including analysis of particular matter, geochemistry and fossil diatom records).

The data of chemical conditions in the Lærdalsfjord and the Lærdalselv shows a moderate level of the PAH Anthracene in the Innermost part of the Inner Lærdalsfjord, a low to moderate level of Zinc in the river Lærdalselv and the Inner Lærdalsfjord basin, as well as a moderate to a high level of Tributyltin (TBT) in the river Lærdalselv and the Inner Lærdalsfjord. To improve the chemical conditions, the sources of TBT and other metal pollutants shall be investigated and mitigated (Matthias Paetzel 2023, *personal communication*).

Like diatoms, foraminifera are also widely utilized as biological indicators of environmental change due to their wide distribution, high abundance, and well-preserved conditions as fossil records. Foraminifera are hence used in the 2022 project to indicate historical environmental and climate changes, and the level of biodiversity in the Lærdalsfjord based on the requirement of the EU Water Framework Directive. In this foraminifera analysis, the high precipitation level during the period 1976-1993 was indicated by the increase in the abundance of foraminifera. This analysis also pointed out that the biodiversity in the Inner Lærdalsfjord is in a moderate level and needs to be improved in the future (Marianne Nilsen 2023, *personal communication*).

Another biological indicator, macroalgae, was also investigated with the help of an underwater drone. Based on the percentage of red, green, and opportunist algae, the shore index was calculated and the ecological condition of the Lærdalsfjord was determined as moderate. The underwater investigation also pointed out the need for further investigations into the ecological impacts of the trash dumped into the Lærdalsfjord, and the distribution of deepwater coral and sea pens. Since sea pens are sensitive to bad water quality and their habitats are vulnerable, protection measurements need to be taken (Marianne Nilsen 2023, *personal communication*).

Sediment cores collected from the Inner and Outer Lærdalsfjord were also analysed based on changes in grain size, mineral matter, organic matter content (Oppermann 2023, *in progress*), and changes in magnetic susceptibility and geochemistry (Hartmann 2023, *in progress*). The changes in geochemistry and particular matter have indicated the effect of changes in precipitation levels and the impacts of hydropower plants and dumping of tunnel masses. The fossil diatom record in these sediment cores will be analysed in this thesis.

4. Materials and Methods

In this chapter, the procedures of data collection and data analysis will be explained.

4.1. Data collection

The smear slide method of Rothwell (1989) will be utilized for the diatom analysis in this thesis. The data collection process consists of three steps, including sampling of sediment cores (material), preparation of smear slides and diatom counting.

4.1.1. Sampling of sediment cores (material)

On August 30th, 2022, two sediment cores with intact sediment-water interfaces were retrieved using a Niemistö (1974) corer at the sampling station 1 in the Inner Lærdalsfjord (Location 1 at 52.6m water depth; number 1 in Figure 19) and the sampling station 2 in the Outer Lærdalsfjord (Location 2 at 123m water depth; number 2 in Figure 19) (Table 1). The sediment core MF2022-2 from the Inner Lærdalsfjord is 23cm long while the core MF2022-3 from the Outer Lærdalsfjord is 28cm long (Table 1). After retrieving the two sediment cores, a general description of both cores was made based on visual inspections of structures, texture, and particulate matter and a colour estimation using the colour code of Munsell (1994).

Based on sedimentation rates obtained by Gjerdingen (2018) and Haflidason (2020), the two sediment cores consist of sediment deposited during the past around 90 years. Thus, the term “recent sediments” used in this thesis refers to sediments with a time span of about 90 years.

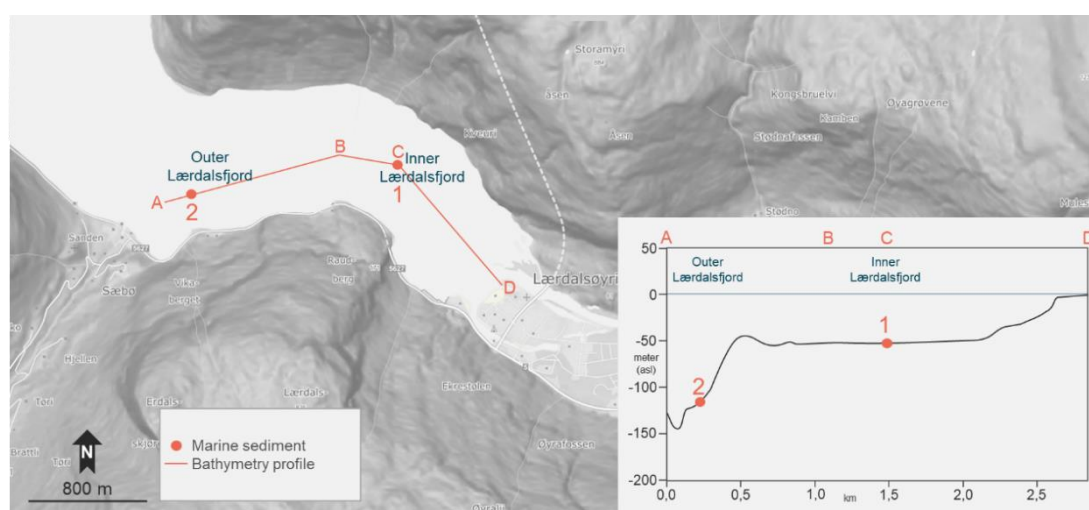


Figure 14. Bathymetry profile of the Inner Lærdalsfjord (Station 1) and the Outer Lærdalsfjord (Station 2). Sampling stations 1 and 2 marked with red numbers. Red letters (A, B, C, D) indicate the transect used for the reconstruction of the bathymetry.

Table 1. Coordinates, water depth and sediment penetration (core length) of two sediment cores MF2022-2 (Station 1, Inner Lærdalsfjord) and MF2022-3 (Station 2, Outer Lærdalsfjord).

Core name	Station name	Longitude (North)	Latitude (East)	Water depth	Sediment penetration (Core length)
MF2022-2	1	61°6'28.84228"N	7°27'9.30960"E	52.6 m	23.0 cm
MF2022-3	2	61°6'22.66596"N	7°25'41.53737"E	123.0 m	28.0 cm

4.1.2 Preparation of smear slides

Since this thesis is part of a marine environmental project and the whole project investigated not only fossil diatom records but a variety of sediment parameters, the parallel analysis of all parameters is essential. The parallel analysis of sediment parameters should preferably take place within the same material, in this case within smear slides (Paetzel & Dale, 2010). Hence, the smear slide method of Rothwell (1989) was utilized in this thesis. Another advantage of the smear slide method is its time- and cost-efficiency. The smear slide method requires only a small sample (<1 mm³), and the preparation and analysis of smear slides can be carried out in a relatively short time. In addition, the smear slide analysis is non-destructive and repeatable.

The smear slides were prepared in the following procedure:

- 1) The collected sediment cores were cut into two halves.
- 2) Since the sedimentation rate is around 0.25 to 0.33cm/year, a frequency of 0.5cm is chosen for subsampling. The sediment cores were then subsampled continuously at the frequency of 0.5cm. Each sediment subsample thus contains a sediment deposition of around 1 to 2 years on average.
- 3) The subsample was then homogenized with the help of a droplet of distilled water and a toothpick. The amount of a needle head (about 1mm³) of the homogenized subsample was then extracted and transferred onto a clean microscope cover glass. A droplet of distilled water was then used to disintegrate the needle head sample. To decrease the surface tension of the distilled water, a drop of Kodak Photo-Flo wetting agent was utilized. Then, the sample was smeared over the cover glass by a toothpick with an empty margin of 0.5cm on both short sides of the cover glass.
- 4) The liquid content in the smear slides was then evaporated on a heating plate with a temperature lower than 50°C.

- 5) Since the diatoms with opaline silica ($\text{SiO}_2 \cdot 2\text{H}_2\text{O}$) cell walls have a low refractive index of 1.43 like glass (Fuhrmann et al., 2004), a mounting agent, Naphrax (Brunel Microscopes Ltd) with a high refraction index of 1.73 was added onto the cover glass to make the finely silicified structures of the diatom frustules visible for identification. Since Naphrax is dissolved in highly carcinogenic and cancerogenic toluene, the whole process was carried out inside a ventilated fume hood cupboard.
- 6) A standard 75x26mm microscope slide was then mounted onto the cover glass and flipped over so that the cover glass was on the top.
- 7) The solvent of the mounting agent, toluene, was then evaporated by heating the slide on heating plate at a temperature between 100°C and 120°C. After the toluene was evaporated, the smear slide was cooled down and stored in a box. Due to the mounting agent, the sediment subsample inside the smear slide can remain in the same position and status for a long time. Examples of smear slides are shown in Figure 15.

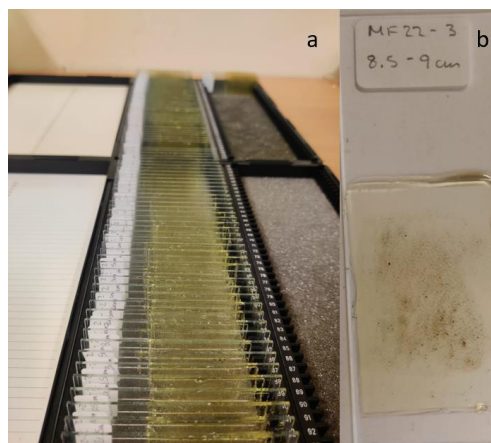


Figure 15. (a) A collection of smear slides for a whole sediment core. (b) A single smear slide with a label showing the sediment core number and the core depth.

4.1.3. Diatom counting

Despite the advantages of the smear slides method stated above, some concerns about this method shall not be neglected. One of the main concerns is that single diatoms could be overlapped by organic or mineral matter. Another concern is that correct diatom determination can be difficult due to the high similarities between certain species and genera. To address these concerns, the counting process followed the following rules:

- 1) A statistically robust number of at least 350 diatoms per smear slide, was counted.

- 2) Diatoms were only counted if more than 50% of their frustule was visible to prevent repeated counting of one single diatom.
- 3) The diatom counting proceeded continuously along three transects across each smear slide using a Leitz Aristoplan translucent light microscope with 40x magnification.
- 4) Most diatoms were determined at the genus level since diatoms within the same genus have similar ecological preferences (Fourtanier & Kociolek, 1999). Exceptions are *Paralia sulcata*, *Tabellaria flocculosa*, *Fragilaria pulchella*, and *Mastogloia elliptica*, *Thalassiosira nordenskiöldii* and *Skeletonema costatum*.
- 5) Diatoms were identified based on the morphology of the valves. Firstly, diatoms were classified into centric (Figure 16: 4) and pennate diatoms based on their general shape. They were further subdivided into diatoms with arcuate (Figure 16: 6,7,9), straight (Figure 16: 2,5), or sigmoid (Figure 16: 10) shapes by closer examination. Other features included the existence of a short sharply pointed tip (Figure 16: 3,7), the existence of a raphe (Figure 16: 1,2,3,6), the existence and shape of a central nodule (Figure 16: 1,2,3,6), three features of striae including density, orientation, and seriation (Figure 16: 1,2,3,6,7), as well as the formation of colonies (Figure 16: 5,8).
- 6) The final determination of the genus was made by comparing the main features of a diatom and the pictures of the diatom (examples of these pictures are shown in Figure 16). Although the pictures only show the most common appearance of a diatom and appearances of a diatom can vary depending on the circumstances, the clear features of the valves shown in the pictures ensured the reliability of the determination result.
- 7) Since percentages of single diatom genera among all the diatoms were later calculated during the data analysis, all the diatoms had to be counted regardless of if they could be clearly identified. Diatoms that could not be clearly identified were recorded as “others”.

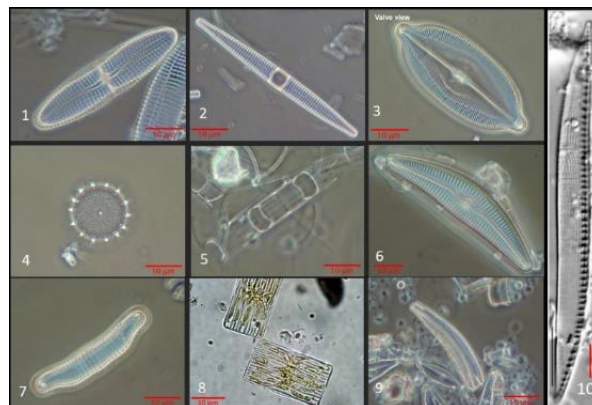


Figure 16. Different diatom valves:(1) *Achnanthes* (2) *Fragilaria pulchella* (3) *Caloneis* (4) *Thalassiosira nordenskiöldii* (5) *Skeletonema costatum* (6) *Cymbella* (7) *Eunotia* (8) *Tabellaria flocculosa* (9) *Rhoicosphenia* (10) *Nitzschia*(Smith, 1853).

4.2. Data analysis

Based on the data collected, the sediment cores were dated by utilizing the diatom-based dating method introduced by Paetzel & Dale (2010). Another dating possibility based on an additional relationship between air (and thus surface water) temperature and the relative abundance of certain diatom species will also be examined. With the available timescale of the sediment cores, the major diatom composition changes in both cores will be identified, compared, and linked to the possible past environmental and/or climate changes.

4.2.1 Data processing

Results of the diatom counting for core MF2022-2 and core MF2022-3 were firstly recorded in two excel tables shown in Appendix 1 and Appendix 2 respectively. Diatoms were grouped into five categories, namely “marine planktonic”, “freshwater planktonic”, “marine benthic”, “freshwater benthic” and “others” based on their habitat and salinity preferences.

The diatom species were divided into freshwater and marine diatoms since freshwater diatoms are transported from land into the fjord and can indicate changes in precipitation levels and runoffs, while marine diatoms grow in the fjord and can reflect environmental and climate (and consequently hydrographic) changes in the fjord. The category, brackish water diatoms, was not relevant in this thesis, since this thesis focuses on the fjord environment, while there are only a few real brackish water diatoms living in land-locked brackish water based on the definition of Snoeijs (2001) (i.e. brackish water diatoms are species that only exist in the transitional zones between freshwater and marine environments).

The marine diatom species were further subdivided into marine planktonic and marine benthic diatoms since the marine benthic diatoms are more sessile and receive more impacts of local environmental and climate changes compared to the marine planktonic diatoms (Cantonati et al., 2021). Freshwater diatoms were also subdivided into freshwater planktonic and freshwater benthic diatoms since freshwater benthic diatoms, whose transportation partially depends on river flow velocity (Stevenson, 1983), can indicate changes in river flow pattern.

Since the ornamentation and morphology of valves of most centric diatoms could not be clearly identified and most centric diatoms are marine planktonic species (Serôdio & Lavaud, 2020; Not et al., 2012), they were recorded as “round type diatoms” and assigned to the “marine planktonic” category. Since these “round type diatoms” may belong to different genera rather than one single genus, their relative abundances will not be specifically analysed. Only centric

diatoms that can be clearly determined as *Thalassiosira nordenskiöldii* were counted as “*Thalassiosira nordenskiöldii*”.

The relative abundances of each diatom genus and each category in the core MF2022-2 and the core MF2022-3 are presented in percentage of total diatom counts in two excel tables shown in Appendix 3 and Appendix 4, respectively.

X-Y scatter graphs of the relative abundance of each category and each diatom genus presented versus depth in the core MF2022-2 and the core MF2022-3 were then created in Excel and are shown in Appendix 5 and Appendix 6, respectively. To facilitate further comparison, the Y-axis of all graphs is set to the same scale, extending from 30 cm to 0 cm sediment depth. The interval of the data points in the graphs is set to 0.5 cm since both sediment cores were subsampled continuously at the frequency of 0.5 cm. For example, the value of a subsample of 10-10.5 cm sediment depth is shown at the point of 10.25 cm sediment depth. The X-axis of the graphs of total freshwater, total marine, freshwater planktonic, freshwater benthic, marine planktonic, and marine benthic diatoms is also set to the same scale, ranging from 0 to 70%.

Based on the relative abundances of each diatom genus and category, the common and the abundant diatom genera were then identified. A table that shows the pictures of these genera and their morphology and ecological preferences was then created to provide a theoretical basis for further diatom analysis. The criteria for the diatom relative abundance suggested by Scherer & Koc (1996) were utilized. Common diatom genera show a relative abundance between 5% and 20% while the relative amount of abundant diatom genera is between 20% and 60% (Scherer & Koc, 1996).

In addition, correlations between the different diatom genera and the five categories were tested by running the Pearson Correlation Test with a two-tailed significance. As the diatom relative abundances can be affected by various factors, a value between 0.44 and 1 (Howarth & Sinding-Larsen, 1983), instead of between 0.7 and 1 (e.g. Ratner, 2009), is defined as a positive correlation while a value between -0.44 and -1 indicates a negative correlation (Howarth & Sinding-Larsen, 1983). The values that are closer to 1 or -1 imply a stronger correlation than values less close to 1 or -1. The results of the correlation tests served as a basis for further selection and analysis of the diatom graphs.

Furthermore, for the diatom species, whose relative abundance shows a clear positive or negative relationship with the depth of sediment cores, a linear trendline with the equation and the R-squared (R^2) value was added on its X-Y scatter graphs presented versus depth. R-

squared (R^2) value implies the extent to which the changes in variable (a) the relative abundance of this diatom species is related to the changes in variable (b) depth in sediment cores. A higher R-squared (R^2) value indicates a stronger relationship and vice versa.

4.2.2 Diatom-based dating

A timescale of both sediment cores was developed prior to further data analysis by applying the relative dating method introduced by Paetzel & Dale (2010) based on the relationship between precipitation level and the relative abundance of total freshwater diatoms. The principle behind this method is that enhanced precipitation can lead to increased transportation of freshwater diatoms into the fjord (Paetzel & Dale, 2010).

Considering that the average sedimentation rates range from 0.25 to 0.33 cm/year (Gjerdingen, 2018; Haflidason, 2020) and the time span of two sediment cores is around 90 years, a graph of the average historical precipitation levels every three year from 1930 to 2020 was computed based on the data from the Maristova meteorological station (Meteorologisk institutt, 2022b) (Figure 19). Compared to the graph of annual average historical precipitation level (Figure 8), the frequent fluctuations within 0-3 years were smoothed in this graph and the peaks and low points can be more easily pointed out. This graph was then compared to the graphs of the relative abundances of total freshwater diatoms in both sediment cores.

Based on the principle of this dating method, a decrease in precipitation would coincide with a decrease in the relative abundance of total freshwater diatoms. Together with the already known average sedimentation rates (Gjerdingen, 2018; Haflidason, 2020), the low points in both graphs were matched with each other and sedimentation rates were then calculated between the low points through dividing the depth differences between low points in the freshwater diatom graph by the time differences between the corresponding low points in the precipitation graph.

Another alternative dating possibility was also examined in this thesis. This approach is based on a negative relationship between temperature levels and the relative abundance of the marine diatom species *Paralia sulcata* that prefers well-mixed water with nutrient upwelling (McQuoid & Nordberg, 2003b). The principle behind this method is that an increase in the air (and thus surface water) temperature level could lead to less frequent water circulation and a longer stratification period in water column (Aksnes et al., 2019), which could furthermore result in a decreasing concentration of *Paralia sulcata*.

To smoothen the data and make major temperature changes more visible, a graph of the average historical temperature levels every three year from 1930 to 2020 was computed based on the records in the Lærdal, Lærdal – Tønjum, Lærdal - Moldo and Lærdal Iv meteorological stations (Meteorologisk institutt, 2022b) (Figure 20; Figure 21). A comparison was then conducted between the temperature graph and the graphs of the relative abundance of *Paralia sulcata* in both sediment cores.

Based on the principle of this dating method, peaks in the graph of *Paralia sulcata* can be matched with low points in the temperature graph, while low points in the graph of *Paralia sulcata* can be associated with peaks in the temperature graph. Sedimentation rates were then calculated through dividing the depth differences between two peaks or low points in the graph of *Paralia sulcata* by the time differences between the corresponding low points or peaks in the temperature graph.

After obtaining the sedimentation rates and time scales based on these two relative diatom-based dating methods, the results were compared with each other to verify their reliability.

4.2.3 Analysis of major changes

Based on the diatom graphs and the correlation test results, major changes in the freshwater and marine diatom compositions were highlighted. These major changes were the focus of the further diatom analysis. To show the corresponding timing of these major changes, the depth scales of the diatom graphs were converted into time scales, using the available dating results based on the relative dating method introduced by Paetzel & Dale (2010).

Potential environmental and/or climate factors that led to these changes were then identified based on the knowledge about the ecological preferences of marine diatom species for the respective biotic and abiotic factors and the deposition patterns of freshwater diatom species, as well as the information about past climate changes and local human activities in the Lærdalsfjord.

In addition, a detailed comparison of the diatom composition changes between the Inner and Outer Lærdalsfjord was conducted to examine the similarities and differences of impacts of external influential factors (climate and environmental factors) on the Inner and Outer Lærdalsfjord. The observed differences and similarities will be shown in a simple box model of the Lærdalsfjord.

5. Results

This chapter will present all the major results obtained in the processes of data collection and data analysis, including a general description of both sediment cores, two sets of dating results based on two diatom-based relative dating methods, major changes in the marine and freshwater diatom compositions, major results of the correlation test between different diatom genera, major changes of common and abundant diatoms, as well as a table of the morphology and ecological preferences of the common and abundant diatoms.

5.1. General description of both sediment cores

The whole core MF2022-2 reveals blackish colour variations with a gradually upward changing structure from a layer with lamination to a patchy layer and then to a homogenous wet layer (Figure 17). It consists of a layer with lamination at the depths from 23 to 17 cm in black (2.5Y 2.5/1), a layer with lamination at the depths from 17 to 11 cm in black (5Y 25/1), a patchy layer at the depths from 11 to 3 cm in black (5Y 25/2), and a homogenous wet layer at the depths from 3 to 0 cm in black (2.5Y 2.5/1) (Figure 17).

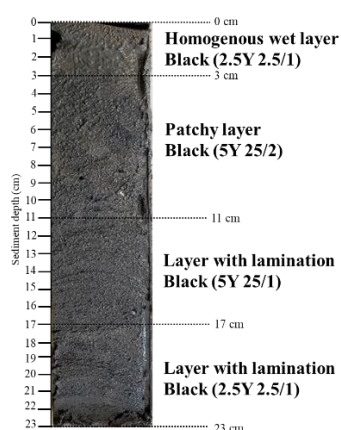


Figure 17. Sediment core MF2022-2 from the Inner Lærdalsfjord and its layers with different colours and structures.

The whole core MF2022-3 reveals a homogenous structure, darker in colour in the bottom and lighter in colour in the upper 23 cm (Figure 18). It consists of a wet layer at the depths from 28 to 26 cm in black (5Y 2.5/1), a dry layer at the depths from 26 to 23.5 cm in very dark grey (5Y 3/1), a wet layer at the depths from 23.5 to 23 cm in very dark grey (5Y 3/1), a dry layer at the depths from 23 to 3 cm in dark grey (5Y 3/2), and a wet layer at the depths from 3 to 0 cm in black (5Y 2.5/2) (Figure 18).

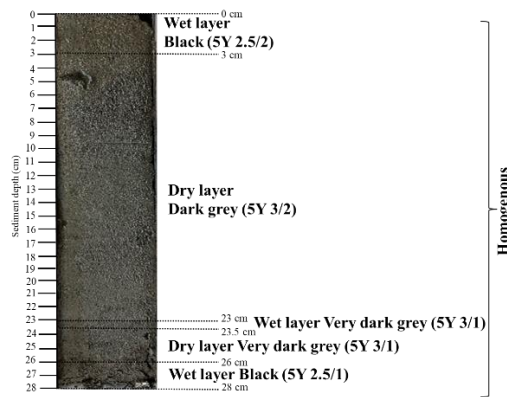


Figure 18. Sediment core MF2022-3 from the Outer Lærdalsfjord and its layers with different colours and structures.

5.2. Dating based on the relationship between precipitation and the relative abundance of freshwater diatoms

In core MF2022-2 from the Inner Lærdalsfjord, the relative abundance of total freshwater diatoms shows noticeable decreases at 15.75cm, 11.25cm, 6.75cm, and 1.75cm sediment depth (Figure 19). Based on the positive relationship between precipitation levels and the relative abundance of freshwater diatoms and the average sedimentation rates in the Lærdalsfjord (Gjerdingen, 2018; Hafliðason, 2020), these four low points in total freshwater diatom graph were matched with the low points in the precipitation graph in 1969, 1981, 1996 and 2014. Since the depth of 1.75cm was dated as 2014 and the average sedimentation rates range from 0.25 to 0.33cm/year (Gjerdingen, 2018; Hafliðason, 2020), the first point in the diatom graph of the Inner Lærdalsfjord may represent the year 2019 or 2020, instead of 2022. In other words, the surface might be lost in the core sampling process.

To ensure the reliability of the dating result, the peaks in the precipitation graph in 1972, 1984, 1990, 1999, 2005 and 2011 were also matched with the peaks in total freshwater diatom graph of the Inner Lærdalsfjord at the depths of 14.25cm, 10.25cm, 8.75cm, 5.25cm, 3.25cm, and 2.25cm correspondingly.

Based on the depth differences and the already known timescale at certain depths, the sedimentation rates of the core from the Inner Lærdalsfjord were calculated and are 0.38 cm/year from 1969 to 1981, 0.30cm/year from 1981 to 1996, and 0.27cm/year from 1996 to 2014. An example of the sedimentation rate calculation is as follows:

$$\text{Sedimentation rate} = (11.25\text{cm} - 6.75\text{cm}) / (1981 - 1969) \text{ year} = 0.375\text{cm/year (round up to 0.38cm/year)}$$

In core MF2022-3 from the Outer Lærdalsfjord, the relative abundance of total freshwater diatoms shows noticeable decreases at the depths of 27.25cm, 16.75cm, 13.25cm, 9.25cm, and 3.25cm (Figure 19). These five low points in the total freshwater diatom graph of the Outer Lærdalsfjord were matched with the low points in the precipitation graph in 1936, 1969, 1981, 1996 and 2014.

To make sure that the dating result is reasonable, the peaks in the precipitation graph in 1972, 1984, 1990, 1999, 2005 and 2011 were matched with the peaks in the total freshwater diatom graph of the Outer Lærdalsfjord at the depths of 15.25cm, 12.25cm, 10.75cm, 8.25cm, 6.75cm, and 4.25cm correspondingly. Since the precipitation level shows no remarkable increase after 2014 and between 2005 and 2011, the peaks in the total freshwater diatom graph of the Outer Lærdalsfjord at the depths of 2.25cm and 5.75cm were identified as enhanced deposition events of unknown causes.

Based on the same calculation method as shown above, the sedimentation rates of the core from the Outer Lærdalsfjord were calculated and are 0.32cm/year from 1936 to 1969, 0.29 cm/year from 1969 to 1981, 0.27cm/year from 1981 to 1996, 0.30cm/year from 1996 to 2014 and 0.31cm/year from 2014 to 2022. The deposition events at the depths of 2.25cm and 5.75cm were subtracted during the sedimentation rate calculation.

Since the dating for both sediment cores before 1969 is uncertain, matches between the precipitation graph and total freshwater graph were only conducted until 1969, except for a match between the low point in 1936 in the precipitation graph and the low point at the depth of 15.25cm in total freshwater diatom graph of the Outer Lærdalsfjord.

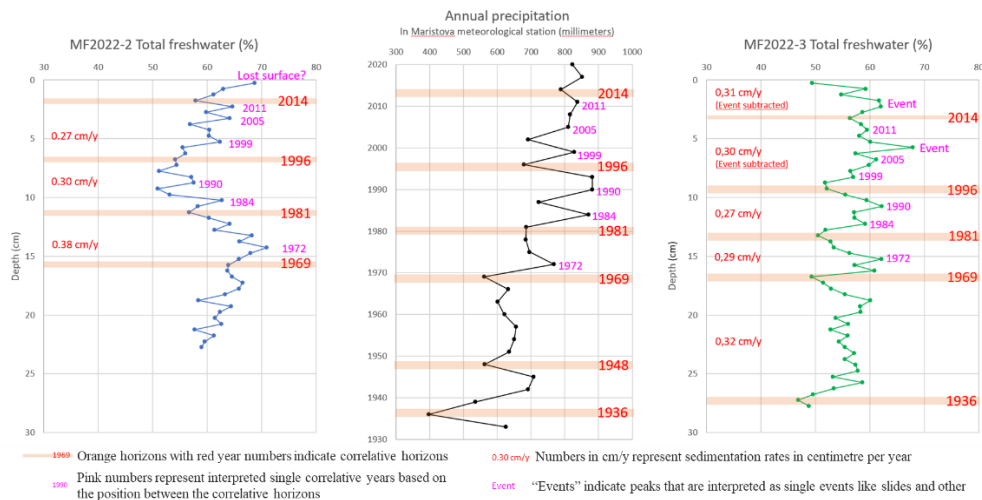


Figure 19. Dating result of core MF2022-2 from the Inner and core MF2022-3 from the Outer Lærdalsfjord based on the relationship between total freshwater diatoms and precipitation levels until 1969(except for 1936 in the Outer Lærdalsfjord).

5.3. Dating based on the relationship between temperature and the relative abundance of *Paralia sulcata*

The average annual temperature and the relative abundance of *Paralia sulcata* show an opposite pattern in the Inner and Outer Lærdalsfjord after 1973 in the temperature graph and at the sediment depth from 13.75cm to 0cm in the *Paralia sulcata* graph of the Inner Lærdalsfjord and at the sediment depth from 14.75cm to 0cm in the *Paralia sulcata* graph of the Outer Lærdalsfjord (Figure 20; Figure 21). Since this opposite pattern after 1973 is utilized to date the two sediment cores, timescales are developed until 1973 (Figure 20; Figure 21). The data points prior to 1973 fall into the grey shaded area of both figures.

In core MF2022-2 from the Inner Lærdalsfjord, *Paralia sulcata* shows significant decreases at the depths of 13.75cm, 1.75cm, and a noticeable increase in the depth of 6.75cm (Figure 20). Based on the negative relationship between the temperature level and relative abundance of *Paralia sulcata*, and the already known average sedimentation rates (Gjerdingen, 2018; Hafliðason, 2020), these three low points and one peak in the *Paralia sulcata* graph were matched with the three peaks and one low point in the temperature graph in 1973, 2013 and 1994. Since the depth of 1.75cm was dated to 2013 and the average sedimentation rates range from 0.25 to 0.33cm/year (Gjerdingen, 2018; Hafliðason, 2020), the first point in the *Paralia sulcata* graph of the Inner Lærdalsfjord may correspond to the year 2018 or 2019, instead of 2022. In other words, there was a surface loss in the core sampling process.

To ensure the reliability of the dating result, four peaks in the temperature graph in 1982, 1988, 1998, 2004 were also matched with the decreases in the *Paralia sulcata* graph of the Inner Lærdalsfjord at the depths of 11.25cm, 9.25cm, 5.75cm, and 3.25cm correspondingly (Figure 20). One low point in the temperature graph in 1979 was also matched with the peak in the *Paralia sulcata* graph at the sediment depths of 12.25cm correspondingly (Figure 20).

Based on the depth differences and the already known timescale of certain sediment depths, the sedimentation rates of the core from the Inner Lærdalsfjord were calculated and are 0.33cm/year from 1973 to 1994, and 0.26cm/year from 1994 to 2013. An example of the sedimentation rate calculation is as follows:

$$\text{Sedimentation rate} = (13.75\text{cm} - 6.75\text{cm}) / (1994 - 1973) \text{ year} = 0.33\text{cm/year (round up to 0.38cm/year)}$$

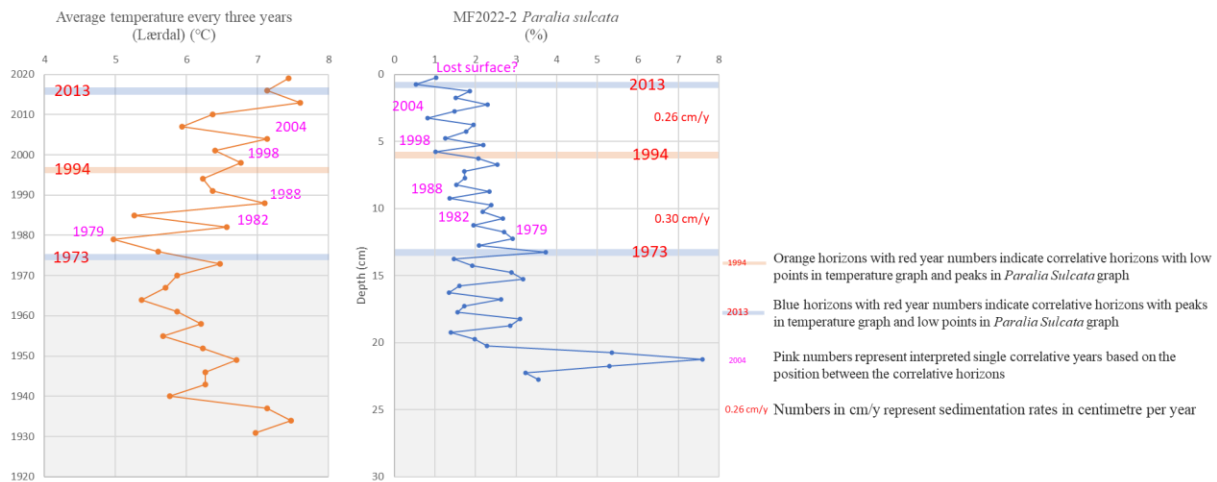


Figure 20. Dating result of core MF2022-2 from the Inner Lærdalsfjord based on the relationship between the relative abundance of *Paralia sulcata* and temperature level until 1973 (the part before 1973 is highlighted in grey in both graphs).

In core MF2022-3 from the Outer Lærdalsfjord, *Paralia sulcata* shows significant decreases at the sediment depths of 25.25cm, 15.25cm, and 2.75cm and a noticeable increase at the sediment depth of 8.75cm (Figure 21). Based on the available average sedimentation rates in the Lærdalsfjord (Gjerdingen, 2018; Hafliðason, 2020), these three low points and one peak in the *Paralia sulcata* graph were matched with the three peaks and one low point in the temperature graph of 1940, 1973, 2013 and 1994. To ensure the reliability of the dating result, four peaks in the temperature graph in 1982, 1988, 1998, 2004 were also matched with the decreases in the *Paralia sulcata* graph at the depths of 12.75cm, 11.75cm, 7.75cm, and 5.75cm correspondingly (Figure 21). Four low points in the temperature graph in 1979, 1985, 2001, 2007 were also matched with the peaks in the *Paralia sulcata* graph at the depths of 13.75cm, 12.25cm, 7.25cm, and 3.75cm (Figure 21).

Based on the depth differences and the already known timescale, the sedimentation rates of the core from the Outer Lærdalsfjord were calculated and are 0.33cm/year from 1940 to 1973, 0.31cm/year from 1973 to 1994, and 0.32cm/year from 1994 to 2013.

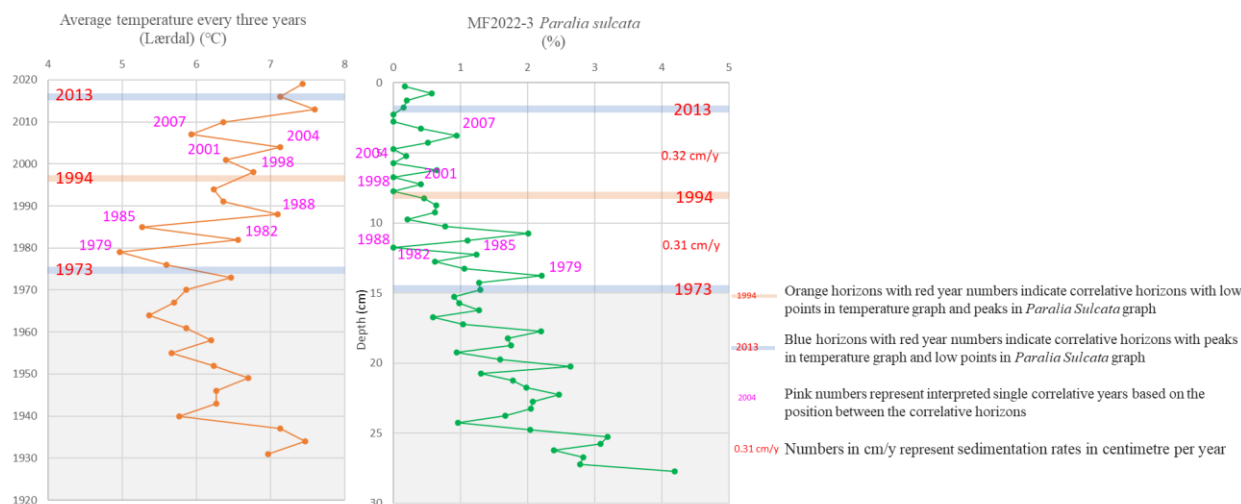


Figure 21. Dating result of core MF2022-2 from the Outer Lærdalsfjord based on the relationship between the relative abundance of *Paralia sulcata* and temperature level until 1973 (the part before 1973 is highlighted in grey in both graphs).

5.4. Major changes of the freshwater diatom compositions in both sediment cores

Since the total percentage of freshwater, marine and other diatoms in both sediment cores is 100% and the percentage of other diatom is very low ($\leq 10\%$), the relative abundances of total freshwater diatoms and total marine diatoms show an opposite pattern in both cores (Figure 22; Figure 24; Figure 26; Figure 28).

In core MF2022-2 from the Inner Lærdalsfjord, total freshwater diatoms account for more than 50% of the total diatoms except at the depths of 9.25cm and 7.75cm, which verifies the dominant position of freshwater diatoms (Figure 22). The changes of total freshwater diatoms are largely determined by the changes of freshwater planktonic diatoms, whose relative abundances range from 30% to 60% among all diatoms (Figure 22).

Freshwater planktonic diatoms showed a pronounced upward decrease between the depth of 14.25cm and 7.25cm from 1974 to 1995 and recovered to the original level gradually between the depth of 7.25cm and 5.75cm from 1995 to 2000 (Figure 22; Figure 23). Freshwater benthic diatoms showed a slight upward increase around the depth of 9.25cm in 1988, followed by a further upward increase around the depth of 5.75cm in the year 2000 (Figure 22; Figure 23). Its average percentage increased from around 10% to around 12% (Figure 22). Total freshwater diatoms follow the changing pattern of freshwater planktonic diatoms, namely decreasing from 1974 to 1995 and returning to the original level between 1995 and 2000 (Figure 23).

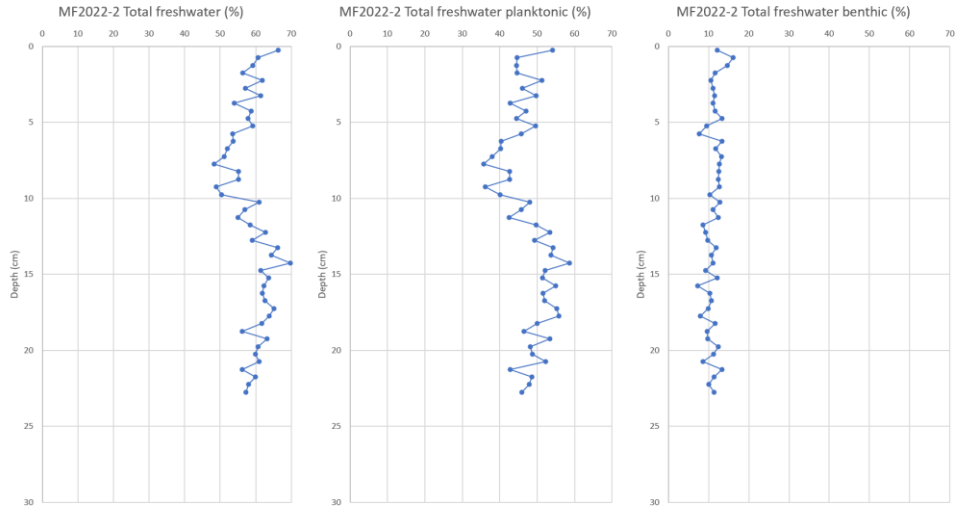


Figure 22. The relative abundances of total freshwater diatoms, freshwater planktonic diatoms, and freshwater benthic diatoms in core MF2022-2 from the Inner Lærdalsfjord presented versus depths.

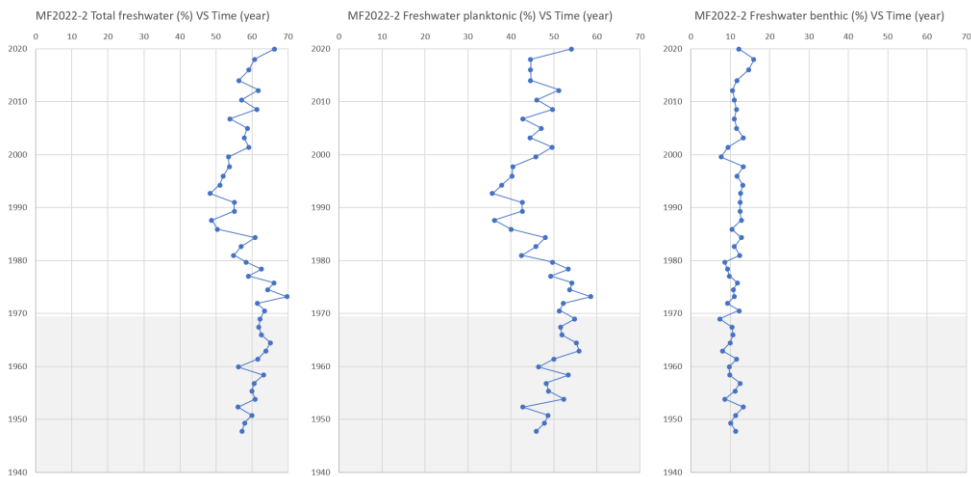


Figure 23. The relative abundances of total freshwater diatoms, freshwater planktonic diatoms, and freshwater benthic diatoms in core MF2022-2 from the Inner Lærdalsfjord presented versus time (part before 1969 without certain dating results is highlighted in grey).

In more than 80% of core MF2022-3 from the Outer Lærdalsfjord, total freshwater diatoms account for more than 50% (Figure 24), which shows the dominant position of freshwater diatoms in the total diatom composition. Freshwater planktonic diatoms with relative abundances ranging from 25% to 55% among all diatoms are in a dominant position among total freshwater diatoms (Figure 24).

Freshwater planktonic diatoms showed a noticeable upward increase at the depth of 7.75 cm in 2000 (Figure 24; Figure 25). Its average percentage increased from around 40% to around 45% (Figure 24). In contrast, freshwater benthic diatoms showed a slight upward decrease between

the depth of 7.75 cm and 0 cm during the period from the year 2000 to 2020 (Figure 24; Figure 25). Its average percentage dropped from around 15% to around 10% (Figure 24). Since the freshwater planktonic and benthic diatoms show an opposite pattern in the upper 5 cm, total freshwater diatoms remain at a relatively stable level across the whole sediment core with minor fluctuations (Figure 24; 25).

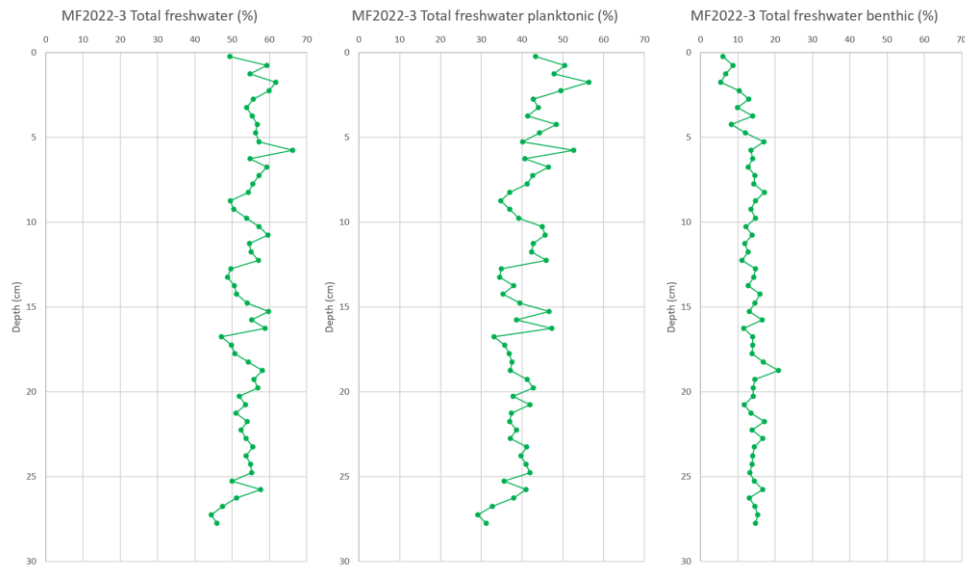


Figure 24. The relative abundances of total freshwater diatoms, freshwater planktonic diatoms, freshwater benthic diatoms in the core MF2022-3 from the Outer Lærdalsfjord presented versus sediment depth.

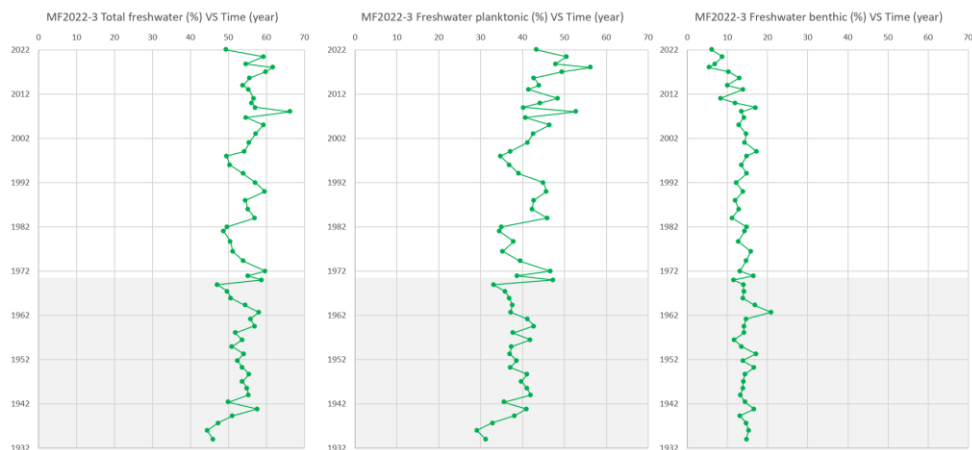


Figure 25. The relative abundances of total freshwater diatoms, freshwater planktonic diatoms, freshwater benthic diatoms in the core MF2022-3 from the Outer Lærdalsfjord presented versus time (parts before 1969 without certain dating results are highlighted in grey).

The changes in the freshwater diatom composition in both cores show pronounced differences. The relative abundance of freshwater planktonic diatoms in core MF2022-2 from the Inner Lærdalsfjord dropped between 1974 and 1995 and returned to a stable level around 2000, while

the relative abundance of freshwater planktonic diatoms in core MF2022-3 from the Outer Lærdalsfjord showed no noticeable changes between 1974 and 2000 and increased slightly after 2000 (Figure 23; Figure 25). In addition, the relative abundance of freshwater benthic diatoms in core MF2022-2 from the Inner Lærdalsfjord increased firstly after 1988 then after 2000, while their relative abundance in the core MF2022-3 from the Outer Lærdalsfjord reduced continuously after 2000 (Figure 23; Figure 25).

5.5. Major changes in the marine diatom compositions in both sediment cores

In core MF2022-2 from the Inner Lærdalsfjord, marine planktonic diatoms with relative abundances ranging from 20% to 50% are in a dominant position among all marine diatoms (Figure 26). Thus, the changes of total marine diatoms are proportionally more impacted by the changes of marine planktonic diatoms than by the changes of marine benthic diatoms.

Marine planktonic diatoms showed a significant increase between the depth of 14.25cm and 9.25cm from 1974 to 1988, followed by a gradual decrease between the depth of 9.25cm and 0cm from 1988 to 2020 (Figure 26; Figure 27). Marine benthic diatoms showed a gradual decrease across the whole core (Figure 26). Its average percentage decreased from around 9% to around 5% (Figure 26).

Total marine diatoms show the combined changes in both marine planktonic and marine benthic diatoms. Its relative abundance increased upward during the period from 1974 to 1988 and decreased upward continuously during the period from 1988 to 2020 (Figure 27).

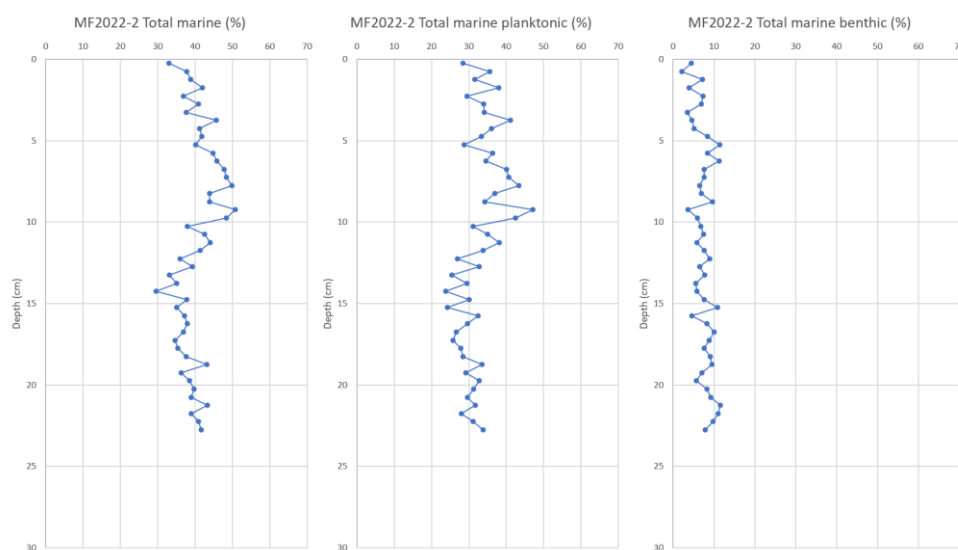


Figure 26. The relative abundances of total marine diatoms, marine planktonic diatoms, and marine benthic diatoms in core MF2022-2 from the Inner Lærdalsfjord presented versus sediment depth.

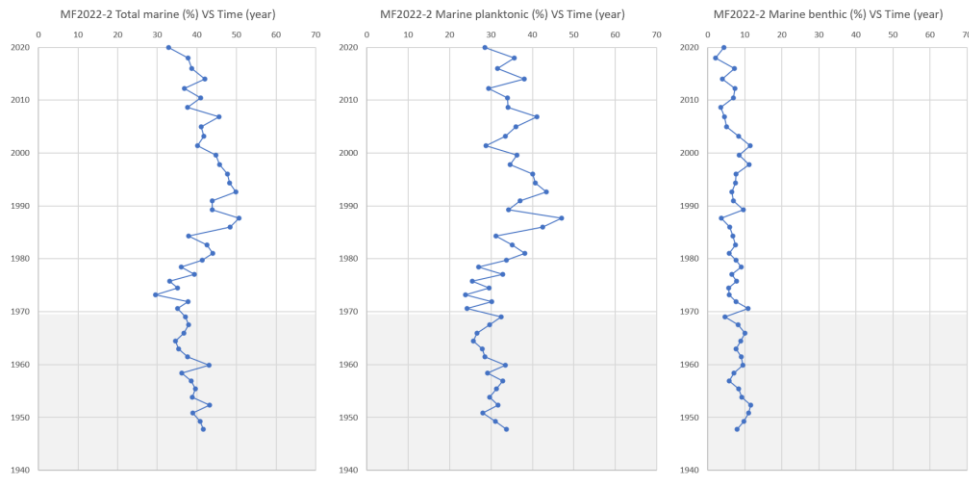


Figure 27. The relative abundances of total marine diatoms, marine planktonic diatoms, and marine benthic diatoms in core MF2022-2 from the Inner Lærdalsfjord presented versus time (parts before 1969 without certain dating results are highlighted in grey).

In core MF2022-3 from the Outer Lærdalsfjord, marine planktonic diatoms with relative abundances ranging from 25% to 50% dominate the marine diatom composition (Figure 28).

Marine planktonic diatoms showed a slight upward decrease around the depth of 7.75cm in 2000 (Figure 28; Figure 29). Its average percentage between the depth of 16.75cm and 7.75cm is around 40% while the average percentage between the depth of 7.75cm and 0cm is only around 35% (Figure 28). Marine benthic diatoms showed a first upward decrease between the depth of 14.25cm and 10.25cm from 1974 to 1985, followed by a second upward decrease between the depth of 10.25cm and 0cm from 1985 to 2022 (Figure 28; Figure 29). Its average percentage dropped from around 6% to around 2% (Figure 28).

Despite the dominant position of marine planktonic diatoms, the changes of total marine diatoms are almost equally influenced by the changes of both marine planktonic and marine benthic diatoms. Its relative abundance reduces continuously upward throughout the whole core from around 45% to around 40% on average (Figure 28).

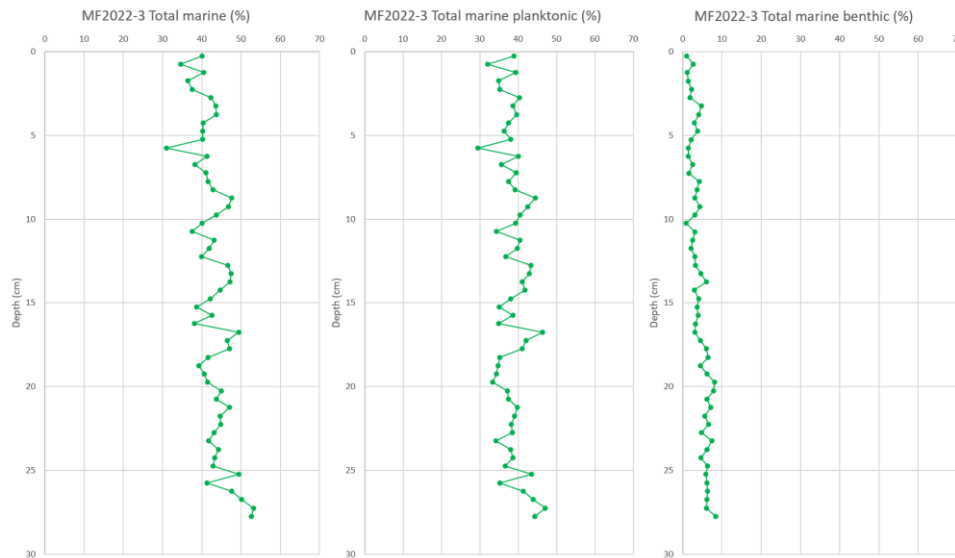


Figure 28. The relative abundances of total marine diatoms, marine planktonic diatoms, and marine benthic diatoms in core MF2022-3 from the Outer Lærdalsfjord presented versus sediment depth.

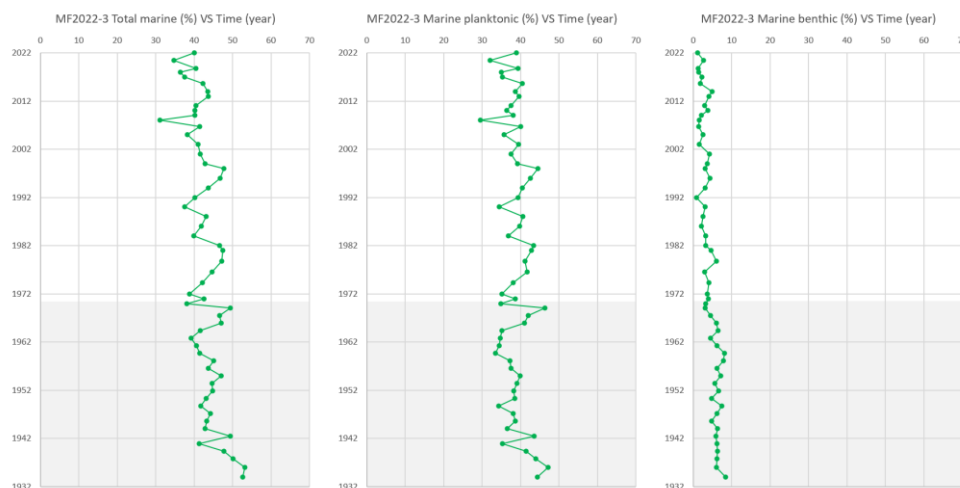


Figure 29. The relative abundances of total marine diatoms, marine planktonic diatoms, and marine benthic diatoms in core MF2022-3 from the Outer Lærdalsfjord presented versus time (parts before 1969 without certain dating results are highlighted in grey).

In both cores, the relative abundance of marine benthic diatoms showed a noticeable gradual upward decrease across the whole cores, and the relative abundance of marine planktonic diatoms decreased after the 1990s (Figure 27; Figure 29). However, an increase in the relative abundance of marine planktonic diatoms between 1974 and 1988 can only be observed in core MF2022-2 from the Inner Lærdalsfjord, while their relative abundance in core MF2022-3 from the Outer Lærdalsfjord showed no significant change during that period (Figure 27; Figure 29).

5.6. Major results of the correlation test

The positive and negative correlations in core MF2022-2 and core MF2022-3 with the absolute values of correlation coefficients (r) being between $r=0.44$ and $r=1$ (Howarth & Sinding-Larsen, 1983) are shown in Table 2 and Table 3 respectively. The complete results of the correlation test (including the correlation coefficients $r < 0,44$) in core MF2022-2 and core MF2022-3 are shown in Appendix 9 and Appendix 10.

In core MF2022-2 from the Inner Lærdalsfjord, total freshwater planktonic diatoms show a positive correlation with total freshwater diatoms with a correlation coefficient (r) of $r=0.95$ (Table 2). *Eunotia* sp. and *Tabellaria flocculosa* show a positive correlation with total freshwater planktonic diatoms with a correlation coefficient (r) of $r=0.81$ and $r=0.55$ respectively (Table 2). *Mastogloia elliptica* shows a positive correlation with total freshwater benthic diatoms with a correlation coefficient (r) of $r=0.68$ (Table 2). Total freshwater planktonic diatoms are in a negative correlation with total freshwater benthic diatoms with a correlation coefficient (r) of $r=-0.53$ (Table 2).

Total marine planktonic diatoms show a positive correlation with total marine diatoms with a correlation coefficient (r) of $r=0.90$ (Table 2). Round type diatoms and *Chaetoceros* sp. show a positive correlation with total marine planktonic diatoms with correlation coefficients (r) of $r=0.86$ and $r=0.50$ respectively (Table 2). There is no correlation between *Thalassiosira nordenskiöldii* and total marine planktonic diatoms (correlation coefficient (r) of $r=0.37$). *Paralia sulcata* shows a positive correlation with total marine benthic diatoms with a correlation coefficient (r) of $r=0.61$ (Table 2). Both *Paralia sulcata* and total marine benthic diatoms are in positive correlation with depths of sediment cores with a correlation coefficient (r) of $r=0.59$ and $r=0.47$ respectively (Table 2).

In core MF2022-3 from the Outer Lærdalsfjord, total freshwater planktonic diatoms show a positive correlation with total freshwater diatoms with a correlation coefficient (r) of $r=0.86$ (Table 3). *Eunotia* sp. shows a positive correlation with total freshwater planktonic diatoms with a correlation coefficient (r) of $r=0.80$ (Table 3) while there is no correlation between *Tabellaria flocculosa* and total freshwater planktonic diatoms (correlation coefficient (r) of $r=0.13$). *Mastogloia elliptica* shows a weak positive correlation with total freshwater benthic diatoms with a correlation coefficient (r) of $r=0.44$ (Table 3). Total freshwater planktonic diatoms are in a negative correlation with total freshwater benthic diatoms with a correlation coefficient (r) of $r=-0.66$ (Table 3).

Total marine planktonic diatoms show a positive correlation with total marine diatoms with a correlation coefficient (r) of r=0.88 (Table 3). *Chaetoceros* sp. and *Thalassiosira nordenskiöldii* show a positive correlation with total marine diatoms with a correlation coefficient (r) of r=0.63 and r=0.58 respectively (Table 3). There is no positive correlation between round type diatoms and total marine diatoms (correlation coefficient (r) of r=-0.08). *Paralia sulcata* shows a positive correlation with total marine benthic diatoms with a correlation coefficient (r) of r=0.78 (Table 3). Both *Paralia sulcata* and total marine benthic diatoms are in positive correlation with depths of sediment cores with a correlation coefficient (r) of r=0.84 and r=0.80 respectively (Table 3).

Table 2. Significant correlations in Core MF2022-2 with absolute value of correlation coefficient (r) of $r \geq 0,44$ (Howarth & Sinding-Larsen, 1983). Variable A and B refer to the two variables whose correlation coefficient is calculated.

Variable A Variable B Correlation Coefficient	Total Freshwater Freshwater/Marine 0,98	Total Marine Freshwater/Marine -0,98	Total Freshwater Total Freshwater Planktonic 0,95	Total Marine Total Freshwater Planktonic -0,94
Variable A Variable B Correlation Coefficient	Total Freshwater Planktonic Freshwater/Marine 0,92	Total Marine Total Marine Planktonic 0,90	Total Freshwater Total Marine Planktonic -0,90	Total Freshwater Planktonic Total Marine Planktonic -0,88
Variable A Variable B Correlation Coefficient	Freshwater/Marine Total Marine Planktonic -0,87	Total Marine Planktonic Round type diatoms 0,86	<i>Achnanthes</i> (Marine Benthic) Total Marine Benthic 0,83	<i>Eunotia</i> (Freshwater Planktonic) Total Freshwater Planktonic 0,81
Variable A Variable B Correlation Coefficient	<i>Eunotia</i> (Freshwater Planktonic) Total Marine -0,81	<i>Eunotia</i> (Freshwater Planktonic) Total Freshwater 0,80	<i>Eunotia</i> (Freshwater Planktonic) Freshwater/Marine 0,79	Round type diatoms Total Freshwater -0,79
Variable A Variable B Correlation Coefficient	Round type diatoms Total Marine 0,77	Round type diatoms Freshwater/Marine -0,77	Total Benthic Total Marine Benthic 0,74	Round type diatoms Total Freshwater Planktonic -0,73
Variable A Variable B Correlation Coefficient	<i>Fragilaria</i> (Freshwater Benthic) Total Benthic 0,70	<i>Mastogloia</i> (Freshwater Benthic) Total Freshwater Benthic 0,68	<i>Eunotia</i> (Freshwater Planktonic) Total Marine Planktonic -0,67	<i>Tabellaria</i> (Freshwater Planktonic) Depth 0,64
Variable A Variable B Correlation Coefficient	<i>Paralia</i> (Marine Benthic) Total Marine Benthic 0,61	Total Freshwater Benthic <i>Fragilaria</i> (Freshwater Benthic) 0,60	<i>Eunotia</i> (Freshwater Planktonic) Round type diatoms -0,60	<i>Paralia</i> (Marine Benthic) Depth 0,59
Variable A Variable B Correlation Coefficient	Total Benthic <i>Achnanthes</i> (Marine Benthic) 0,57	<i>Tabellaria</i> (Freshwater Planktonic) <i>Mastogloia</i> (Freshwater Benthic) -0,57	<i>Tabellaria</i> (Freshwater Planktonic) Total Freshwater Planktonic 0,55	<i>Gomphonema</i> (Freshwater Benthic) Depth -0,55
Variable A Variable B Correlation Coefficient	<i>Tabellaria</i> (Freshwater Planktonic) Total Marine Planktonic -0,55	Total Freshwater Benthic Total Benthic 0,53	Total Freshwater Benthic Total Freshwater Planktonic -0,53	<i>Tabellaria</i> (Freshwater Planktonic) Total Freshwater Benthic -0,51
Variable A Variable B Correlation Coefficient	<i>Chaetoceros</i> (Marine Planktonic) Total Marine Planktonic 0,50	<i>Paralia</i> (Marine Benthic) Total Benthic 0,49	<i>Diatoma tenuis Agardh</i> (Freshwater Planktonic) <i>Meridon</i> (Marine Planktonic) -0,49	Total Marine Benthic Depth 0,47
Variable A Variable B Correlation Coefficient	<i>Skeletonema</i> (Marine Planktonic) Depth 0,47	<i>Melosira</i> sp. (Freshwater Benthic) Total Freshwater Benthic 0,47	<i>Tabellaria</i> (Freshwater Planktonic) Total Marine Benthic 0,45	<i>Fragilaria</i> (Freshwater Benthic) Total Freshwater Planktonic -0,45
Variable A Variable B Correlation Coefficient	<i>Mastogloia</i> (Freshwater Benthic) Depth -0,45	<i>Tabellaria</i> (Freshwater Planktonic) Total Freshwater 0,44	<i>Surirella</i> (Marine Benthic) Others 0,44	

Table 3. Significant correlations in Core MF2022-3 with absolute value of correlation coefficient (r) of $r \geq 0,44$ (Howarth & Sinding-Larsen, 1983). Variable A and B refer to the two variables whose correlation coefficient is calculated.

Variable A Variable B Correlation Coefficient	Total Marine Total Freshwater -0,94	Total Benthic Total Freshwater Benthic 0,89	Total Marine Benthic <i>Achnanthes</i> (Marine Benthic) 0,88	Total Marine Total Marine Planktonic 0,88
Variable A Variable B Correlation Coefficient	Total Marine Total Freshwater Planktonic -0,88	Total Freshwater Total Marineine Planktonic -0,88	Total Freshwater Total Freshwater Planktonic 0,86	<i>T. Nordenskiöldii</i> (Marine Planktonic) Depth 0,86
Variable A Variable B Correlation Coefficient	<i>Paralia</i> (Marine Benthic) Depth 0,84	<i>Caloneis</i> (Marine Benthic) <i>Licmophora</i> (Marine Planktonic) 0,83	Total Freshwater Planktonic <i>Eunotia</i> (Freshwater Planktonic) 0,80	Total Marine Benthic Depth 0,80
Variable A Variable B Correlation Coefficient	Total Marine Benthic <i>Paralia</i> (Marine Benthic) 0,78	Round type diatoms Depth -0,78	Total Benthic Total Marine Benthic 0,77	Total Benthic Depth 0,77
Variable A Variable B Correlation Coefficient	Total Benthic <i>Eunotia</i> (Freshwater Planktonic) -0,76	<i>Paralia</i> (Marine Benthic) <i>T. Nordenskiöldii</i> (Marine Planktonic) 0,75	Total Freshwater Planktonic Total Marine Planktonic -0,75	<i>T. Nordenskiöldii</i> (Marine Planktonic) Round type diatoms -0,74
Variable A Variable B Correlation Coefficient	Total Benthic Total Freshwater Planktonic -0,72	Total Benthic <i>Fragilaria</i> (Freshwater Benthic) 0,71	Total Freshwater Benthic <i>Eunotia</i> (Freshwater Planktonic) -0,71	<i>Eunotia</i> (Freshwater Planktonic) Depth -0,69
Variable A Variable B Correlation Coefficient	Total Marine <i>Eunotia</i> (Freshwater Planktonic) -0,69	Total Freshwater Benthic <i>Fragilaria</i> (Freshwater Benthic) 0,67	Total Benthic <i>Achnanthes</i> (Marine Benthic) 0,66	Total Benthic <i>Melosira</i> sp. (Freshwater Benthic) 0,66
Variable A Variable B Correlation Coefficient	Total Marine Benthic Round type diatoms -0,66	Total Freshwater Benthic Total Freshwater Planktonic -0,66	Freshwater Planktonic Freshwater Benthic -0,66	Total Benthic <i>Paralia</i> (Marine Benthic) 0,65
Variable A Variable B Correlation Coefficient	<i>T. Nordenskiöldii</i> (Marine Planktonic) <i>Chaetoceros</i> (Marine Planktonic) 0,65	Total Freshwater Benthic <i>Melosira</i> sp. (Freshwater Benthic) 0,65	<i>Eunotia</i> (Freshwater Planktonic) <i>T. Nordenskiöldii</i> (Marine Planktonic) -0,65	<i>Eunotia</i> (Freshwater Planktonic) <i>Chaetoceros</i> (Marine Planktonic) -0,64
Variable A Variable B Correlation Coefficient	<i>Chaetoceros</i> (Marine Planktonic) Depth 0,63	<i>Caloneis</i> (Marine Benthic) <i>Eunotia</i> (Freshwater Planktonic) 0,63	Total Marine <i>Chaetoceros</i> (Marine Planktonic) 0,63	Total Freshwater Planktonic <i>Chaetoceros</i> (Marine Planktonic) -0,63
Variable A Variable B Correlation Coefficient	Total Benthic Round type diatoms -0,63	Total Marine Benthic <i>T. Nordenskiöldii</i> (Marine Planktonic) 0,62	<i>Paralia</i> (Marine Benthic) Round type diatoms -0,62	Total Freshwater Planktonic Depth -0,61
Variable A Variable B Correlation Coefficient	Total Benthic <i>Chaetoceros</i> (Marine Planktonic) 0,60	Total Benthic <i>T. Nordenskiöldii</i> (Marine Planktonic) 0,60	Total Freshwater Planktonic <i>T. Nordenskiöldii</i> (Marine Planktonic) -0,60	Total Marine Benthic <i>Chaetoceros</i> (Marine Planktonic) 0,59
Variable A Variable B Correlation Coefficient	<i>Paralia</i> (Marine Benthic) <i>Pinnularia</i> (Freshwater Benthic) 0,59	Total Marine <i>T. Nordenskiöldii</i> (Marine Planktonic) 0,58	Total Marine Benthic <i>Pinnularia</i> (Freshwater Benthic) 0,57	Total Marine <i>Paralia</i> (Marine Benthic) 0,57
Variable A Variable B Correlation Coefficient	Total Marine Depth 0,57	Total Freshwater <i>Eunotia</i> (Freshwater Planktonic) 0,57	<i>Caloneis</i> (Marine Benthic) <i>Gomphonema</i> (Freshwater Benthic) -0,57	<i>Achnanthes</i> (Marine Benthic) Depth 0,56
Variable A Variable B Correlation Coefficient	<i>Paralia</i> (Marine Benthic) <i>Eunotia</i> (Freshwater Planktonic) -0,56	<i>Encyonema</i> (Freshwater Planktonic) Depth 0,54	<i>Paralia</i> (Marine Benthic) <i>Chaetoceros</i> (Marine Planktonic) 0,54	Others <i>Licmophora</i> (Marine Planktonic) 0,54
Variable A Variable B Correlation Coefficient	Total Marine Total Marine Benthic 0,54	<i>Paralia</i> (Marine Benthic) Total Freshwater Planktonic -0,54	Total Marine Benthic <i>Eunotia</i> (Freshwater Planktonic) -0,54	Total Freshwater Benthic Depth 0,53
Variable A Variable B Correlation Coefficient	<i>Encyonema</i> (Freshwater Planktonic) <i>T. Nordenskiöldii</i> (Marine Planktonic) 0,53	<i>Fragilaria</i> (Freshwater Benthic) Depth 0,53	<i>Melosira</i> sp. (Freshwater Benthic) Depth 0,53	Other <i>Caloneis</i> (Marine Benthic) 0,53
Variable A Variable B Correlation Coefficient	Round type diatoms <i>Chaetoceros</i> (Marine Planktonic) -0,53	Total Marineine Benthic Total Freshwater Planktonic -0,53	Total Freshwater <i>Chaetoceros</i> (Marine Planktonic) -0,53	<i>Pinnularia</i> (Freshwater Benthic) Depth 0,52
Variable A Variable B Correlation Coefficient	Total Marine Benthic <i>Encyonema</i> (Freshwater Planktonic) 0,52	<i>Grammatophora</i> (Marine Benthic) <i>Eunotia</i> (Freshwater Planktonic) 0,52	Total Benthic <i>Pinnularia</i> (Freshwater Benthic) 0,51	Total Freshwater <i>Diatoma tenuis</i> Agardh (Freshwater Planktonic) 0,51
Variable A Variable B Correlation Coefficient	<i>Paralia</i> (Marine Benthic) <i>Encyonema</i> (Freshwater Planktonic) 0,51	<i>Eunotia</i> (Freshwater Planktonic) Total Marine Planktonic -0,51	Others <i>Gomphonema</i> (Freshwater Benthic) -0,51	<i>Pinnularia</i> (Freshwater Benthic) Round type diatoms -0,51
Variable A Variable B Correlation Coefficient	<i>Eunotia</i> (Freshwater Planktonic) <i>Licmophora</i> (Marine Planktonic) 0,50	<i>Achnanthes</i> (Marine Benthic) Round type diatoms -0,50	Total Freshwater <i>T. Nordenskiöldii</i> (Marine Planktonic) -0,50	Total Marine Total Benthic 0,49
Variable A Variable B Correlation Coefficient	Total Marine Benthic <i>Fragilaria</i> (Freshwater Benthic) 0,49	<i>Melosira</i> sp. (Freshwater Benthic) Total Freshwater Planktonic -0,49	<i>Caloneis</i> (Marine Benthic) Total Freshwater Benthic -0,49	<i>Melosira</i> sp. (Freshwater Benthic) <i>Chaetoceros</i> (Marine Planktonic) 0,48
Variable A Variable B Correlation Coefficient	<i>Achnanthes</i> (Marine Benthic) <i>Chaetoceros</i> (Marine Planktonic) 0,48	<i>Gomphonema</i> (Freshwater Benthic) <i>Licmophora</i> (Marine Planktonic) -0,48	<i>Melosira</i> sp. (Freshwater Benthic) <i>T. Nordenskiöldii</i> (Marine Planktonic) 0,46	Total Benthic <i>Caloneis</i> (Marine Benthic) -0,46
Variable A Variable B Correlation Coefficient	Others Total Benthic -0,46	<i>Melosira</i> sp. (Freshwater Benthic) Round type diatoms -0,45	<i>Fragilaria</i> (Freshwater Benthic) Round type diatoms -0,45	Total Freshwater <i>Paralia</i> (Marine Benthic) -0,45
Variable A Variable B Correlation Coefficient	<i>Melosira nummuloides</i> Agardh (Freshwater Benthic) <i>T. Nordenskiöldii</i> (Marine Planktonic) 0,44	Total Freshwater Benthic <i>Chaetoceros</i> (Marine Planktonic) 0,44	Total Marine <i>Meridon</i> (Marine Planktonic) 0,44	Total Freshwater Benthic <i>Mastogloia</i> (Freshwater Benthic) 0,44
Variable A Variable B Correlation Coefficient	Total Freshwater Depth -0,44	<i>Eunotia</i> (Freshwater Planktonic) <i>Meridon</i> (Marine Planktonic) -0,44	Total Freshwater Benthic Round type diatoms -0,44	

5.7. Major changes of common and abundant diatoms in both cores

Based on the criteria for the diatom relative abundance stated in section 4.2.1 and the results of the correlation test (Table 2; Table 3), the following 6 diatoms are chosen for further analysis: *Eunotia* sp., *Tabellaria flocculosa*, *Mastogloia elliptica*, *Chaetoceros* sp., *Thalassiosira nordenskiöldii*, *Paralia sulcata*. Their morphology and ecological preferences are illustrated with pictures in Table 4. The X-Y scatter graphs of their relative abundances presented versus sediment depths and time are analysed in this section.

In core MF2022-2 from the Inner Lærdalsfjord, like total freshwater planktonic diatoms, the relative abundances of both *Eunotia* sp., and *Tabellaria flocculosa* also showed a pronounced decrease between the depths from 14.25cm to 7.25cm from 1974 to 1995 and recovered to the original level between the depths of 7.25cm and 5.7 cm from 1995 to 2000 (Figure 30; Figure 31). However, between the depth from 5.75cm to 0cm from 2000 and 2020, *Eunotia* sp. showed a noticeable increase while *Tabellaria flocculosa* decreases slightly (Figure 30; Figure 31).

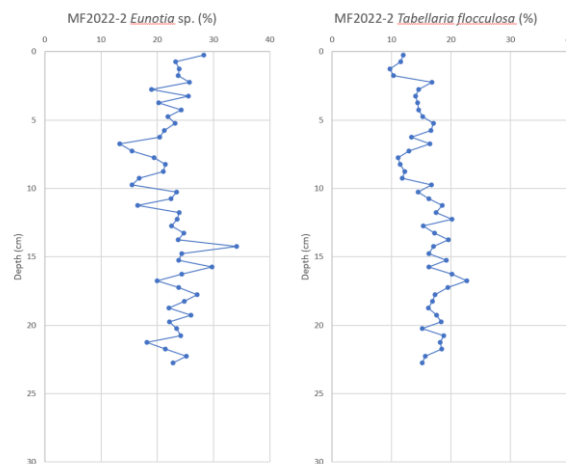


Figure 30. X-Y scatter graphs of the relative abundances of major freshwater planktonic diatom genus, *Eunotia* sp. and *Tabellaria flocculosa*, presented versus sediment depths, in core MF2022-2 from the Inner Lærdalsfjord.

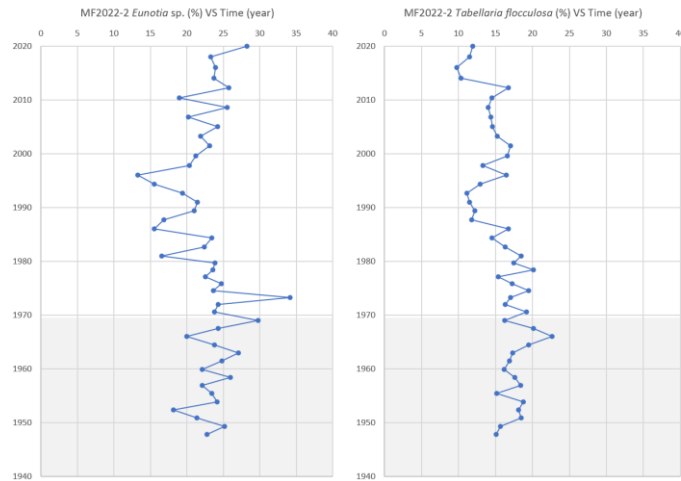


Figure 31. X-Y scatter graphs of the relative abundances of major freshwater planktonic diatoms, *Eunotia* sp. and *Tabellaria flocculosa*, presented versus time, in core MF2022-2 (part before 1969 without certain dating results is highlighted in grey).

In core MF2022-3 from the Outer Lærdalsfjord, the relative abundances of *Eunotia* sp. and *Tabellaria flocculosa* showed a similar opposite trend to that in core MF2022-2 from the Inner Lærdalsfjord between 2000 and 2022 (Figure 31; Figure 33). *Eunotia* sp. increased significantly between the depths from 7.75cm to 0cm from 2000 to 2022 from 17% on average to 25% on average, while the relative abundance of *Tabellaria flocculosa* decreased slightly during the same period (Figure 32; Figure 33). However, in contrast to core MF2022-2 from the Inner Lærdalsfjord, there was no significant change in the relative abundances of both genus between 1974 and 2000 in the Outer Lærdalsfjord (Figure 31; Figure 33).

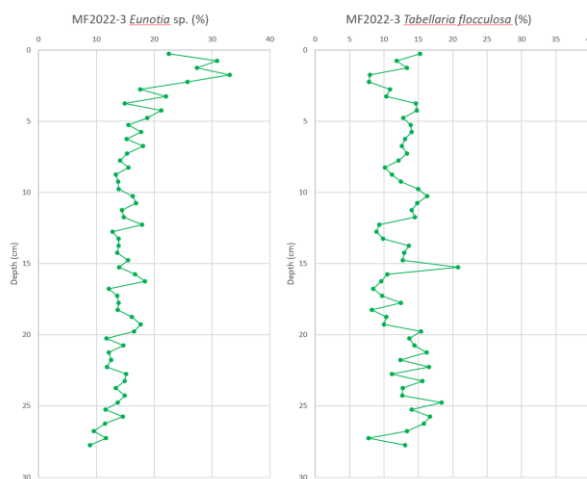


Figure 32. X-Y scatter graphs of the relative abundances of major freshwater planktonic diatom genus, *Eunotia* sp., *Tabellaria flocculosa*, presented versus, in core MF2022-3 from the Outer Lærdalsfjord.

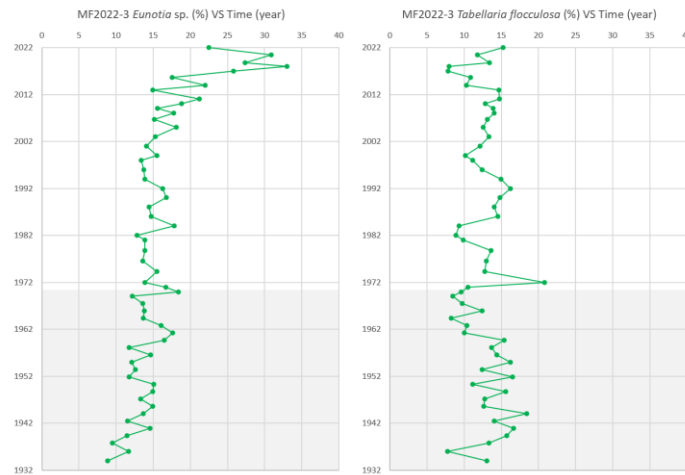


Figure 33. X-Y scatter graphs of the relative abundances of major freshwater planktonic diatoms, *Eunotia* sp. and *Tabellaria flocculosa*, presented versus time, in core MF2022-3 (part before 1969 without certain dating results is highlighted in grey).

The relative abundance of *Mastogloia elliptica* shows similar and slightly more pronounced changes with total freshwater benthic diatoms (Figure 22; Figure 24; Figure 34). Its relative abundance in core MF2022-2 from the Inner Lærdalsfjord increased drastically at the depths from 5.75cm to 0cm between 2000 and 2020 from 2.5% on average to 4% on average, while that in the core MF2022-3 from the Outer Lærdalsfjord decreased significantly between the depths from 7.75cm to 0cm during the same period (Figure 34; Figure 35).

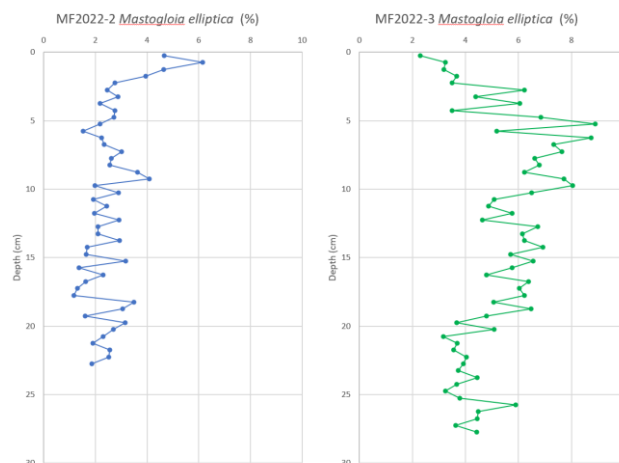


Figure 34. X-Y scatter graphs of the relative abundance of major freshwater benthic diatom, *Mastogloia elliptica*, presented versus sediment depth, in core MF2022-2 and core MF2022-3.

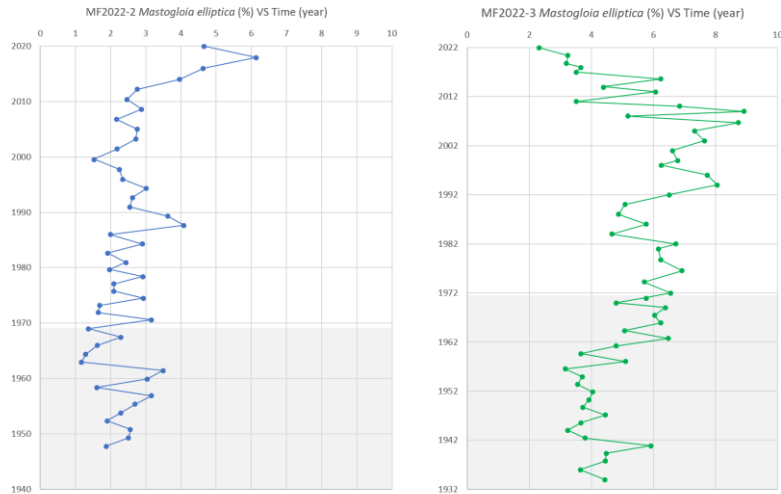


Figure 35. X-Y scatter graphs of the relative abundance of major freshwater benthic diatom, *Mastogloia elliptica*, presented versus time, in core MF2022-2 and core MF2022-3 (part before 1969 without certain dating results is highlighted in grey).

In core MF2022-2 from the Inner Lærdalsfjord, the relative abundances of both *Chaetoceros* sp. and *Thalassiosira nordenskiöldii* showed a noticeable increase between the depth of 14.25cm and 0cm from 1974 to 2020 (the unusual peak at the depth of 9.25cm in the *Chaetoceros* sp. graph is considered as an outlier and thus not taken into consideration) (Figure 36; Figure 37). A decrease from 1988 to 2000, which is observed in the graph of total marine planktonic diatoms (Figure 26), cannot be seen in the graphs of *Chaetoceros* sp. and *Thalassiosira nordenskiöldii*.

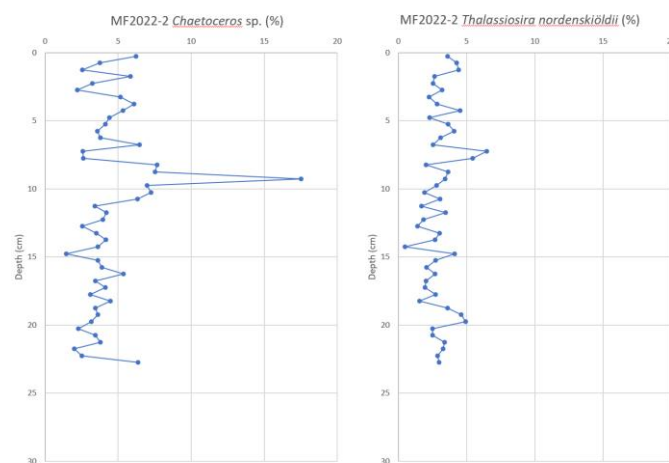


Figure 36. X-Y scatter graphs of the relative abundances of major marine planktonic diatom genus, *Chaetoceros* sp. and *Thalassiosira nordenskiöldii*, presented versus sediment depths, in core MF2022-2 from the Inner Lærdalsfjord.

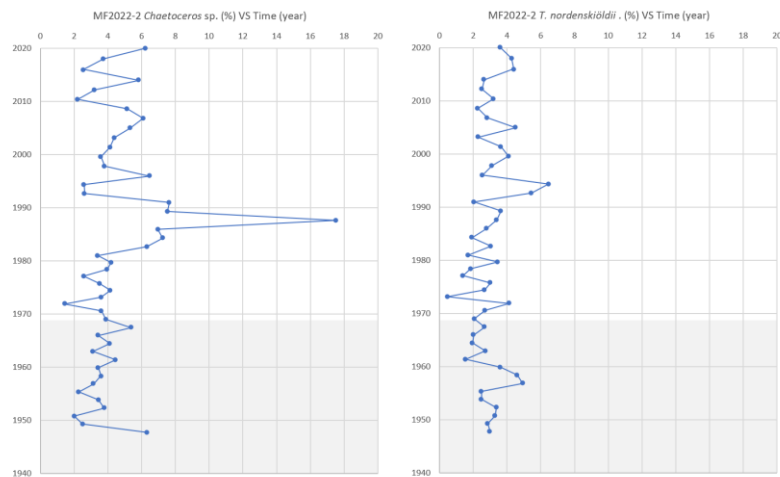


Figure 37. X-Y scatter graphs of the relative abundances of major marine planktonic diatom genus, *Chaetoceros* sp. and *Thalassiosira nordenskiöldii*, presented versus time, in core MF2022-2 (parts before 1969 without certain dating results are highlighted in grey).

In core MF2022-3 from the Outer Lærdalsfjord, the relative abundances of both *Chaetoceros* sp. and *Thalassiosira nordenskiöldii* showed a first significant decrease between the depth from 14.75cm to 7.75cm between 1974 and 2000, followed by a second decrease between the depth from 7.75cm to 0cm from 2000 to 2022 (Figure 38; Figure 39). In contrast, only a slight decrease around the depth of 7.75cm in 2000 can be observed in the graph of total marine planktonic diatoms (Figure 28).

The relative abundances of these two major marine planktonic diatoms show different changing patterns in the Inner and Outer Lærdalsfjord. While the relative abundances of *Chaetoceros* sp. and *Thalassiosira nordenskiöldii* in the Inner Lærdalsfjord increased after the 1970s, their relative abundances decreased continuously after the 1970s in the Outer Lærdalsfjord. (Figure 37; Figure 39).

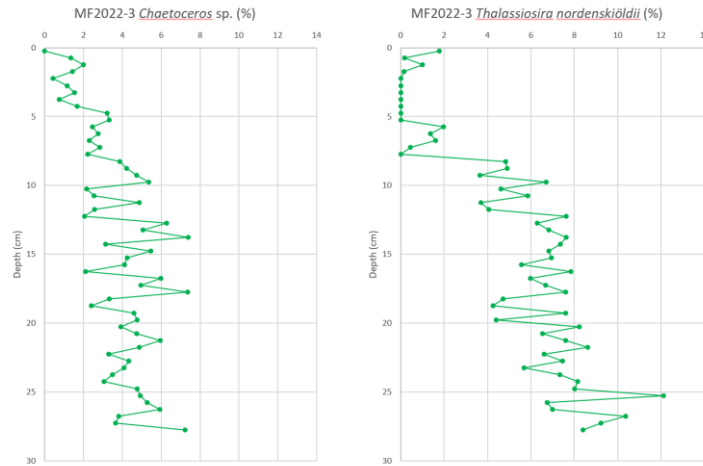


Figure 38. X-Y scatter graphs of the relative abundances of major marine planktonic diatom genus, *Chaetoceros* sp. and *Thalassiosira nordenskiöldii*, presented versus sediment depths, in core MF2022-3 from the Outer Lærdalsfjord.

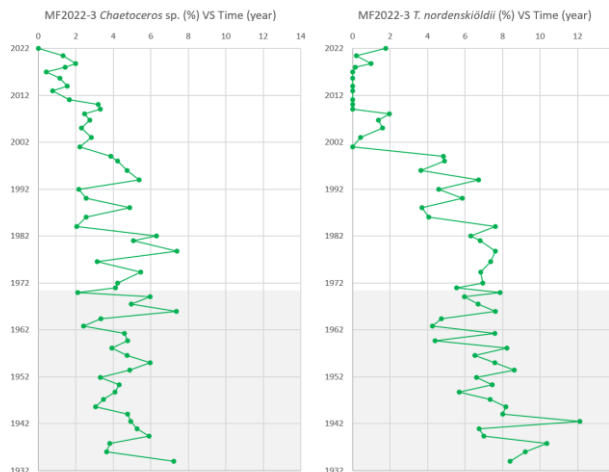


Figure 39. X-Y scatter graphs of the relative abundances of major marine planktonic diatom genus, *Chaetoceros* sp. and *Thalassiosira nordenskiöldii*, presented versus time, in core MF2022-3 (parts before 1969 without certain dating results are highlighted in grey).

In core MF2022-2 and core MF2022-3, the relative abundances of *Paralia sulcata* show a continuous decrease towards the sediment surface (Figure 40). The decrease in both the Inner and Outer Lærdalsfjord was more significant after 1985, and its relative abundance in the Outer Lærdalsfjord remained at a rather low level after the 1990s (Figure 41). In addition, the R-squared (R^2) value in the graph of core MF2022-3 ($R^2 = 0,7020$) is larger than that of core MF2022-2 ($R^2 = 0,3363$) (Figure 40). In other words, the positive correlation between *Paralia sulcata* and depth is more pronounced in the Outer Lærdalsfjord than in the Inner Lærdalsfjord (Figure 40).

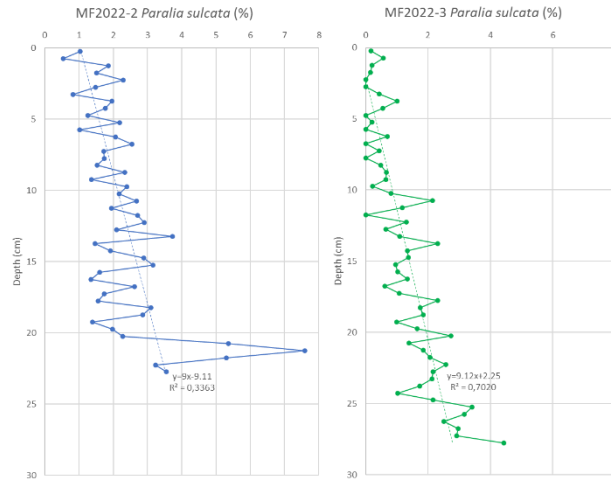


Figure 40. X-Y scatter graphs of the relative abundance of major marine benthic diatom genus, *Paralia sulcata*, presented versus sediment depths, in core MF2022-2 and core MF2022-3 with trendlines and trendline equations.

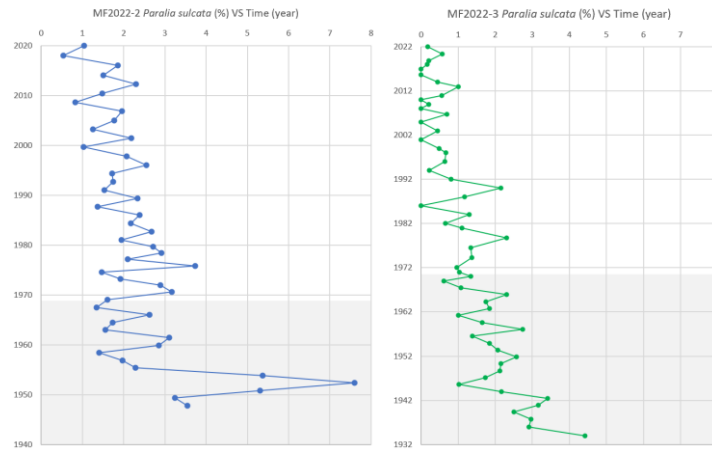
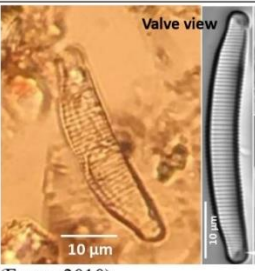
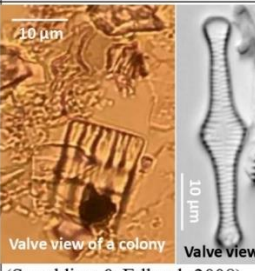


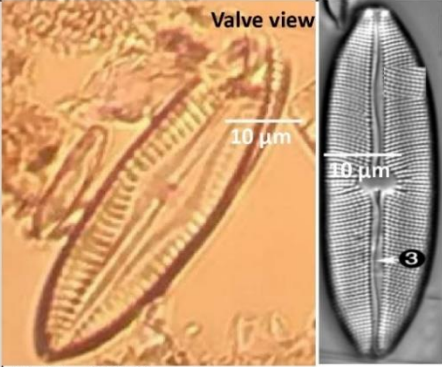
Figure 41. X-Y scatter graphs of the relative abundance of major marine benthic diatom genus, *Paralia sulcata*, presented versus time, in core MF2022-2 and core MF2022-3 (part before 1969 without certain dating results is highlighted in grey).

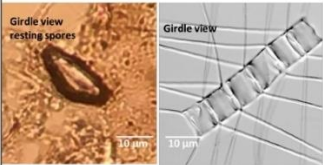
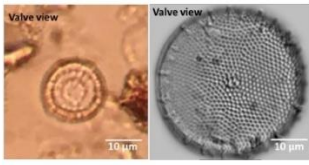
5.8. Table of the morphology, classification, and ecological preferences of common and abundant diatoms

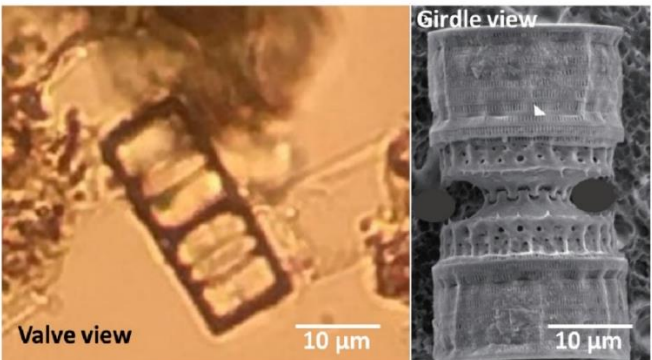
Information about the ecological preferences and morphology of the common (5 to 20% of the total diatom composition; Scherer & Koc (1996)) and abundant diatoms (20 to 60% of the total diatom composition; Scherer & Koc (1996)) is necessary for the analysis of potential causes of the major changes in their relative abundances. Thus, the information about the six common and abundant diatoms is summarized in Table 4 in the following order: freshwater planktonic diatoms, freshwater benthic diatoms, marine planktonic diatoms, and marine benthic diatoms.

Table 4. Morphology, classification, and ecological preferences of the six common and abundant diatoms; read from left to right. Pictures without references are taken from the Lærdalsfjord smear slides.

Genus	Freshwater planktonic diatoms	<i>Eunotia</i> sp.	<i>Tabellaria flocculosa</i>
Mean occurrence in core MF2022-2 in Inner Lærdalsfjord (%)	47,68	22,64	15,88
Mean occurrence in core MF2022-3 in Outer Lærdalsfjord (%)	40,75	15,90	12,76
Morphology		<p>a. Valves have arcuate shape, are asymmetric to the apical axis. b. The raphe is short and extends from valve mantle onto valve face. c. Striae are uniseriate, are positioned usually in single lines. d. The terminal nodules are positioned on the mantle. (Furey, 2010)</p>	<p>a. Valves are elongate and have capitate ends. The center is wider than the ends. b. Valves have no raphe. c. Valves form zig-zag colonies. d. Striae are uniseriate and positioned with irregular spaces in between. (Spaulding & Edlund, 2008)</p>
Classification		<p>Class: Bacillariophyceae Order: Eunotiales Family: Eunotiaceae (Furey, 2010)</p>	<p>Class: Fragilariophyceae Order: Tabellariales Family: Tabellareaceae (Spaulding & Edlund, 2008)</p>
Ecological preferences		<p>It can tolerate low nutrient level (Furey, 2010). It prefers more acidic water (Barber & Haworth, 1981).</p>	<p>It is a typical freshwater planktonic diatom in the fjord sediment in Norway, and hence it is an indicator of enhanced freshwater runoff or enhanced primary productivity in main origin rivers or lakes (Paetzel & Dale, 2010). It is acidophilus and prefers slightly acid water (Paetzel & Dale, 2010). Its abundance decreases when there is heavy metal pollution, especially when the concentrations of Copper and Zinc are high (Cattaneo et al., n.d.).</p>
Pictures		 <p>(Furey, 2010)</p>	 <p>(Spaulding & Edlund, 2008)</p>

Genus	Freshwater benthic diatoms	<i>Mastogloia elliptica</i>
Mean occurrence in core MF2022-2 in Inner Lærdalsfjord (%)	11,19	2,61
Mean occurrence in core MF2022-3 in Outer Lærdalsfjord (%)	13,48	5,28
Morphology		<p>a. Valves are elliptical to linear-elliptical with convex to nearly parallel sides.</p> <p>b. Its raphe is straight or undulate.</p> <p>c. Axial area is almost as narrow as the raphe and the central area is circular and slightly expanded.</p> <p>d. Striae are radiate and are composed of single rows of areolae.</p> <p>e. Raphe branches are lateral and sinuous, with slightly expanded ends. (Krammer & Lange-Bertalot, 1986; Patrick & Reimer, 1966; Agardh, 1824)</p>
Classification		<p>Class: Bacillariophyceae</p> <p>Order: Naviculales</p> <p>Family: Mastogloiaceae</p> <p>(Spaulding & Edlund, 2008)</p>
Ecological preferences		<p>It prefers brackish waters in coastal areas or saline inland waters (Krammer & Lange-Bertalot, 1986). It was found even in a water environment with high chloride content up to 13200 mg/L (Patrick & Reimer, 1966).</p>
Pictures		 <p>(Bahls, 2012)</p>

Genus	Marine planktonic diatoms	<i>Chaetoceros</i> sp.	<i>Thalassiosira nordenskiöldii</i>
Mean occurrence in core MF2022-2 in Inner Lærdalsfjord (%)	32,81	4,49	3,04
Mean occurrence in core MF2022-3 in Outer Lærdalsfjord (%)	38,69	3,68	4,98
Morphology		a. Filamentous colonies are often formed. b. Valves are elliptic. c. Setae that extend from the pole of each valve connect neighboring valves. d. The setae of the terminal valve are twisted strongly away from the colony. (Spaulding & Edlund, 2008)	a. Valves have a disc-like centric shape b. Areolae are positioned in radial or tangential rows. (Spaulding & Edlund, 2008)
Classification		Class: Coscinodiscophyceae Order: Chaetocerotales Family: Chaetoceraeae (Spaulding & Edlund, 2008)	Class: Coscinodiscophyceae Order: Thalassiosirales Family: Thalassiosiraceae (Spaulding & Edlund, 2008)
Ecological preferences		It is a typical marine planktonic diatom in spring bloom, and hence indicates the primary productivity level. Its abundance increases with more nutrients available (UBC Department of Earth, Ocean and Atmospheric Sciences, 2012). It can tolerate stratified water and reduced salinity (Jensen et al., 2004). The common species <i>Chaetoceros muelleri</i> has a pH preference of from 7.6 to 8.3 (Blinn & Bailey, 2001) and can tolerate heavy metal pollution (Cattaneo et al., n.d.). It forms resting stages under unfavorable conditions (Witon et al., 2006).	It is a typical marine planktonic diatoms in the spring bloom in Norway and thus indicates primary productivity level (UBC Department of Earth, Ocean and Atmospheric Sciences, 2012). It is a neritic Arctic-boreal species, which prefers well-mixed water, reaches its population maximum in 2.8 degrees Celsius (+/- 1.8) temperature, and can tolerate warmer temperatures than <i>Detonula confervacea</i> (McQuoid & Nordberg, 2003).
Pictures		 <p>(Spaulding & Edlund, 2008)</p>	 <p>(Spaulding & Edlund, 2008)</p>

Genus	Marine benthic diatoms	<i>Paralia sulcata</i>
Mean occurrence in core MF2022-2 in Inner Lærdalsfjord (%)	7,42	2,32
Mean occurrence in core MF2022-3 in Outer Lærdalsfjord (%)	4,24	1,28
Morphology		<p>a. Valves are circular and slightly convex.</p> <p>b. Valves form solid chain colonies connected by well-developed interlocking ridges and marginal spines. Each chain consists of intercalary and separation valves.</p> <p>b. Valves at the end of each chain have reduced ridges and no marginal spines.</p> <p>(Yun et al., 2016)</p>
Classification		<p>Class: Bacillariophyceae</p> <p>Order: Paraliales</p> <p>Family: Achnantheaceae</p> <p>(Spaulding & Edlund, 2008)</p>
Ecological preferences		<p>It is a marine benthic diatom, and an indicator of salt-marsh environment and a silty tidal flat habitat (McQuoid & Nordberg, 2003). Its abundance decreases when there is a shortage of nutrient, especially a lack of Phosphorus (McQuoida & Nordberg, 2003). Small sized <i>P.sulcata</i> prefers more well-mixed water with more upwelling of nutrient-rich, high salinity water and mild winter weather (McQuoida & Nordberg, 2003). The relative proportion of cells larger than 20 μm increases in more stratified water with low salinity and low Phosphorus concentration (McQuoida & Nordberg, 2003).</p>
Pictures		 <p>(Yun et al., 2016)</p>

6. Discussion

This section aims to answer the three objective questions by comparing the two dating results and analysing the causes of the major changes in the relative abundances of freshwater and marine diatoms in the Inner and Outer Lærdalsfjord.

6.1. Reliability of diatom-based dating methods

To compare the two dating results (Figure 19, Figure 20, and Figure 21), X-Y scatter graphs of the relative abundance of total freshwater diatoms, and of the relative abundance of *Paralia sulcata* presented versus time based on the two dating results were computed (Figure 42; Figure 43). The differences between the two dating results are within 0 or 2 years (with one outlier of 5 years) across both sediment cores (Figure 42; Figure 43). In other words, the dating result based on temperature and the marine benthic diatom, *Paralia sulcata* can be verified by the dating result based on precipitation and total freshwater diatoms, and vice versa. Thus, it is reasonable to conclude that changes in the diatom compositions can be used to date the recent sediment cores over the past 90 years.

In addition, the decrease in sedimentation rates from 0.38 cm/year (from 1969 to 1981) to 0.27 cm/year (from 1996 to 2014) can be linked back to the impacts of two hydropower plants (Borgund kraftverk, 2021) on the reduction in the flow velocity of the river Lærdalselv (Torbjørn Dale 2023, *personal communication*). With the river flow velocity decreasing, the amount of mineral and organic matter transported and deposited into the Inner Lærdalsfjord sediment decreases correspondingly. In contrast, the sedimentation rates in the Outer Lærdalsfjord remain relatively stable. This implies that the Outer Lærdalsfjord is impacted less by the two hydropower plants.

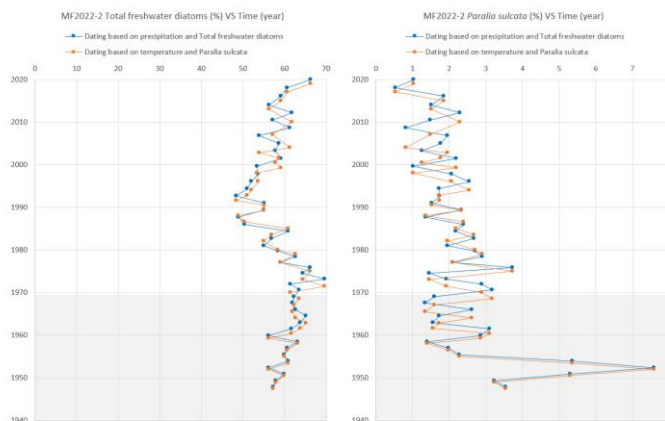


Figure 42. X-Y scatter graphs of total freshwater diatoms and *Paralia sulcata* presented versus time based on two dating results of the core MF2022-2 (Figure 24; Figure 25) (part before 1969 without certain dating results is highlighted in grey).

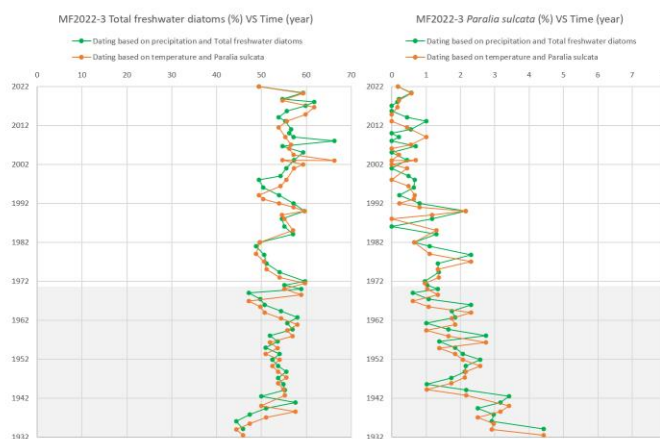


Figure 43. X-Y scatter graphs of total freshwater diatoms and *Paralia sulcata* presented versus time based on two dating results of the core MF2022-3 (Figure 24; Figure 26) (part before 1969 without certain dating results is highlighted in grey).

6.2. Causes of changes in the freshwater planktonic diatom compositions

Based on the correlation coefficients shown in Table 2 and Table 3, *Eunotia* sp. and *Tabellaria flocculosa* are the dominant genera among freshwater planktonic diatoms in the Inner Lærdalsfjord, while *Eunotia* sp. is the dominant freshwater planktonic diatom genus in the Outer Lærdalsfjord.

The decreases in freshwater planktonic diatom concentrations and in the relative abundances of the two major freshwater planktonic diatoms, *Eunotia* sp. and *Tabellaria flocculosa* in the Inner Lærdalsfjord between 1974 and 1995 (Figure 23; Figure 31) can also be attributed to the impacts of the two hydropower plants at Borgund and Stuvane on the resulting decrease in river flow velocity (Borgund kraftverk, 2021). However, such decreases cannot be observed in the

Outer Lærdalsfjord during the same period (Figure 25). This shows that the impact of hydropower plants is insignificant in the Outer Lærdalsfjord.

Between 1995 and 2000, the relative abundance of freshwater planktonic diatoms shows a gradual increase to the original level in the Inner Lærdalsfjord and a remarkable increase in 2000 in the Outer Lærdalsfjord (Figure 23; Figure 25). This can be explained by the significant increase in the precipitation level after the 1990s due to climate change (Figure 8) since more freshwater planktonic diatoms can be transported into the Inner and Outer Lærdalsfjord when the precipitation level goes up.

In addition, *Eunotia* sp. showed a significant increase while *Tabellaria flocculosa* decreased slightly after 2000 in the Inner and Outer Lærdalsfjord (Figure 31; Figure 33). One potential cause of these opposite changes is the decrease in nutrient availability in the river Lærdalselv in the recent 20 years (Figure 1). The dams of two hydropower plants (Borgund kraftverk, 2021) may have partially caused the reduction in nutrients like silicium (Si) in the river Lærdalselv. Since freshwater diatoms must compete for the limited nutrients and *Eunotia* sp. has a better adaptability to a low trophic level than *Tabellaria flocculosa* (Table 4), *Eunotia* sp. outcompetes *Tabellaria flocculosa*.

6.3. Causes of changes in the freshwater benthic diatom compositions

Based on the correlation coefficients shown in Table 2 and Table 3, *Mastogloia elliptica* is the dominant freshwater benthic diatom genus in Inner and Outer Lærdalsfjord.

While the relative abundance of freshwater benthic diatoms in the Inner Lærdalsfjord increased first in 1988 and then in 2000, their relative abundance in the Outer Lærdalsfjord decreased slightly after 2000 (Figure 23; Figure 25). A similar changing pattern can be observed more clearly in the changes in the relative abundance of the major freshwater benthic diatom, *Mastogloia elliptica* (Figure 35). This can be explained by the increased impact of the two hydropower plants on river flow pattern (Borgund kraftverk, 2021). Since most freshwater benthic diatoms are attached to plants, sediments, or rocks, their transportation requires a sufficient level of river flow velocity (Stevenson, 1983; Dixit et al., 1992).

After the construction of the first hydropower plant at Borgund in 1974, the partially regulated river still maintained a natural seasonal flow pattern and an equilibrium was established between the natural delta and the partially regulated river (Torbjørn Dale 2023, *personal*

communication). Thus, the amount of freshwater benthic diatoms transported into the Inner and Outer Lærdalsfjord remained largely unchanged.

After the construction of the second hydropower plant at Stuvane in 1988, the river flow was further regulated (Torbjørn Dale 2023, *personal communication*). Due to the reduced river flow velocity, its capacity to transport freshwater benthic diatoms further out to the Outer Lærdalsfjord was limited. As a result, a higher portion of freshwater benthic diatoms was directly deposited in the Inner Lærdalsfjord rather than being transported further out into the Outer Lærdalsfjord. This explains the first increase in the relative abundance of freshwater benthic diatoms in the Inner Lærdalsfjord in 1988. At this time point, the reduction in the relative abundance of freshwater benthic diatoms in the Outer Lærdalsfjord was still insignificant and could be compensated by the increase in precipitation level in the 1990s (Figure 8) and the runoffs from the river Erdalselv (Figure 1).

Due to the loss of the original natural delta during and after the Lærdal Tunnel building between 1995 and 2000 (Engineering.com, 2006), the equilibrium between the natural delta and the partially regulated river disappeared. Thus, the capacity of the river to transport the freshwater benthic further out to the Outer Lærdalsfjord was reduced further. A much higher portion of freshwater benthic diatoms was deposited in the Inner Lærdalsfjord than in the Outer Lærdalsfjord. This is the reason for the second increase in the relative abundance of freshwater benthic diatoms in the Inner Lærdalsfjord in 2000 and the decrease in their relative abundance in the Outer Lærdalsfjord after 2000. However, it is important to emphasize that the increase in the relative abundance of freshwater benthic diatoms in the Inner Lærdalsfjord does not necessarily imply the increase in their absolute amount.

6.4. Causes of changes in the marine planktonic diatom compositions

Based on the correlation coefficients shown in Table 2 and Table 3, round type diatoms and the *Chaetoceros* sp. are dominant marine planktonic diatoms in the Inner Lærdalsfjord while the *Chaetoceros* sp. and *Thalassiosira nordenskiöldii* dominate the marine planktonic diatoms in the Outer Lærdalsfjord.

The relative abundance of marine planktonic diatoms in the Inner Lærdalsfjord increased slightly between 1974 and 1988 and decreased gradually between 1988 and 2020 (Figure 27). One possible explanation can be the increased impacts of two hydropower plants on the

resulting reduction in nutrients transported out into the Lærdalsfjord (Borgund kraftverk, 2021) since primary productivity in fjords is partially determined by nutrient availability.

After the construction of the first Borgund hydropower plant in 1974, the river flow velocity was reduced slightly (Torbjørn Dale 2023, *personal communication*), and thus the river Lærdalselv could only transport a smaller portion of nutrients further out from the Inner Lærdalsfjord to the Outer Lærdalsfjord. As a result, a larger portion of nutrients was deposited directly in the Inner Lærdalsfjord rather than being further transported out into the Outer Lærdalsfjord. This can be the cause for the increase in the relative abundance of marine planktonic diatoms in the Inner Lærdalsfjord between 1974 and 1988 (Figure 32).

In 1988, after the building of the second hydropower plant, the flow velocity of the river Lærdalselv dropped further (Torbjørn Dale 2023, *personal communication*). Hence, its capacity to transport nutrients out into the Inner Lærdalsfjord started to decrease and the amount of nutrients transported into the Inner Lærdalsfjord was reduced to a critically low level. Due to the lack of nutrients in the Inner Lærdalsfjord, the primary productivity in the Inner Lærdalsfjord decreased. This explains the decrease in the relative abundance of marine planktonic diatoms in the Inner Lærdalsfjord between 1988 and 2020 (Figure 27).

If this is the cause of the changes in the Inner Lærdalsfjord, the relative abundance of marine planktonic diatoms in the Outer Lærdalsfjord should show a continuous decrease from 1974 via 1988 to 2020. However, such an anticipated decrease can only be seen in the decrease in the relative abundance of the two dominating marine planktonic diatom species, *Chaetoceros* sp. and *Thalassiosira nordenskiöldii*, between 1974 and 2020 (Figure 39). In contrast, the relative abundance of total marine planktonic diatoms in the Outer Lærdalsfjord only decreased slightly around 2000 (Figure 29).

One possible reason why there was no significant decrease in the relative abundance of total marine planktonic diatoms between 1974 and 2020 is that the relative abundance of round type diatoms showed no decrease between 1974 and 2020 and their relative abundance is much higher than other marine planktonic diatoms. Since round type diatoms cannot be clearly identified, they might not be marine planktonic diatoms although they were counted as marine planktonic diatoms. Thus, their response to the changes in nutrient availability may differ from other marine planktonic diatoms. Alternatively, these unidentified species might belong to a diatom species that favourably lives on low level nutrient conditions.

Another noticeable change is that the relative abundances of *Chaetoceros* sp. and *Thalassiosira nordenskiöldii* increased in the Inner Lærdalsfjord not only between 1974 and 1988 but also after 1988 (Figure 37). This can be explained by the rise in both air temperature (Figure 8) and water temperature (Kaufmann 2014; Reß 2015), as well as the corresponding extension of the stratification period in the Lærdalsfjord. With the air (and thus surface water) temperature rising continuously (Figure 8), the inflow of Norwegian Coastal Water or North Atlantic Water with high salinity into the basin becomes less frequent, and the stratification period in the Inner Lærdalsfjord may become longer (Darelius, 2020). As a result, *Chaetoceros* sp. and *Thalassiosira nordenskiöldii*, who can tolerate stratified water and reduced salinity, outcompeted other species (Table 4). However, it is noteworthy that their increasing relative abundances does not necessarily mean that their absolute abundances increased despite the reduced nutrient availability in the Inner Lærdalsfjord.

However, the relative abundances of *Chaetoceros* sp. and *Thalassiosira nordenskiöldii* show decreases rather than increases in the Outer Lærdalsfjord after 1988. This implies that the impact of the decrease in nutrient availability is more pronounced than the impact of temperature and stratification in the Outer Lærdalsfjord. The amount of nutrients in the Outer Lærdalsfjord might have reduced to a critical level after the construction of the second hydropower plant in 1988. Since both species have a low tolerance to low trophic level (Table 4), they might be outcompeted by other primary producers with a better tolerance on low trophic levels after 1988.

6.5. Causes of changes in the marine benthic diatom compositions

The correlation coefficients (Table 2; Table 3) imply that *Paralia sulcata* is the dominant marine benthic diatom genus, and its relative abundance decreases towards the sediment surface.

The decrease in the relative abundance of *Paralia sulcata* throughout the whole sediment cores in the Inner and Outer Lærdalsfjord (Figure 40) can be explained by reduced nutrient upwelling and longer stratification periods in the Lærdalsfjord since the 1960s. With the air (and thus surface water) temperature in Lærdal increasing since the 1960s (Figure 8), the density of the North Atlantic Oceanic Water reduces, and the basin water exchange becomes less frequent (Darelius, 2020). As a result, *Paralia sulcata*, who prefers well-mixed water with more nutrient upwelling (McQuoid & Nordberg, 2003b), was outcompeted by other species with a better adaptability of stagnant water with less nutrient upwelling. The more pronounced decrease in

its relative abundance after 1985 in both cores can be attributed to the more pronounced increase in water temperatures in the Norwegian Sea since 1985 (Kaufmann 2014; Reß 2015).

6.6. Differences in the environmental setting between the Inner and Outer Lærdalsfjord

There are similarities and differences in how the external influential factors (summarised as environmental and climate factors) exert impacts on the Inner and Outer Lærdalsfjord (Figure 44). The Inner and Outer Lærdalsfjord receive mainly four external influences, namely (a) precipitation, (b) the inflow of North Atlantic Oceanic Water, (c) the runoff of the river Lærdalselv and the river Erdalselv, and (d) the water exchange between the Inner and Outer Lærdalsfjord (Figure 44). Impacts of water exchange between the Inner and Outer Lærdalsfjord are rather minor and hence will not be discussed in this thesis.

(a). The increase in total freshwater diatom concentrations as a consequence of increasing precipitation levels can be seen in the Inner and Outer Lærdalsfjord (Figure 44).

(b). However, the Outer Lærdalsfjord is more influenced by the inflow of North Atlantic Oceanic Water than the Inner Lærdalsfjord since the Outer Lærdalsfjord is located closer to the open ocean (Figure 1; Figure 44). As a result, the increasing water temperatures of the Norwegian Sea lead to a reduction in the marine benthic diatom *Paralia sulcata*, which is more pronounced in the Outer Lærdalsfjord than in the Inner Lærdalsfjord (Figure 44).

(c). Although both, the Inner and the Outer Lærdalsfjord receive runoff from the river Lærdalselv, the Outer Lærdalsfjord is located more distant to the river Lærdalselv and receives additional river runoff from the river Erdalselv (Figure 44). Thus, the Outer Lærdalsfjord is less impacted by the decreasing flow velocity of the river Lærdalselv after the construction of the first hydropower plant in 1974. The decrease in the relative abundance of the freshwater planktonic diatoms after 1974 is more pronounced in the Inner Lærdalsfjord (Figure 44).

However, the flow velocity in the river Lærdalselv decreased utterly after the construction of the second hydropower plant in 1988, resulting in a further reduction in nutrients transported out to the Lærdalsfjord. This loss in nutrients seems to be more significant in the Outer Lærdalsfjord (Figure 44). Thus, the decrease in marine planktonic diatoms is more pronounced in the Outer Lærdalsfjord than in the Inner Lærdalsfjord (Figure 44). Similarly, the impact of the loss of the natural delta results in a decrease in freshwater benthic diatoms transported out to the Lærdalsfjord (Figure 44). The loss in benthic freshwater diatoms is also more pronounced in the Outer Lærdalsfjord (Figure 44).

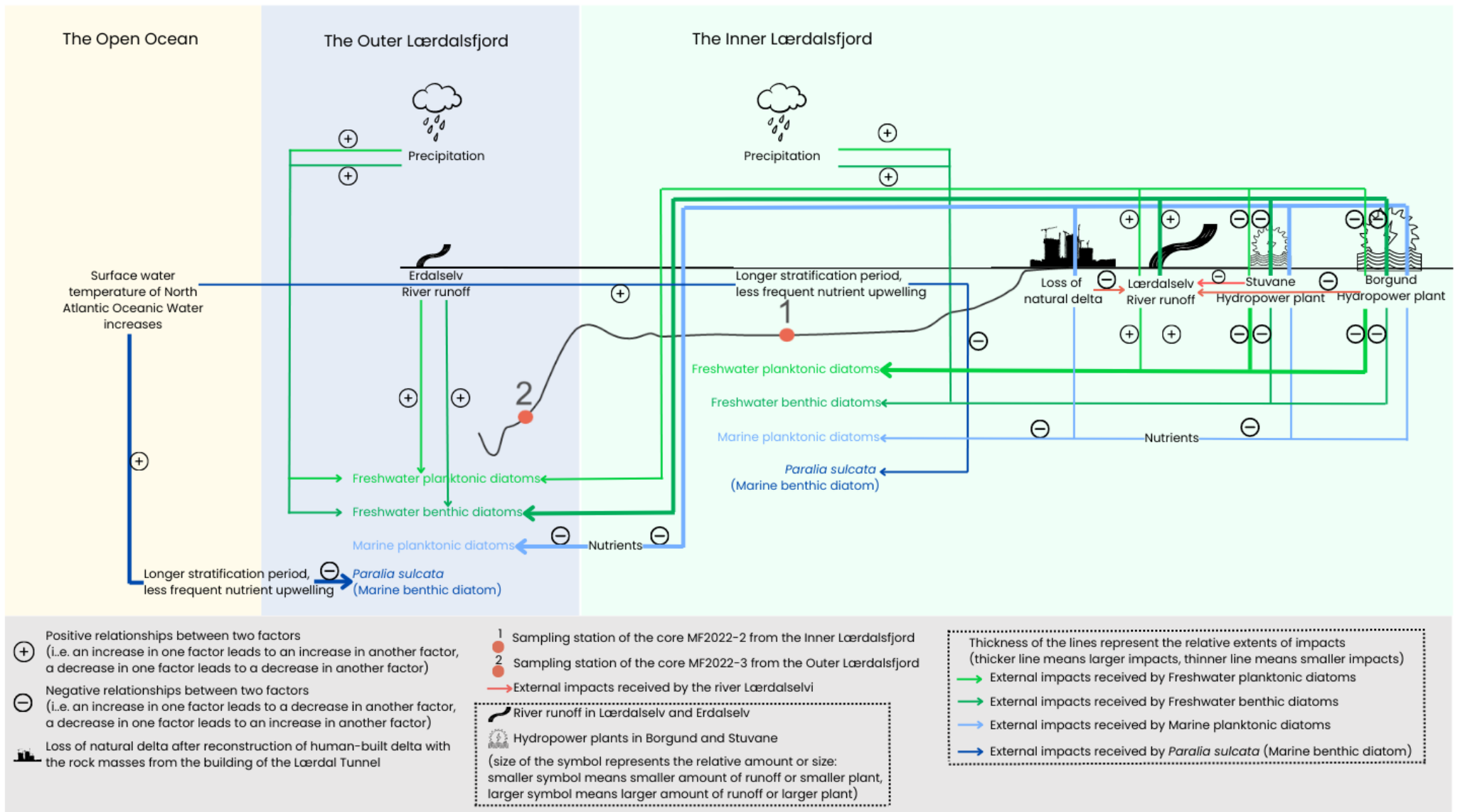


Figure 44. The box model of the Lærdalsfjord, which shows similarities and differences in how the main external influential factors (the precipitation, the inflow of North Atlantic Oceanic Water, river runoff of the river Lærdalselv and the river Erdalselv) exert impacts on the diatom composition in the Inner and Outer Lærdalsfjord. The runoff of the river Lærdalselv is influenced by hydropower plants and loss of natural delta.

7. Conclusion

The major conclusions of this thesis are as follows:

(1). The relative dating method introduced by Paetzel & Dale (2010) based on the relationship between the historical local precipitation records and the relative abundance of freshwater diatoms can be used to date the two sediment cores from the Inner and Outer Lærdalsfjord back to 1969 (with the exception of dating of the year 1936 in the Outer Lærdalsfjord). The sedimentation rates range from 0.27 cm/year to 0.38 cm/year. This dating is confirmed by an additional dating based on the negative relationship between fjord water temperature change and the relative abundance of a marine benthic diatom species, *Paralia sulcata*. These two datings show differences within 0 to 2 years (and one single maximum of 5 years).

(2). Changes in the freshwater diatom composition hold signals of past natural and human-caused climate and environmental change. The positive relationship between the precipitation level and the relative abundance of freshwater planktonic diatoms is confirmed in both sediment cores. In addition, the impact of two hydropower plants on the river flow pattern is reflected by the decrease in the freshwater planktonic diatoms in the Inner Lærdalsfjord. This impact is less significant in the Outer Lærdalsfjord due to its different environmental surrounding. Furthermore, an increase in the freshwater benthic diatoms in the Inner Lærdalsfjord and their decrease in the Outer Lærdalsfjord after 2000 indicate that the impact of the two hydropower plants results in a decrease in the transportation capacity of the river Lærdalselv. This effect is additionally enhanced by the loss of the natural delta.

(3). Changes in the marine diatom composition can also indicate the past natural and human-caused climate and environmental change. Decreases in the marine planktonic diatoms in both sediment cores after 1988 can be linked to the increased impacts of the two hydropower plants on the resulting reduction in river transportation capacity of nutrients after the construction of the second hydropower plant. Additionally, a continuous decrease in the marine benthic diatom species, *Paralia sulcata*, throughout the whole cores in the Inner and Outer Lærdalsfjord reflects the global warming trend and the corresponding decrease in the frequency of basin water circulation in the Lærdalsfjord. The reduction in the marine benthic diatom *Paralia sulcata* in the Outer Lærdalsfjord is more pronounced since the Outer Lærdalsfjord is more influenced by the increasing water temperature of the Norwegian Sea (Kaufmann 2014; Reß 2015).

8. Reference

- Agardh, C.A. (1824) *Systema algarum*. Literis Berlingianis, 1-312.
- Aksnes, D. L., Aure, J., Johansen, P.-O., Johnsen, G. H., & Veia Salvanes, A. G. (2019). Multi-decadal warming of Atlantic Water and associated decline of dissolved oxygen in a Deep Fjord. *Estuarine, Coastal and Shelf Science*, 228, 106392. Retrieved February 21, 2023, from <https://doi.org/10.1016/j.ecss.2019.106392>
- Alverson, A. J., Cannone, J. J., Gutell, R. R., & Theriot, E. C. (2006). The Evolution Of Elongate Shape In Diatoms 1. *Journal of Phycology*, 42(3), 655-668.
- Archibald, J. M. (2017). *Handbook of the protists*. Springer Berlin Heidelberg. Retrieved February 21, 2023, from https://link.springer.com/content/pdf/10.1007%2F978-3-319-28149-0_29.pdf
- Bahls, L. (2012). *Mastogloia elliptica*. *Diatoms of North America*. Retrieved March 8, 2023, from https://diatoms.org/species/mastogloia_elliptica
- Barber, H., & Haworth, E. (1981). *A Guide to the Morphology of the Diatom Frustule*.
- Bianchi, T. S., Arndt, S., Austin, W. E. N., Benn, D. I., Bertrand, S., Cui, X., Faust, J. C., Kozirowska-Makuch, K., Moy, C. M., Savage, C., Smeaton, C., Smith, R. W., & Syvitski, J. (2020). Fjords as aquatic critical zones (aczs). *Earth-Science Reviews*, 203, 103145. Retrieved February 21, 2023, from <https://doi.org/10.1016/j.earscirev.2020.103145>
- Blinn, D. W., & Bailey, P. C. (2001). Land-use influence on stream water quality and diatom communities in Victoria, Australia: A response to secondary salinization. *Saline Lakes*, 231–244. https://doi.org/10.1007/978-94-017-2934-5_21
- Blumberg, A. F., & Di Toro, D. M. (1990). Effects of Climate Warming on Dissolved Oxygen Concentrations in Lake Erie. *Transactions of the American Fisheries Society*, 119(2), 210–223. Retrieved February 21, 2023, from [https://doi.org/10.1577/1548-8659\(1990\)119](https://doi.org/10.1577/1548-8659(1990)119)
- Borgund kraftverk. (2021). *Store Norske Leksikon*. Retrieved March 10, 2023, from https://snl.no/Borgund_kraftverk

Cantonati, M., Zorza, R., Bertoli, M., Pastorino, P., Salvi, G., Platania, G., Prearo, M., & Pizzul, E. (2021). Recent and subfossil diatom assemblages as indicators of environmental change (including fish introduction) in a high-Mountain Lake. *Ecological Indicators*, 125, 107603.

Cattaneo, A., Couillard, Y., Wunsam, S., & Courcelles, M. (n.d.). Diatom taxonomic and morphological changes as indicators of metal pollution and recovery in Lac Dufault (Québec, Canada) - *journal of paleolimnology*. SpringerLink. Retrieved January 21, 2023, from <https://link.springer.com/article/10.1023/B:JOPL.0000029430.78278.a5>

Cox, E. J. (2011). Ontogeny, homology, and terminology-wall morphogenesis as an aid to character recognition and character state definition for pennate diatom SYSTEMATICS1. *Journal of Phycology*, 48(1), 1–31. Retrieved February 21, 2023, from <https://doi.org/10.1111/j.1529-8817.2011.01081.x>

Dale, T. (2023) Professor at the Western Norway University of Applied Science (HVL), personal communication

Darelius, E. (2020). On the effect of climate trends in coastal density on deep water renewal frequency in sill fjords—a statistical approach. *Estuarine, Coastal and Shelf Science*, 243, 106904. Retrieved February 21, 2023, from <https://doi.org/10.1016/j.ecss.2020.106904>

Durbin, E. G. (1974). Studies on the autecology of the marine diatom *thalassiosira nordenskiöldii* cleve. 1. the influence of daylength, light intensity, and temperature on growth1. *Journal of Phycology*, 10(2), 220–225. Retrieved February 21, 2023, from <https://doi.org/10.1111/j.1529-8817.1974.tb02702.x>

Dixit, S. S., Smol, J. P., Kingston, J. C., & Charles, D. F. (1992). Diatoms: Powerful indicators of environmental change. *Environmental Science & Technology*, 26(1), 22–33. <https://doi.org/10.1021/es00025a002>

Engineering.com. (2006). Laerdal Tunnel. Engineering.Com. Retrieved March 10, 2023, from <https://www.engineering.com/story/laerdal-tunnel>

European Commission. (2014). Directive 2000/60/EC of the European Parliament and of the Council of 23 October 2000 establishing a framework for Community action in the field of water policy. EUR-Lex Access to European Union Law. Retrieved February 28, 2023, from <https://eur-lex.europa.eu/eli/dir/2000/60/2014-11-20>

European Environmental Agency. (2022). Oxygen concentrations in coastal and marine waters surrounding Europe. Site. Retrieved March 1, 2023, from <https://www.eea.europa.eu/ims/oxygen-concentrations-in-coastal-and>

Faust, J. C., Fabian, K., Milzer, G., Giraudeau, J., & Knies, J. (2016). Norwegian fjord sediments reveal NAO related winter temperature and precipitation changes of the past 2800 years. *Earth and Planetary Science Letters*, 435, 84–93. Retrieved February 21, 2023, from <https://doi.org/10.1016/j.epsl.2015.12.003>

Fourtanier, E., & Kocielek, J. P. (1999). Catalogue of the diatom genera. *Diatom Research*, 14(1), 1–190. Retrieved February 21, 2023, from <https://doi.org/10.1080/0269249x.1999.9705462>

Fuhrmann, T., Landwehr, S., El Rharbi-Kucki, M., & Sumper, M. (2004). Diatoms as living photonic crystals. *Applied Physics B*, 78(3-4), 257–260. Retrieved February 21, 2023, from <https://doi.org/10.1007/s00340-004-1419-4>

Furey, P. (2010). *Eunotia*. In *Diatoms of North America*. <https://diatoms.org/genera/eunotia>

Gjerdingen, H. (2018). Identifisering av flomavsetninger i fjorder på Vestlandet - Aurlandsfjorden og Lærdalsfjorden (Master's thesis, Universitetet i Bergen).

Haflidason, H. (2020). Marine Geological Cruise Report (Master's thesis, Universitetet i Bergen)

Hartmann, S. (2023). The effect of recent (0-80 years) environmental change on the geochemical (XRF and magnetic susceptibility) record of Lærdalsfjord sediments, Western Norway (Master's thesis, Carl von Ossietzky Universität Oldenburg), in progress

Heggøy, E., Johansen, P.-O., & Johannessen, P. (2007). Marinbiologisk miljøundersøkelse i Lærdalsfjorden i 2006. Seksjon for anvendt miljøforskning – marin.

Howarth, R. J. & Sinding-Larsen, R. (1983). Multivariate analysis. In: R. J. Howarth (ed.): *Statistics and data analysis in geochemical prospecting*. Elsevier Science, Amsterdam, 207-289.

Jensen, K. G., Kuijpers, A., Koç, N., & Heinemeier, J. (2004). Diatom evidence of hydrographic changes and ice conditions in Igaliku Fjord, South Greenland, during the past 1500 years. *The Holocene*, 14(2), 152–164. Retrieved February 21, 2023, from <https://doi.org/10.1191/0959683604hl698rp>

Johannessen, P., & Lønning, T. (1988). Resipientundersøkelser. (I. f. Marinbiologi, Hrsg.) UNIFOB.

Johnsen, T. M., & Golmen, L. G. (1992). Kosekvensanalyse Av Dumping Av Tunnelmasse I Sjøen I Lærdalsområdet. Norsk institutt for vannforskning. Retrieved February 21, 2023, from <http://hdl.handle.net/11250/207047>

Kasim, M., & Mukai, H. (2006). Contribution of benthic and epiphytic diatoms to clam and oyster production in the Akkeshi-Ko Estuary. *Journal of Oceanography*, 62(3), 267–281. Retrieved February 21, 2023, from <https://doi.org/10.1007/s10872-006-0051-9>

Kaufmann, S. (2014). A 100 year hydrographical record of the Barsnesfjord, Western Norway and its environmental application (Bachelor's thesis, Sogn og Fjordane University College)

Klamer, T. (2017). River Deltas of the Inner Sognefjord (inner Sogn Region) Consequences of Anthropogenic Change (Bachelor's thesis, Western Norway University of Applied Science (HVL))

Kociolek, J.P., Blanco, S., Coste, M., Ector, L., Liu, Y., Karthick, B., Kulikovskiy, M., Lundholm, N., Ludwig, T., Potapova, M., Rimet, F., Sabbe, K., Sala, S., Sar, E., Taylor, J., Van de Vijver, B., Wetzel, C.E., Williams, D.M., Witkowski, A. & Witkowski, J. (2023). DiatomBase. Retrieved February 21, 2023, from <https://www.diatombase.org> on 2023-03-02. doi:10.14284/504

Koide, M., Soutar, A., and Goldberg, E. D. (1972). Marine geochronology with ²¹⁰Pb. *Earth and Planetary Science Letters*, 14, 442–446.

Kong, F., Ran, Z., Zhang, J., Zhang, M., Wu, K., Zhang, R., Liao, K., Cao, J., Zhang, L., Xu, J., & Yan, X. (2021). Synergistic effects of temperature and light intensity on growth and physiological performance in *Chaetoceros Calcitrans*. *Aquaculture Reports*, 21, 100805. Retrieved February 21, 2023, from <https://doi.org/10.1016/j.aqrep.2021.100805>

- Kotzsch, A., Gröger, P., Pawolski, D., Bomans, P. H., Sommerdijk, N. A., Schlierf, M., & Kröger, N. (2017). Silicanin-1 is a conserved diatom membrane protein involved in silica biomineralization. *BMC Biology*, 15(1). Retrieved February 21, 2023, from <https://doi.org/10.1186/s12915-017-0400-8>
- Krammer, K. & Lange-Bertalot, H. (1986) Bacillariophyceae. 1. Teil: Naviculaceae In: Ettl, H., J. Gerloff, H. Heynig and D. Mollenhauer (eds.) Süßwasserflora von Mitteleuropa, Band 2/1. Gustav Fisher Verlag, Jena. 876.
- Lauritano, C., Orefice, I., Procaccini, G., Romano, G., & Ianora, A. (2015). Key genes as stress indicators in the ubiquitous diatom *Skeletonema Marinoi*. *BMC Genomics*, 16(1). Retrieved February 21, 2023, from <https://doi.org/10.1186/s12864-015-1574-5>
- Lewis, W. M. (1984). The Diatom Sex Clock and Its Evolutionary Significance. *The American Naturalist*, 123(1), 73–80. Retrieved February 21, 2023, from <http://www.jstor.org/stable/2460887>
- McQuoid, M. R., & Nordberg, K. (2003a). Environmental influence on the diatom and silicoflagellate assemblages in Koljö Fjord (Sweden) over the last two centuries. *Estuaries*, 26(4), 927–937. <https://doi.org/10.1007/bf02803351>
- McQuoid, M. R., & Nordberg, K. (2003b). The diatom *Paralia sulcata* as an environmental indicator species in coastal sediments. *Estuarine, Coastal and Shelf Science*, 56(2), 339–354. [https://doi.org/10.1016/s0272-7714\(02\)00187-7](https://doi.org/10.1016/s0272-7714(02)00187-7)
- Medlin, L. K. (2009). The use of the terms centric and pennate. *Diatom Research*, 24(2), 499–501.
- Medlin, L. K., & Desdevises, Y. (2020). Phylogenetic reconstruction of diatoms using a seven-gene dataset, multiple outgroups, and morphological data for a total evidence approach. *Phycologia*, 59(5), 422–436. Retrieved February 21, 2023, from <https://doi.org/10.1080/00318884.2020.1795962>
- Medlin, L., & Kaczmarska, I. (2004). Evolution of the diatoms: V. Morphological and cytological support for the major clades and a taxonomic revision. *Phycologia*, 43(3), 245–270. Retrieved February 21, 2023, from <https://doi.org/10.2216/i0031-8884-43-3-245.1>
- Meteorologisk institutt. (2022a). Klimaprofil Sogn og Fjordane. Klimaservicesenter. Retrieved March 1, 2023, from <https://klimaservicesenter.no/kss/klimaprofiler/sogn-og-fjordane>

Meteorologisk institutt. (2022b). Norwegian Centre for Climate Services. Seklima – Observations and weather statistics. Retrieved March 6, 2023, from <https://seklima.met.no/>.

Mitra, A., Roy, A., & Trivedi, S. (2018). Phytoplankton diversity in the World Heritage Site of Indian sundarbans: An overview. *Examines in Marine Biology & Oceanography*, 1(2). Retrieved February 21, 2023, from <https://doi.org/10.31031/eimbo.2018.01.000507>

Munsell (1994). Munsell Soil Color Charts. Munsell Color 1994 revised edition, GretagMacbeth, NY, USA.

Niemistö, L. (1974). A gravity corer for studies of soft sediments. *Merentutkimuslait Julk/Havsforskningsinstituttets Skrifter*, 238, 33–38.

Norgeskart. (n.d.). Retrieved September 1, 2022, from <https://norgeskart.no/>

Not, F., Siano, R., Kooistra, W. H., Simon, N., Vaultot, D., & Probert, I. (2012). Diversity and Ecology of Eukaryotic Marine Phytoplankton. In *Advances in Botanical Research. Genomic Insights into the Biology of Algae: Diversity and Ecology of Eukaryotic Marine Phytoplankton* (Vol. 64, pp. 1–53). Elsevier. Retrieved February 21, 2023, from <https://doi.org/10.1016/B978-0-12-391499-6.00001-3>

Oppermann, J. (2023). Signals of environmental change based on the particulate matter record in recent (0-80 years) sediments from the Lærdalsfjord, Western Norway. (Master's thesis, Carl von Ossietzky Universität Oldenburg), in progress

Otu, M. & Spaulding, S. (2011). *Cavinula cocconeiformis*. In *Diatoms of North America*. Retrieved March 22, 2023, from https://diatoms.org/species/cavinula_cocconeiformis

Paetzel, M., & Dale, T. (2010). Climate proxies for recent fjord sediments in the Inner Sognefjord region, Western Norway. *Geological Society, London, Special Publications*, 344(1), 271–288. <https://doi.org/10.1144/sp344.19>

Paetzel, M. & Schrader, H. (1992). Recent environmental changes recorded in anoxic Barsnesfjord sediments: Western Norway. *Marine Geology*, 105, 23–36.

Patrick, R.M. & Reimer, C.W. (1966). *The Diatoms of the United States exclusive of Alaska and Hawaii*, V. 1 Monographs of the Academy of Natural Sciences of Philadelphia, 13.

- Pérez-Martínez, C., Cruz-Pizarro, L., & Sánchez-Castillo, P. (1992). Auxosporulation In *Cyclotella Ocellata* (Bacillariophyceae) Under Natural And Experimental Conditions 1. *Journal of phycology*, 28(5), 608-615.
- Ratner, B. (2009). The correlation coefficient: Its values range between +1/-1, or do they? *Journal of Targeting, Measurements and Analysis for Marketing* 17, 139-142.
- Reß, T. (2015). Some hydrographical changes in the Sognefjord and its tributaries, the Sogndalsfjord and the Barsnesfjord (Western Norway), the last century (Bachelor's thesis, Sogn og Fjordane University College)
- Ross, R., Cox, E.J., Karayeva, N.I., Mann, D.G., Paddock, T.B.B., Simonsen, R. and Sims, P.A. (1979). An amended terminology for the siliceous components of the diatom cell *Nova Hedwigia*, Beihefte 64: 513-533
- Rothwell, R. G. (1989). *Minerals and Mineraloids in Marine Sediments: An Optical Identification Guide*. Elsevier Science Publishers Ltd, London
- Round, F. E., Crawford, R. M., & Mann, D. G. (1990). *Diatoms: biology and morphology of the genera*. Cambridge university press.
- Scherer, R. P., & Koc, N. (1996). Late Paleogene diatom biostratigraphy and paleoenvironments of the northern Norwegian-Greenland Sea. *Proceedings of the Ocean Drilling Program, 151 Scientific Results*. Retrieved February 21, 2023, from <https://doi.org/10.2973/odp.proc.sr.151.155.1996>
- Serôdio, J., & Lavaud, J. (2020). Diatoms and their ecological importance. *Encyclopedia of the UN Sustainable Development Goals*, 1–9. Retrieved February 21, 2023, from https://doi.org/10.1007/978-3-319-71064-8_12-1
- Smith, W. (1853). *Synopsis of British Diatomaceae* John Van Voorst, London 1853. 89 pp., pls 1-31
- Smith, R. D., Bianchi, T. S., Allison, M. A., Savage, C., & Galy, V. (2015). High rates of organic carbon burial in fjord sediments globally. *Nature Geoscience*, 8(6), 450–453. Retrieved February 21, 2023, from <https://doi.org/10.1038/ngeo2421>
- Snoeijs, P. (2001). 14 Diatoms and environmental change in brackish waters. *The diatoms: applications for the environmental and earth sciences*, 298.

Spaulding, S. & Edlund, M. (2008). Genera. In *Diatoms of North America*. Retrieved February 21, 2023, from <https://diatoms.org/genera/>

SSBS API (2022). Retrieved February 21, 2023, from <https://data.ssb.no/api/v0/en/table/01223/>

Stevenson, R. J. (1983). Effects of current and conditions simulating autogenically changing microhabitats on benthic diatom immigration. *Ecology*, 64(6), 1514–1524. Retrieved February 21, 2023, from <https://doi.org/10.2307/1937506>

Taylor, F., Whitehead, J., & Domack, E. (2001). Holocene paleoclimate change in the Antarctic Peninsula: Evidence from the diatom, sedimentary and geochemical record. *Marine Micropaleontology*, 41(1-2), 25–43. Retrieved February 21, 2023, from [https://doi.org/10.1016/s0377-8398\(00\)00049-9](https://doi.org/10.1016/s0377-8398(00)00049-9)

Theriot, E. C., Cannone, J. J., Gutell, R. R., & Alverson, A. J. (2009). The limits of nuclear-encoded SSU rDNA for resolving the diatom phylogeny. *European Journal of Phycology*, 44(3), 277–290. Retrieved February 21, 2023, from <https://doi.org/10.1080/09670260902749159>

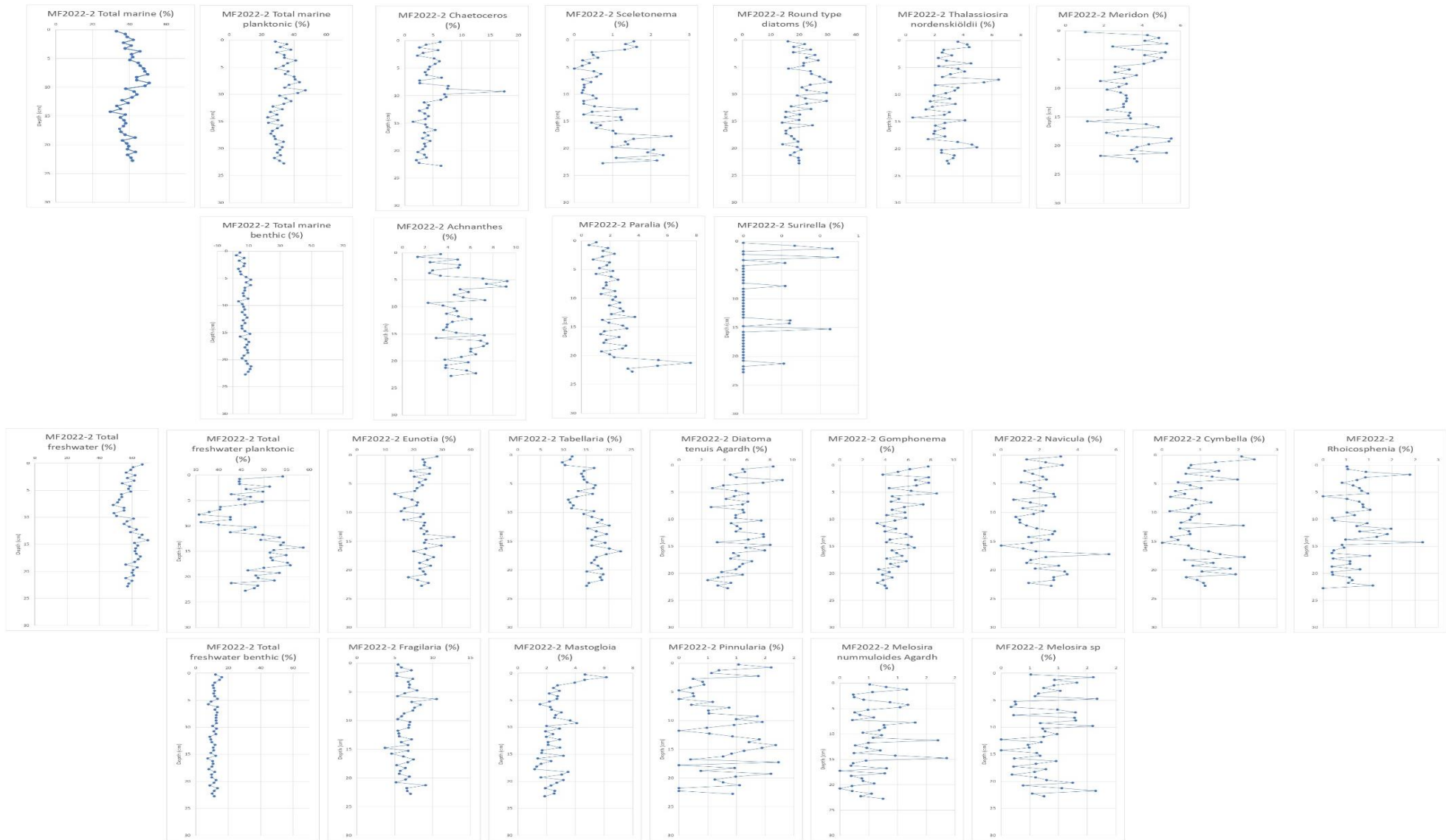
UBC Department of Earth, Ocean and Atmospheric Sciences. (2012). The phytoplankton encyclopaedia project. Retrieved February 21, 2023, from <https://www.eoas.ubc.ca/research/phytoplankton/diatoms/centric.html>

Vann-nett.no. (2022). Hva er et miljømål? Vannnett-Portal. Retrieved February 28, 2023, from <https://vann-nett.no/portal/#/waterenvgoalinformation>

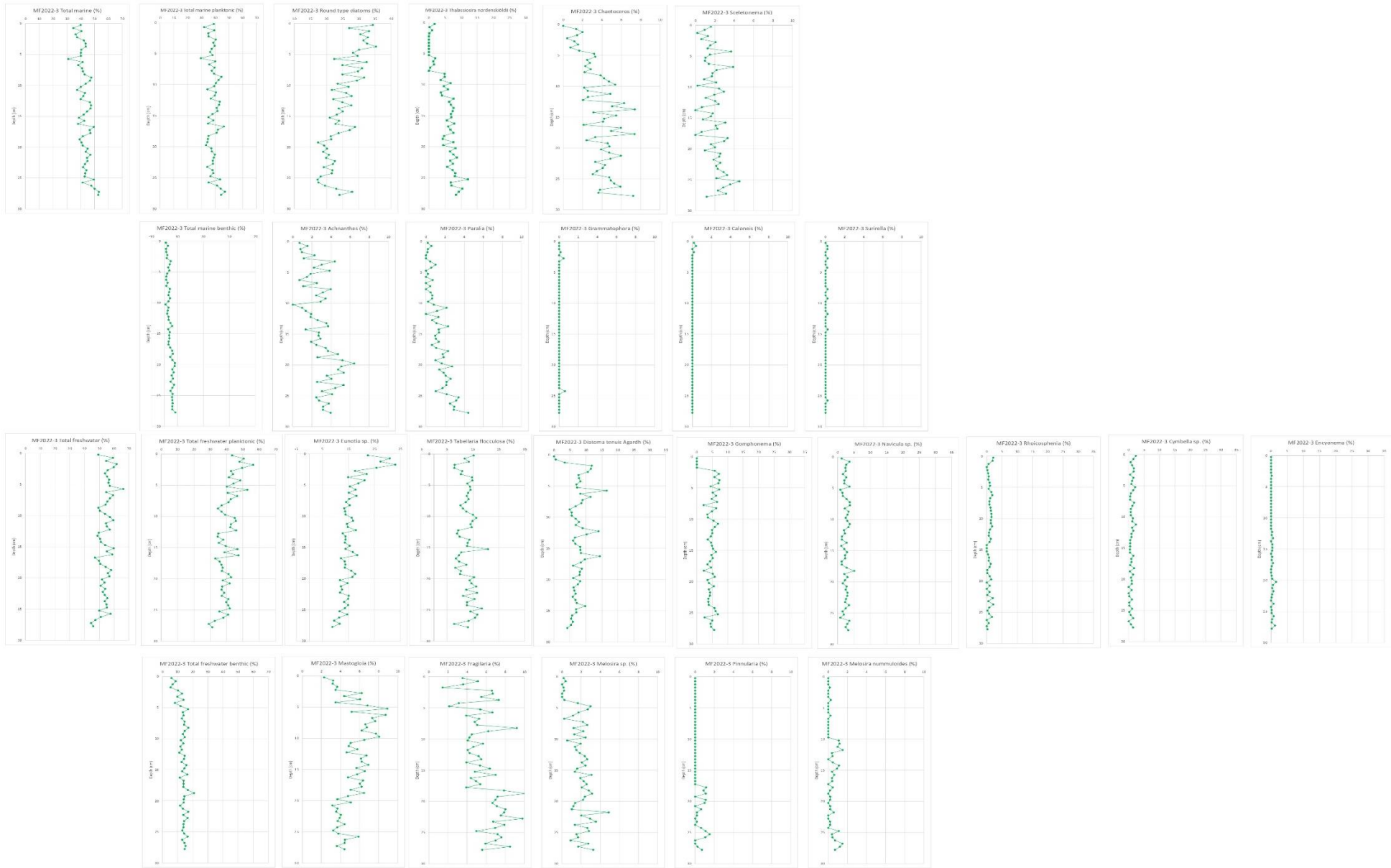
Witon, E., Malmgren, B., Witkowski, A., & Kuijpers, A. (2006). Holocene marine diatoms from the Faeroe Islands and their paleoceanographic implications. *Palaeogeography, Palaeoclimatology, Palaeoecology*, 239(3-4), 487–509. <https://doi.org/10.1016/j.palaeo.2006.02.006>

Yun, S. M., Lee, S. D., Park, J. S., & Lee, J. H. (2016). A new approach for identification of the genus *paralia* (bacillariophyta) in Korea based on morphology and morphometric analyses. *ALGAE*, 31(1), 1–16. Retrieved February 21, 2023, from <https://doi.org/10.4490/algae.2016.31.3.7>

Appendix 5. X-Y scatter graphs of the relative abundance of each category and each diatom genus (in % of total diatoms) in the core MF2022-2

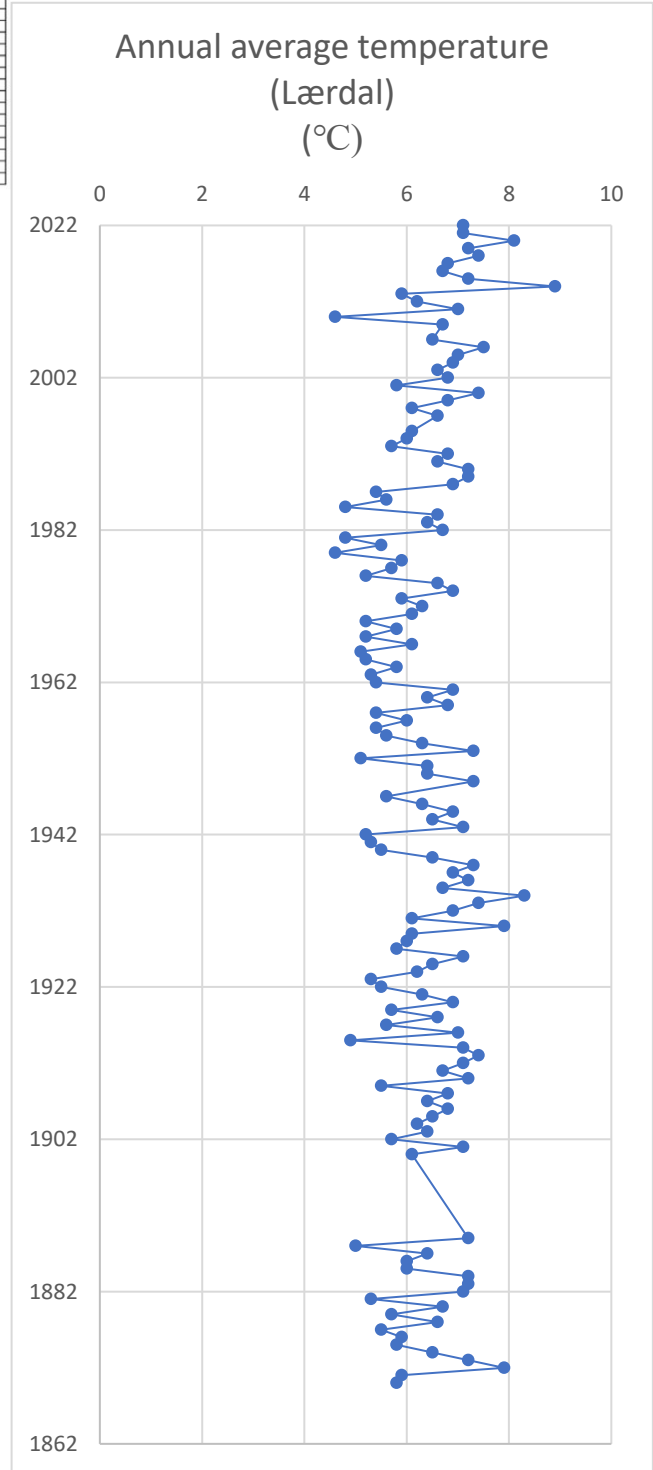


Appendix 6. X-Y scatter graphs of the relative abundance of each category and each diatom genus (in % of total diatoms) in the core MF2022-3



Appendix 8. Historical annual average temperature records, the data from the meteorological stations in Lærdal, Lærdal/Tønjum, Lærdal/Moldo, and Lærdal IV

Location	Station	Year	Annual average temperature (degree Celsius)	Annual average temperature (degrees Celsius) (average of every 3 years)	Year
Lærdal	SNS4100	1870	5,8	6,956666667	1931
Lærdal	SNS4100	1871	5,9	7,466666667	1934
Lærdal	SNS4100	1872	7,9	7,133333333	1937
Lærdal	SNS4100	1873	7,2	5,766666667	1940
Lærdal	SNS4100	1874	6,5	6,266666667	1943
Lærdal	SNS4100	1875	5,8	6,266666667	1946
Lærdal	SNS4100	1876	5,9	6,7	1949
Lærdal	SNS4100	1877	5,5	6,233333333	1952
Lærdal	SNS4100	1878	6,6	5,666666667	1955
Lærdal	SNS4100	1879	5,7	6,2	1958
Lærdal	SNS4100	1880	6,7	5,866666667	1961
Lærdal	SNS4100	1881	5,3	5,366666667	1964
Lærdal	SNS4100	1882	7,1	6,7	1967
Lærdal	SNS4100	1883	7,2	5,866666667	1970
Lærdal	SNS4100	1884	7,2	6,466666667	1973
Lærdal	SNS4100	1885	6	5,6	1976
Lærdal	SNS4100	1886	6	4,956666667	1979
Lærdal	SNS4100	1887	6,4	6,566666667	1982
Lærdal	SNS4100	1888	5	6,266666667	1985
Lærdal	SNS4100	1889	7,2	7,1	1988
Lærdal	SNS4100	1900	6,1	6,366666667	1991
Lærdal	SNS4100	1901	7,1	6,233333333	1994
Lærdal	SNS4100	1902	5,7	6,766666667	1998
Lærdal	SNS4100	1903	6,4	6,4	2001
Lærdal	SNS4100	1904	6,2	7,133333333	2004
Lærdal	SNS4100	1905	6,5	5,933333333	2007
Lærdal	SNS4100	1906	6,8	6,366666667	2010
Lærdal	SNS4100	1907	6,4	7,6	2013
Lærdal	SNS4100	1908	6,8	7,133333333	2016
Lærdal	SNS4100	1909	5,5	7,433333333	2019
Lærdal	SNS4100	1910	7,2		
Lærdal	SNS4100	1911	6,7		
Lærdal	SNS4100	1912	7,1		
Lærdal	SNS4100	1913	7,4		
Lærdal	SNS4100	1914	7,1		
Lærdal	SNS4100	1915	4,9		
Lærdal	SNS4100	1916	7		
Lærdal	SNS4100	1917	5,6		
Lærdal	SNS4100	1918	6,6		
Lærdal	SNS4100	1919	5,7		
Lærdal	SNS4100	1920	6,9		
Lærdal	SNS4100	1921	6,3		
Lærdal	SNS4100	1922	5,5		
Lærdal	SNS4100	1923	5,3		
Lærdal	SNS4100	1924	6,2		
Lærdal	SNS4100	1925	6,5		
Lærdal	SNS4100	1926	7,1		
Lærdal	SNS4100	1927	5,8		
Lærdal	SNS4100	1928	6		
Lærdal	SNS4100	1929	6,1		
Lærdal	SNS4100	1930	7,9		
Lærdal	SNS4100	1931	6,1		
Lærdal	SNS4100	1932	6,9		
Lærdal	SNS4100	1933	7,4		
Lærdal	SNS4100	1934	8,3		
Lærdal	SNS4100	1935	6,7		
Lærdal	SNS4100	1936	7,2		
Lærdal	SNS4100	1937	6,9		
Lærdal	SNS4100	1938	7,3		
Lærdal	SNS4100	1939	6,5		
Lærdal	SNS4100	1940	5,5		
Lærdal	SNS4100	1941	5,3		
Lærdal	SNS4100	1942	5,2		
Lærdal	SNS4100	1943	7,1		
Lærdal	SNS4100	1944	6,5		
Lærdal	SNS4100	1945	6,9		
Lærdal	SNS4100	1946	6,3		
Lærdal	SNS4100	1947	5,6		
Lærdal - Tønjum	SNS4130	1949	7,3		
Lærdal - Tønjum	SNS4130	1950	6,4		
Lærdal - Tønjum	SNS4130	1951	6,4		
Lærdal - Tønjum	SNS4130	1952	5,1		
Lærdal - Tønjum	SNS4130	1953	7,3		
Lærdal - Tønjum	SNS4130	1954	6,3		
Lærdal - Tønjum	SNS4130	1955	5,6		
Lærdal - Tønjum	SNS4130	1956	5,4		
Lærdal - Tønjum	SNS4130	1957	6		
Lærdal - Tønjum	SNS4130	1958	5,4		
Lærdal - Tønjum	SNS4130	1959	6,8		
Lærdal - Tønjum	SNS4130	1960	6,4		
Lærdal - Tønjum	SNS4130	1961	6,9		
Lærdal - Tønjum	SNS4130	1962	5,4		
Lærdal - Tønjum	SNS4130	1963	5,3		
Lærdal - Tønjum	SNS4130	1964	5,8		
Lærdal - Tønjum	SNS4130	1965	5,2		
Lærdal - Tønjum	SNS4130	1966	5,1		
Lærdal - Tønjum	SNS4130	1967	6,1		
Lærdal - Tønjum	SNS4130	1968	5,2		
Lærdal - Tønjum	SNS4130	1969	5,8		
Lærdal - Tønjum	SNS4130	1970	5,2		
Lærdal - Tønjum	SNS4130	1971	6,1		
Lærdal - Tønjum	SNS4130	1972	6,3		
Lærdal - Tønjum	SNS4130	1973	5,9		
Lærdal - Tønjum	SNS4130	1974	6,9		
Lærdal - Tønjum	SNS4130	1975	6,6		
Lærdal - Tønjum	SNS4130	1976	5,2		
Lærdal - Tønjum	SNS4130	1977	5,7		
Lærdal - Tønjum	SNS4130	1978	5,9		
Lærdal - Tønjum	SNS4130	1979	4,6		
Lærdal - Tønjum	SNS4130	1980	6,6		
Lærdal - Tønjum	SNS4130	1981	4,8		
Lærdal - Tønjum	SNS4130	1982	6,7		
Lærdal - Tønjum	SNS4130	1983	6,4		
Lærdal - Tønjum	SNS4130	1984	6,6		
Lærdal - Tønjum	SNS4130	1985	4,8		
Lærdal - Tønjum	SNS4130	1986	5,6		
Lærdal - Tønjum	SNS4130	1987	5,4		
Lærdal - Tønjum	SNS4130	1988	6,9		
Lærdal - Tønjum	SNS4130	1989	7,2		
Lærdal - Tønjum	SNS4130	1990	7,2		
Lærdal - Tønjum	SNS4130	1991	6,6		
Lærdal - Tønjum	SNS4130	1992	6,8		
Lærdal - Tønjum	SNS4130	1993	5,7		
Lærdal - Tønjum	SNS4130	1994	6		
Lærdal - Tønjum	SNS4130	1995	6,1		
Lærdal - Moldo	SNS4120	1997	6,6		
Lærdal - Moldo	SNS4120	1998	6,1		
Lærdal - Moldo	SNS4120	1999	6,8		
Lærdal - Moldo	SNS4120	2000	7,4		
Lærdal - Moldo	SNS4120	2001	5,8		
Lærdal - Moldo	SNS4120	2002	6,8		
Lærdal - Moldo	SNS4120	2003	6,6		
Lærdal - Moldo	SNS4120	2004	6,9		
Lærdal - Moldo	SNS4120	2005	7		
Lærdal - Moldo	SNS4120	2006	7,5		
Lærdal - Moldo	SNS4120	2007	6,5		
Lærdal - Moldo	SNS4110	2009	6,7		
Lærdal - Moldo	SNS4110	2010	4,6		
Lærdal - Moldo	SNS4110	2011	7		
Lærdal - Moldo	SNS4110	2012	6,2		
Lærdal - Moldo	SNS4110	2013	5,9		
Lærdal - Moldo	SNS4110	2014	8,9		
Lærdal - Moldo	SNS4110	2015	7,2		
Lærdal - Moldo	SNS4110	2016	6,7		
Lærdal - Moldo	SNS4110	2017	6,8		
Lærdal - Moldo	SNS4110	2018	7,4		
Lærdal - Moldo	SNS4110	2019	7,2		
Lærdal - Moldo	SNS4110	2020	8,1		
Lærdal - Moldo	SNS4110	2021	7,1		
Lærdal - Moldo	SNS4110	2022	7,1		



Erklärung

Hiermit erkläre ich, dass ich die vorliegende Bachelor-Thesis mit dem Titel

“The environmental signal of diatoms in recent (0-90 years) sediments from the Lærdalsfjord, Western Norway”

selbständig verfasst und hierzu keine anderen als die angegebenen Hilfsmittel verwendet habe. Alle Stellen der Arbeit, die wörtlich oder sinngemäß aus fremden Quellen entnommen wurden, sind als solche kenntlich gemacht. Die Arbeit wurde bisher in gleicher oder ähnlicher Form in keinem anderen Studiengang als Prüfungsleistung vorgelegt oder an anderer Stelle veröffentlicht.

YANG Yang

Birkenfeld, 05/2023